ISTANBUL TECHNICAL UNIVERSITY ★ GRADUATE SCHOOL

ZEIN OR GELATIN NANOFIBERS LOADED WITH Au NANOSPHERES, SnO_2 OR BLACK ELDERBERRY EXTRACT USED AS ACTIVE AND SMART PACKAGING LAYERS FOR VARIOUS FISH FILLETS

Ph.D. THESIS

Turgay ÇETİNKAYA

Department of Food Engineering

Food Engineering Programme

DECEMBER 2022

ISTANBUL TECHNICAL UNIVERSITY ★ GRADUATE SCHOOL

ZEIN OR GELATIN NANOFIBERS LOADED WITH Au NANOSPHERES, SnO_2 OR BLACK ELDERBERRY EXTRACT USED AS ACTIVE AND SMART PACKAGING LAYERS FOR VARIOUS FISH FILLETS

Ph.D. THESIS

Turgay ÇETİNKAYA
(506162508)

Department of Food Engineering

Food Engineering Programme

Thesis Advisor: Prof. Dr. Filiz ALTAY
Thesis Co-Advisor: Assoc. Prof. Dr. Zafer CEYLAN

DECEMBER 2022

İSTANBUL TEKNİK ÜNİVERSİTESİ ★ LİSANSÜSTÜ EĞİTİM ENSTİTÜSÜ

ALTIN NANOKÜRECİKLERİ, SnO_2 VEYA KARA MÜRVER EKTRESİ İLE YÜKLENEN ZEİN VE JELATİN NANOLİFLERİNİN FARKLI BALIK FİLETOLARI İÇİN AKTİF VE AKILLI AMBALAJ KATMANI OLARAK KULLANILMASI

DOKTORA TEZİ

Turgay ÇETİNKAYA
(506162508)

Gıda Mühendisliği Anabilim Dalı

Gıda Mühendisliği Programı

Tez Danışmanı: Prof. Dr. Filiz ALTAY
Eş Danışman: Doç. Dr. Zafer CEYLAN

ARALIK 2022

Turgay ÇETINKAYA, a Ph.D. student of İTU Graduate School student ID 506162508, successfully defended the thesis/dissertation entitled "ZEIN OR GELATIN NANOFIBERS LOADED WITH Au NANOSPHERES, SnO_2 OR BLACK ELDERBERRY EXTRACT USED AS ACTIVE AND SMART PACKAGING LAYERS FOR VARIOUS FISH FILLETS", which he prepared after fulfilling the requirements specified in the associated legislations, before the jury whose signatures are below.

Thesis Advisor :	**Prof. Dr. Filiz ALTAY** Istanbul Technical University	.....
Co-advisor :	**Assoc. Prof.Dr. Zafer CEYLAN** Van Yüzüncü Yıl University	.....
Jury Members :	**Prof. Dr. Neşe ŞAHİN YEŞİLÇUBUK** Istanbul Technical University	.....
	Assoc Prof. Dr. Derya KAHVECİ KARINCAOĞLU Istanbul Technical University	.....
	Assoc. Prof. Dr. Salih KARASU Yıldız Technical University	.....
	Assoc. Prof. Dr. Raciye MERAL Van Yüzüncü Yıl University	.....
	Dr. Fatih BİLDİK Istanbul Technical University	.....

Date of Submission : 25 November 2022
Date of Defense : 23 December 2022

To my family,

FOREWORD

Firstly, I would like to express my special thanks to my advisor Prof. Dr. Filiz ALTAY for her contribution to the emergence of the idea of this dissertation subject. I appreciate her guidance, valuable comments and criticisms which allowed me to make great progress in my Ph.D. studies. I would like to thank my co-advisor Assoc. Prof. Dr. Zafer CEYLAN for leading the way to find solutions, and suggestions for this presented dissertation. I'm grateful to him for sharing his valuable experiences.

I would like to thank Dr. Fatih BİLDİK for his contributions regarding the examination of spectroscopic analysis results and support, Zahide KIRBAŞ for sharing her experimental analysis materials, Evren DEMİRCAN for providing chemicals and equipment assistance, Ümit ALTUNTAŞ, for his company, Dr. Kausar RAJAR for her experimental assistance on nanoparticle production, Rukhsana SALEH for her advises, Zahra NAJAFİ and to all other labmates and researchers of Istanbul Technical University, Food Enginering Department.

I would like to acknowledge the Istanbul Technical University, Scientific Research Projects Unit (Project ID number: 42144) for the financial support. I also would like to thank other authors of published articles from this dissertation for their cooperation.

Finally, I would like to thank my beloved mother Leyla ÇETİNKAYA, my dear father Hasan ÇETİNKAYA, my older brother Tolga ÇETİNKAYA and his wife Tuğba ÇETİNKAYA for their encouragement, great effort, and endless support.

November 2022

Turgay ÇETİNKAYA
(Food Engineer, M.S.c.)

TABLE OF CONTENTS

Page

ABBREVIATIONS

ANOVA : Analysis of Variance
ATR : Attenuated Total Reflectance
AuZ-Nm : Gold-zein Nanomats
AZN : Samples treated with zein nanofibers loaded with gold nanospheres
BE : Black Elderberry
DLS : Dynamic Light Scattering
DMA : Dimethlyamine
DSC : Differantial Scanning Calorimetry
EDS : Energy Dispersive X-ray Spectroscopy
FTIR : Fouier Transfrom Infrared Spectroscopy
NF : Nanofiber
NP : Nanoparticle
PCA : Plate Count Agar
PDI : Polydispersity Index
PLGA : Poly (lactic-co-glycolic acid)
PS : Particle Size
PVC : Polyvinly Chloride
PVP : Polyvinylpyrrolidone
SEM : Scanning Electron Microscopy
TGA : Thermogravimetric Analysis
TMA : Trimethylamine
TMAB : Total Mesophilic Aerobic Bacteria
TMAO : Trimethylamine N-oxide
TPB : Total Psychrophilic Bacteria
TVBN : Total Volatile Basic Nitrogen
TYM : Total Yeast and Mold
U : Uncoated samples

SYMBOLS

a	**:** Redness
Au	**:** Gold
b	**:** Yellowness
°C	**:** Degree
CFU	**:** Colony Forming Unit
ε″	**:** Dielectric Loss Factor
ε′	**:** Dielectric Constant
ε″/ε′	**:** Loss Tangent
GHz	**:** Gigahertz
MHz	**:** Megahertz
kV	**:** Kilovolt
L	**:** Lightness
mV	**:** Milivolts
mm	**:** Milimeter
nm	**:** Nanometer
ms cm^{-1}	**:** millisiemens centimeter^{-1}
mN m^{-1}	**:** milliNewton meter^{-1}
mL	**:** Mililiter
pH	**:** Potential of hydrogen
SnO_2	**:** Tin dioxide
T_0	**:** Band beginning transmittance
T_e	**:** Band end transmittance
T_m	**:** Melting temperature
µm^2/s	**:** Diffusion coefficients
µg	**:** Microgram

LIST OF TABLES

Page

LIST OF FIGURES

Page

ZEIN OR GELATIN NANOFIBERS LOADED WITH Au NANOSPHERES, SnO_2 OR BLACK ELDERBERRY EXTRACT USED AS ACTIVE AND SMART PACKAGING LAYERS FOR VARIOUS FRESH FISH FILLETS

SUMMARY

Fresh fish products spoil in a shorter time than other meat products. Consumers would prefer the freshest fish products that have higher initial quality. Therefore, it is important to investigate alternative methods to preserve the quality of fresh fish products and increase their shelf life. Furthermore, estimating the shelf life of fresh fish products in fast and easy methods has started to gain importance in recent years. These developments increase researchers' interest in active and smart packaging layers that are produced by nanotechnological methods. In this dissertation preparation, characterization, and practical application of biopolymer-based electrospun nanofibers as active and smart packaging layers are presented.

First, the purpose and objectives are explained and recent studies are presented in Chapter l. Then, preliminary microbiological analyzes were applied to smoked fish products after their packages being opened (Chapter *2*), suggesting that the smoking process inhibit microbial growth only if the package is not being opened. Then, the quality of three different fish meat samples (local salmon: YS, bream: Ç, sea bass: L) was determined in terms of the electrical conductivity value, surface tension values, and the ε″. Sensory evaluation results were also evaluated by photos and point scales. The electrical conductivity value of the YS, Ç, and L samples on the initial day (0.21, 0.24, and 0.233 mS cm^{-1}) increased on the 4^{th} day of storage (0.35, 0.39, and 0.47 mS cm^{-1}), respectively (~65%, 63%, and 101% change). Dielectric loss factor values calculated at a frequency of 30 MHz were also increased with the highest change of L samples (29.68%) on the 4^{th} day. On the contrary, surface tension values decreased with storage time. The surface tension of YS, Ç, L, declined from 38.22, 42.56, 37.57 mN m^{-1} to 16.2, 29.45, 25.94 mN m^{-1} on the 2^{nd} day of storage. Results revealed these analyzes can be accepted as an important and rapid quality techniques in fish meat samples.

Chapter 2 results revealed that active coating layers could be used to preserve shelf life and inhibit microbial growth. Therefore, in Chapter 3, skinless fish fillets nanocoated with fabricated AuZ-Nm (530 ± 377 nm) and TMAB growth at 4 ± 1 °C compared with the uncoated group during the 8-days storage. Microbiological results indicated that the use of zein nanofibers with gold nanospheres delayed the TMAB growth up to ~1 log CFU/g (p<0.05) and sensory deterioration. The monitoring dielectric properties of fresh fish fillets for evaluating their quality (Chapter 2), was also used in Chapter 3. In this sense, dielectric properties (ε′ and ε″) of the fish fillets were treated with AuZ-Nm and were investigated. ε′ values of the uncoated fish samples were more variable (34.53%) compared to the nanocoated group (<30%) on the 7th day of storage. Similarly, a 40.55% decrease was recorded for the uncoated group according to the initial ε″ value, while this decrease was 22.75% for nanocoated samples (p<0.05 between groups). It has been concluded that zein based nanofibers

with Au nanospheres have the potential as an active food packaging layer to extend the shelf life of fish fillets.

In Chapter 4, the effect of electrical conductivity, ε′, ε″, and loss tangent (ε″/ε′) values (at 300 and 3000 MHz), on feed solution electospinnability was investigated. For the first time, the aggregation behavior of nanofibers was determined by ZetaSizer equipment. Electrospun samples dispersed in the ethanol had lower translational diffusion coefficient (water:2.03 $\mu m^2/s$; ethanol: 1.85 $\mu m^2/s$) and higher hydrodynamic radius (water: 242 nm; ethanol: 221 nm). Zein-gold nanofiber stability was also studied by zeta potential measurements (ethanol: +41.73 mV; water: +5.1 mV). In addition, the antimicrobial effects of AuZ-Nm were investigated and physicochemical characteristics were compared without Au. Specific shoulders in Au-zein nanofiber spectrum indicated C=O carbonyl stretch vibrations in the amide I and amide II region, which does not appear for pure zein, but is observed also in the pure Au spectrum. After addition of Au, bands in the pure zein spectrum converted to stretching peaks, indicating the vibration frequency of Au–O ionic bond groups. These molecular observations and other signs (narrowing band, shifting wavenumber, transmittance changes) confirmed the successful integration of Au molecules.

All these results indicated that although the process of smoking decreased the initial TMAB load, after opening the package, the TMAB values of the smoked fish increased more (Chapter 2). Using Au in nanofiber coating layers inhibited microbial growth more than the smoking process as explained in Chapter *3* and Chapter 4. However, since disruption is inevitable, it is also important to use these nanofiber materials as indicator layers to predict shelf life. In this context, gelatin-based nanofibers were developed to evaluate their color changing functions (Chapter *5*). At first, the production of liquid gold NPs and dried gold nanopowders from gold salt ($HAuCl_4$) was explained as stated in supplementary material. Then liquid gold added to feed solutions. SEM results of gelatin nanofibers the average diameter of pure gelatin nanofibers (GL) was 81.4 nm without any beads. The addition of 10% BE extract to the solution increased diameter to 277 nm (GLE). EDS elemental mapping peaks and Figures indicated that after 5% SnO_2 incorporation into the feed solution, SnO_2 NPs both encapsulated inside the nanofiber and attached to the surfaces of gelatin nanofibers (GLES). Small spots on nanofibers were observed with the addition of produced Au nanopowders at 2%, and the average diameter increased to 554 nm (GLESA). Nanofibers were deeply characterized by FTIR before and after exposed to fish meat for 30 hours (no direct contact). New methods were proposed for the first time to evaluate nanofiber stability by transmittance ratio values and produced degradation metabolites confirmed with the band differences in spectrums. Specific spectral changes indicated absorption/attachment of volatile amines to the nanofibers during deterioration of fresh fish samples. Thermal stability between samples was compared by DSC and TGA. Thermal characteristic results of gelatin nanofiber samples also proved the new ionic bond complexes (initial) and thermal decomposition of absorbed volatiles (30^{th} hour). Furthermore, *L a b* values of the nanofiber showed that interaction between flavonoids/phenolic acids and metal ions modified the color produced by the anthocyanins. Therefore, the lowest brightness values (L=64.23) with the highest redness (a=10.37) for the gelatin nanofiber that contains gold nanopowders (p<0.05) were obtained in the first measurement before the spoilage (GLESA). During 30 hour storage period the absorption of volatile amines influenced *L a b* in different directions. On the 24^{th} hour, the color of the gold nanopowder added gelatin sample (GLESA) became more intense and turned to dark

purple with the lowest *b* value (-3.11) and the lowest *L* value (24.14) ($p<0.05$; between nanofiber samples and between initial, 3rd, 6th hours). When all chapters are evaluated together, the results of this study enable a better insight into a) understanding of the determination of fish quality by rarely studied parameters such as electrical conductivity, surface tension, and dielectric loss factor, b) evaluation of various properties of prepared feed solutions for electospinnability, c) molecular, morphological, elemental characterization of nanofibers and NPs, d) searching aggregation behavior and stability of nanofibers by novel techniques such as DLS data calculations e) practical application of fabricated nanofibers containing Au nanospheres, SnO_2, and BE extract on fish samples for gas sensing performance. These chapters guide possible nanoapplications of the nanofibers incorporated with antimicrobial agents, plant extracts, and metal-based NPs for active and intelligent packaging functions on meat products.

ALTIN NANOKÜRECİKLERİ, SnO_2 VEYA KARA MÜRVER EKSTRESİ İLE YÜKLENEN ZEİN VE JELATİN NANOLİFLERİNİN FARKLI BALIK FİLETOLARI İÇİN AKTİF VE AKILLI AMBALAJ KATMANI OLARAK KULLANILMASI

ÖZET

Taze balık ürünleri diğer et ürünlerine göre daha kısa sürede bozulmaktadır. Tüketiciler, başlangıç kalitesi daha yüksek olan ve en taze balık ürünlerini tercih etmektedirler. Bu nedenle taze balık ürünlerinin kalitesini korumak ve raf ömürlerini artırmak için alternatif yöntemlere ihtiyaç vardır. Ayrıca taze balık ürünlerinin raf ömürlerinin hızlı ve kolay yöntemlerle tahmin edilmesi son yıllarda önem kazanmaya başlamıştır. Bu gelişmeler, araştırmacıların nanoteknolojik yöntemlerle üretilen aktif ve akıllı ambalaj katmanlarına olan ilgisini artırmıştır. Bu doktora tez çalışmasında altın nanokürecikleri, SnO_2 veya mürver ekstresi içeren zein ve gelatin nanoliflerinin hazırlanması, karakterizasyonu ve aktif ve akıllı ambalaj katmanlarının pratik uygulamaları sunulmuştur. Nanoliflerin bir antimikrobiyal ambalaj tabakası olarak taze balıkların raf ömrünü uzatma veya akıllı ambalaj sistemleri olarak balık eti kalite değişimlerini algılama potansiyelleri araştırılmıştır. Birinci bölümde tezin konusu ve amaçları açıklanarak literatürde bu konuyla ilgili yapılan güncel çalışmalara yer verilmiştir. 2. Bölümde bu çalışmanın ön denemelerinde tütsülenmiş balık eti ürünlerinin ambalajı açıldıktan sonra raf ömrünü belirlemek amacıyla toplam mezofilik aerobik bakteri, toplam psikrofilik bakteri, küf-maya analizleri yapılmıştır. Sonuçlar tütsüleme işleminin raf ömrünü uzatmasına rağmen, ancak paket açılmadığında mikrobiyal büyümeyi engellediğini göstermektedir. Daha sonra yenilikçi bir yaklaşım ortaya konularak, elekriksel iletkenlik, yüzey gerilimi, dielektrik kayıp fakötürü gibi parametreler ile 10 ± 2 ºC'de muhafaza edilen taze balıketlerindeki kalite değişimleri 0. 2. ve 4. günlerde incelenmiştir. Üç farklı balık eti örneğinin (yerel somon: YS, çipura: Ç, levrek: L) literatürde fazla yer almayan ve nadir çalışılan elektriksel iletkenlik değeri, yüzey gerilimi değerleri, dielektrik kayıp faktörü (ε″), partikül boyutu gibi bazı parametreler açısından kaliteleri belirlenmiştir. Duyusal değerlendirme sonuçları da fotoğraflar ve puan cetvelleri ile gösterilmiştir. YS, Ç ve L numunelerinin elektriksel iletkenlik ölçer cihazı ile ölçülen ilk günkü değerleri (0,21, 0,24 ve 0,233 mS cm^{-1}) depolamanın 4. gününde sırasıyla (0,35, 0,39 ve 0,47 mS cm^{-1}) olarak ölçülmüştür (~%65, %63 ve %101 artış). Bu sonuçlara göre elektriksel iletkenlik değerleri bozulmayla birlikte artış göstermektedir. Bunun nedeni bozulma ile yağların ve proteinlerin yapısındaki değişme ve bozulmalar nedeniyle iyon miktarının değişmesi olabilir. Ağ analizörü cihazının probu homojenize balık örneklerine daldırılarak 30 MHz frekansında ölçülen dielektrik kayıp faktörü değerleri de balıketi numunelerinde artış göstermiştir. Gıdanın nem miktarının dielektrik kayıp faktörü değerini etkileyen özelliklerin başında geldiği bilinmektedir. Bu nedenle depolama süresince bozulmaya bağlı olarak örneklerdeki nem kayıpları ürünlerin dielektrik kayıp faktörü değerlerini de etkilemiştir. İlk güne kıyasla depolamanın 4. Gününde YS örnekerinde 423,59'dan 47627'e; Ç örneklerinde 419,72'den 482,45'e; L örneklerinde ise en yüksek artış hızıyla (29,68%) 408,21'den 529,40'a yükselmiştir.

Buna karşılık depolama süresince yüzey gerilimi değerleri azalmıştır. YS, Ç, L, yüzey gerilimi depolamanın 2. gününde 38,22, 42,56, 37,57 mN m^{-1}'den 16,2, 29,45, 25,94 mN m^{-1}'e gerilemiştir. Adhezyon olarak tanımlanan yapışkanlık özelliğinin yüzey gerilimini etkileyen önemli bir fonksiyon olduğu literatürde belirtilmiştir. Depolama süresinin artışına bağlı olarak yağların oksidasyonu ve proteinlerin parçalanması söz konusudur. Bozulma süreci adhezif yapışkanlık gibi tekstürel özellikleri de etkilediğinden balıketinin sahip olduğu protein ve yağlardaki değişimlerin etin yapışma mekanizması üzerinde önemli bir rol oynadığı belirtilmiştir. Sonuçlar, bu analizlerin balık eti örneklerinde önemli ve hızlı kalite yöntemleri olarak kullanılabileceğini ortaya koymuştur.

2. Bölümün sonuçları tütsüleme işlemine alternatif olarak aktif ambalaj katmanlarının raf ömrünü korumak ve mikrobiyal büyümeyi engellemek için kullanılabileceğini ortaya koymuştur. Bu nedenle, 3. Bölümde, elektroeğirme yöntemiyle üretilen altın-zein bazlı nanolifler (530 ± 377 nm) derisiz balık filetolarıyla kaplanmış ve 4 ± 1 °C'de 8 gün boyunca balıklardaki TMAB artışı kontrol grubuyla karşılaştırılmıştır. Mikrobiyolojik sonuçlar, altın nanoküreler ile zein nanoliflerinin birlikte kullanımının TMAB artışını ~1 log CFU/g'a (p<0.05) yavaşlatarak duyusal bozulmayı geciktirdiğini göstermiştir.

Ayrıca 2. Bölümde balıkların kalitelerini değerlendirmek için depolamaya bağlı olarak dielektrik özelliklerinin analizleri, 3. Bölümde de uygulanarak altın-zein nanolifi ile muamele edilmiş balık filetolarının dielektrik özellikleri (ε′ ve ε″) incelenmiştir. Depolamanın 7. gününde, kaplanmayan balık örneklerinin ε′ değerlerinin (%34,53), kaplanan gruba (<%30) kıyasla daha değişken olduğu tespit edilmiştir. Benzer şekilde, kaplanmayan grupta başlangıç ε″ değerinde %40,55 azalma kaydedilirken, nanolifle kaplanan numunelerde bu azalma %22,75 olarak elde edilerek gruplar arasında önemli derece fark tespit edilmiştir (p<0.05). Altın nanokürelere sahip zein bazlı nanoliflerin, balık filetolarının raf ömrünü uzatmak için aktif bir gıda paketleme katmanı olarak potansiyele sahip olabileceği sonucuna varılmıştır.

4. Bölümde, öncelikle besleme çözeltisinin bazı özelliklerinin elektroeğirme üzerindeki etkisini incelemek amaçıyla elektriksel iletkenlik, dielektrik sabiti (ε′), dielektrik kayıp faktörü (ε″) ve kayıp tanjant (ε″/ε′) değerleri (300 ve 3000 MHz'de) araştırılmıştır. Eletriksel iletkenlik değeri 808.67 ± 2.082 μs/cm olarak bulunmuştur. Elektriksel iletkenlik değeri, düzgün nanoliflerin oluşumu için önemli bir parametre olarak değerlendirilmektedir. Besleme çözeltisindeki yüksek iletkenlik (> 10 mS/cm) değerleri boncuklu, tek biçimli olmayan ve stabil olmayan lif oluşumuna sebep olabilmektedir. Bu nedenle besleme çözeltisi için düşük bir elektrik iletkenliği tercih edilir ki böylece daha düşük elektriksel kuvvet ile nanolif üretilebilir. Ancak yapılan çalışmalarda çok düşük iletkenlik değerlerinin de (örneğin; 0.06 mS/cm) nanolif oluşmasına engel olduğu bildirilmiştir. Bu nedenle elektriksel iletkenlik değeri polimer konsantrasyonuna ve türüne bağlı olarak nanolif yapısını etkilemektedir. Çalışmada elde edilen değer (808.67 ± 2.082 μS/cm), pürüzsüz altın-zein nanoliflerini (ortalama 438 nm çapında) üretmek için uygun bir değer olarak bulunmuştur. Besleme çözeltisinin dielektrik özellikleri nanoliflerin yapısını ve çapını da etkilemektedir. Yapılan çalışmalar nispeten yüksek ε'ye sahip besleme çözeltisinin, ince liflerin oluşumunu kolaylaştırabiliceğini göstermiştir. Çalışmada 3000 MHz frekansındaki dielektrik kayıp faktörü (11.08) ve kayıp tanjant (0.145) değerlerinin 300 MHz'deki değerlerden (sırasıyla 1.06 ve 0.135) daha yüksek olduğu tespit edilmiştir. Bu bölümde ayrıca ilk kez, üretilen nanoliflerin etanol ve su içindeki kümeleşme davranışı, dinamik ışık saçılması cihazıyla yapılan ölçümler ile belirlenmiştir. Öncelikle nanolifler,

0,1g/100 mL olacak şekilde Silent Crusher S (Heidolph Instruments, GmbH & Co. KG, Schwabach, Almanya) cihazı kullanılarak etanol içinde 60 saniye ve suda ise manyetik karıştırıcı ile 180 saniye dağıtıldı. Daha sonra dispersiyonlar, bir Whatman® Schleicher & Schuell filtre kağıdından (Sınıf: 595 ½, 90 mm çap) süzülmüş ve dinamik ışık saçılımı cihazı kullanılarak ölçümler yapılmıştır. Suda dağılan nanoliflerin daha büyük olan hidrodinamik yarıçapları (su: 242 nm; etanol: 221 nm), zeinin hidrofobik karakterine bağlanmıştır. Yüksek difüzyon katsayısı süspansiyonda polimerin daha fazla hareketli olduğunu göstermektedir ki bu da polimer yüzeyinde düşük su emilimine yol açabilir. Bu nedenle bu çalışmada suda dağılan nanoliflerin daha yüksek translasyonel difüzyon katsayısına (su: 2,03 $\mu m^2/s$; etanol: 1,85 $\mu m^2/s$) sahip olması etanol içindeki dispersiyona kıyasla, su dispersiyonunda hidrofobik zein nanoliflerinin yüzeyinde daha düşük su absorpsiyonunun göstergesi olabilir. Polidispersite indeksi sonuçları çok modlu bir boyut dağılımını ve dispersiyonda farklı büyüklüklerde toplanan nanoyapıların varlığını kanıtlamıştır. Bu sonuçlar nanoenkapsüle olan altın nanokürecikleri (15 nm) ile zein moleküllerinin çaplarının farklı olmasına bağlanmıştır. Ana eksen (uçları en geniş noktalar olan merkez ve odaklardan geçen bir elipsin en uzun çapı) değerlerinin ölçümü için öncelikle denklem ile geometrik katsayı (F_d) hesaplanmıştır. Daha sonra bu değer ikinci bir denklem kullanılarak (Bölüm 4.4.3) elips şeklinde olan liflerin ana eksen değeri hesaplanmıştır. Zein-altın nanolif stabilitesi, farklı solüsyonlarda zeta potansiyeli ölçümleri ile de incelenmiştir (etanol: +41.73 mV; su: +5.1 mV). Antimikrobiyal etkilere ek olarak, saf zein ve altınlı-zein nanoliflerinin fizikokimyasal özellikleri araştırılmıştır. Altın-zein nanolif spektrumundaki spesifik omuzlar, saf zein için oluşmayan, ancak saf altın spektrumunda da gözlenen amid I ve amid II bölgesinde C=O karbonlu germe titreşimlerini göstemiştir. Altın ilavesinden sonra, saf zein spektrumundaki esnek bantlar, Au–O iyonik bağ gruplarının titreşim frekansı ile germe tepe noktalarına dönüşmüştür. Bu moleküler gözlemler ve diğer değişiklikler (daralan bantlar, dalga boyunun kayması, geçirgenlik değişimleri) altın moleküllerinin hassas bir şekilde nanokapsülasyonunu doğrulamıştır.

Tüm bu sonuçlar göstermektedir ki, tütsüleme işlemi başlangıçtaki TMAB yükünü azaltmasına rağmen, paket açıldıktan TMAB değerlerinin daha fazla arttırmaktadır. Bu nedenle nanolif kaplama materyallerinde Au kullanılarak, Bölüm 3 ve Bölüm 4'te açıklandığı gibi, mikrobiyal büyüme tütsüleme işleminden daha fazla engellenmiştir. Ancak taze balık ürünlerinde kısa sürede bozulma kaçınılmaz olduğundan, nanolif materyallerini raf ömrünü tahmin etmek için akıllı indikatör göstergeleri olarak kullanmak da önemlidir. Bu amaçla Bölüm 5'te öncelikle açıklandığı üzere altın tuzundan ($HAuCl_4$) sıvı altın nanoparçacıklarının ve kurutulmuş altın nanotozlarının üretiminden bahsedilmiştir. Daha sonra dört farklı jelatin bazlı besleme çözeltisi hazırlanarak üretim yapılmıştır. Hazırlanan solüsyonlarda 1:1 (ağırlık/ağırlık) oranında asetik asit ve üretilen sıvı altın kullanılmıştır. Kontrol grubu sadece 20% jelatin içerirken, ikinci gruba 10% karamürver esktresi, üçüncü gruba ek olarak 5% SnO_2 ve dördüncü gruba ek olarak 2% altın nanotozları eklenmiştir. Taramalı elektron mikroskobu sonuçlarına göre sadece jelatin içeren nanoliflerin ortalama çapı 81.4 nm olarak ölçülmüştür. Çözeltiye %10 karamürver ekstresinin eklenmesi ile, ortalama çap 277 nm'ye yükselmiştir. SnO_2 eklenen örneklere elektron mikroskobuna entegre edilmiş Enerji Dağılımlı X-ışını Spektroskopisi dedektörü ile elementel haritalama işlemi de uygulanmıştır. Spektrumdaki tepe noktaları (Figür 5.2) SnO_2 nanoparçacıklarının hem nanolif içinde kapsüllendiğini hem de jelatin nanoliflerinin yüzeylerine bağlandığını göstermiştir. Çünkü nanoekapsülasyonla birlikte lif çaplarının ortalaması 398 nm'ye yükselmiştir. Üretilen altın nanotozları eklendiğinde

ise nanolifler üzerinde bazı noktalar gözlemlenmiş ve ortalama çap 554 nm'ye kadar yükselmiştir. Nanoliflerin ilk üretilmiş halleri detaylı karakterizasyon ile FTIR, DSC, TGA ekipmanlarında incelenmiştir. Daha sonra nanolifler oda sıcaklığında çiğ taze balık eti içeren petri kaplarındaki PVC film yüzeyine yerleştirilip (balıketiyle doğrudan temas olmadan) 30 saat boyunca değişimleri gözlemlenmiştir. 30. saatte nanoliflere ikinci bir karakterizasyon işlemi yapılmıştır. FTIR sonuçlarına göre spektrumdaki bant alanlarının oranları karşılaştırılarak ve bantların arasındaki uzaklıklar ölçülerek nanolif stabilitesi değerlendirilmiş, bozulmaya bağlı olarak üretilen metabolitlerin tespiti için yeni yaklaşımlar ortaya konulmuştur. Spektrumdaki spesifik değişiklikler, çiğ balık numunelerinin bozulmasından sonra uçucu aminlerin nanoliflere absorpsiyonunu/bağlandığını göstermiştir (Bölüm 5.4.2.2). Numuneler arasındaki ısıl stabilite farklılıkları, diferansiyel tarama kalorimetre ve termogravimetrik analizler ile karşılaştırılmıştır. Jelatin nanolif numunelerinin ısıl karakteristik sonuçları, metallerin varlığıyla ortaya çıkan başlangıçtaki yeni iyonik bağ yapıları ve 30. saat sonunda absorbe olan uçucu gazların ısıl bozulma bölgeleri kanıtlanmıştır. Uçucu gazlar ve nanoenkapsüle olan metaller arasındaki etkileşimler ile erime, ayrışma veya oksidasyon piklerinde değişimler (genişleme, kayma, yeni pikler vb.) gözlemlenmiştir. Ayrıca, nanoliflerin farklı saatlerde renk ölçümleri yapılarak balıklardaki bozulmanın *L, a, b,* değerlerine etkisi incelenmiştir. Kontrol örneğiyle (sadece jelatin) katı materyal eklenmiş nanolif örnekler arasındaki farklı renk sonuçları (sırasıyla, ekstre, SnO_2 ve altın nanotozu), flavonoidler/fenolik asitler ve metal iyonları arasındaki etkileşimin renk özelliklerini ortaya çıkaran antosiyaninlere bağlanmıştır. Bu nedenle ilk ölçümlerde altın nanotozlarını içeren jelatin nanoliflerinde en yüksek kırmızılık (*a* 10.37) ile en düşük parlaklık değerleri (*L* 64.23) elde edilmiştir ($p<0.05$). 30 saatlik depolama süresi boyunca uçucu aminlerin absorpsiyonu *L, a, b* değerlerini numunelerde farklı yönlerde etkilemiştir. 24. saatte altın nanotoz katkılı jelatin numunesinin rengi daha yoğun hale gelmiş ve en düşük *b* değeri (-3.11) ve en düşük *L* değeri (24.14) ile koyu mor renge dönmüştür ($p<0.05$). Aminlerin metalik nanopartiküllerin yüzeyine azot bağlarıyla kolaylıkla tutunabildiği bilinmektedir. Buna göre altın nanotozlu numunede absorbe edilen gazların çapraz bağlanmayla altın nanotoz toplanmasını teşvik ettiği ve daha güçlü bir *L* ve *b* değişikliği üretmesine sebep olduğu varsayılmıştır. Böylece nanolif numuneleri arası ve aynı zamanda 0., 3., 6. saatler arasında istatistiksel olarak anlamlı farklar bulunmuştur. Bu sonuçlar altın nanopartiküllerin/nanotozların ve SnO_2 gibi metal oksitlerin fonksiyonel özelliklere sahip nanoliflerin ambalaj katmanı olarak üretilmesinde faydalı olabileceğini kanıtlamıştır.

Tüm bölümler birlikte değerlendirildiğinde, yapılan çalışmanın sonuçları a) elektriksel iletkenlik, yüzey gerilimi, dielektrik kayıp faktörü gibi nadiren incelenen parametrelerle balık kalitesinin belirlenmesi b) hazırlanan besleme çözeltilerinin dielektrik, elektiksel iletkenlik gibi özelliklerinin nanolif oluşumuna etkisinin değerlendirilmesi c) nanoliflerin ve nanopartiküllerin moleküler, morfolojik ve elemental karakterizasyonu d) nanoliflerin kümelenme davranışı ve stabilitesinin dinamik ışık saçılımı ve spektroskopik yöntemlerle yorumlanması e) uçucu gaz algılama özellikleri için balık numuneleri üzerinde karamürver, kalay dioksit, altın nanopartikülleri içeren nanoliflerin pratik uygulanabilirliğini göstermiştir. Böylece bu tez çalışması, et ürünlerinde aktif ve akıllı ambalajlama işlevleri için antimikrobiyal nanoaltın, bitki ekstreleri, kalay dioksit ve altın nanotozu gibi materyallerle entegre edilmiş nanoliflerin antimikrobiyal ve/veya akıllı nanosistemlerin geliştirilmesine rehberlik edecektir.

1. INTRODUCTION

1.1 Purpose of Thesis

Preservation of the quality and safety of food from producer to consumer are important concerns in the food industry. Consumers should know whether the food they are about to consume or prepare is healthy and safe. Therefore, there is an increasing demand for traceability in the food chain and pressure to develop novel traceability systems. Fish is a common source of protein within human nutrition, but it is also a rich source of nutrients for bacteria. Spoilage processes inside fish occur fastly with the creation of volatiles caused by microbial growth, autolysis of muscles, and degradation of proteins. Microbial production of volatile amines increases TVBN concentration which affects the quality of fish meat. Therefore, in the preservation of seafood, various conventional methods such as cold preservation, freezing preservation, processes such as salting technology, drying technology, or different packaging methods have been widely used (Speranza et al, 2021). However, there is a need to find alternative methods to avoid quality loss also prediction of seafood freshness in a fast and simple way. This reason leads to interest in real-time indicators for seafood quality control and new approaches for shelf life extension.

In recent years, nanotechnological applications have been implemented as promising approaches for active and intelligent packaging. Researchers have been focused on electrospraying and electrospinning methods to produce nanomaterials with various functions. When the solution concentration is high, the jet from the conical shape as the “Taylor cone” is stabilized. As the jet is driven towards the collector, the unevenly distributed charges cause the whipping or bending motion of the jet. So, with the elongation of jet fiber is deposited on the collector. If the solution concentration is low, the jet is destabilized due to varicose instability and hence fine droplets are formed. Biopolymer-based nanofibers are one of the example of these nanostructures that can be produced by electrospinning of liquid solutions with functional antimicrobial or colorimetric agents for active and intelligent packaging. Therefore, in this dissertation study, electrospun nanofibers are explored for their potential

capability to increase or maintain the quality during the shelf life of fresh fish or function as a packaging layer for sensing fish meat quality.

Aim of the Chapter 2 was firstly to determine of shelf life of fish products by microbiological analysis and by rarely studied parameters such as electrical conductivity, dielectric properties, and particle size as preliminary experiments. In Chapters 3 and 4, some of these equipment were used on fresh fish products, feeding solutions, and produced nanofibers. Aim of the Chapter 3 was to evaluate the active packaging functions of integrated Au nanospheres on fresh fish. In Chapter 4, feed solution properties were determined to evaluate electrosppinability, fabricated nanofibers were characterized by FTIR to prove the integration of Au nanospheres. The translational diffusion coefficient, hydrodynamic radius, PDI, major axis and, zeta potential values in dispersed solvents were measured to define the mobility of the polymer in the suspension, aggregation behavior, size distribution of nanostructures, and stability, respectively. In Chapter 5, gelatin-based nanofiber samples were produced to evaluate the effect of BE extract, SnO_2 and gold nanopowders, on color-changing functions. Infrared spectrums, thermal behaviors, and color properties were examined to find specific favourable linkages between volatile gases and nanofibers.

1.2 Literature Review

1.2.1 Volatile fish spoilage compounds

Oxidation (chemical), enzymatic autolysis and microbial growth are three basic spoilage mechanisms in fish products. After capture, chemical and biological changes take place in dead fish due to the enzymatic breakdown of major fish molecules The digestive enzymes cause extensive autolysis that results in softening, rupture of the belly wall and drain out of the blood water. During storage peptides and amino acids can be produced as a result of the autolysis of fish muscle proteins, which leads to the spoilage of fish meat. Lipid oxidation is another major cause of deterioration and spoilage for fish species with high oil/fat content. Lipid oxidation may occur enzymatically or non-enzymatically. Microbial growth is a major cause of fish spoilage which produces amines, organic acids, sulfides, alcohols, aldehydes, and ketones (Ghaly et al, 2010).

Volatile compounds such as TMA, NH_3, and DMA are considered TVBN, produced because of the destructive activities of microorganisms. These compounds are considered as main microbial degradation metabolites since bacteria are responsible for the creation of volatiles via the metabolic breakdown of protein in fish. In this context, TVBN levels are quality indices for fish spoilage, that increase because of bacterial metabolism with the time of storage (Howgate, 2009). Amines, NH_3, and H_2S can be produced with the proteolytic microorganism's activity. TMAO is a small colorless, odorless amine oxide generated by gut microbial metabolism found in the tissue of aquatic products in high concentrations. TMAO serves as an important substrate in the anaerobic metabolism of bacteria. The source of DMA and TMA in fish is TMAO. Specific spoilage organisms reduce TMAO to TMA by enzymes. TMA, formed with microbial growth in the fish muscle, is considered one of the major metabolites responsible for spoilage upper 4 °C (Serdaroğlu and Deniz, 2001). DMA is produced by autolytic enzymes during frozen storage. Other important metabolites are biogenic amines such as histamine, cadaverine, and pyridine. Bacteria that can decarboxylate amino acids present in the fish muscle lead to the formation of biogenic amines. NH_3, a toxic gas produced by the metabolic breakdown of amino-acids and other compounds such as nucleotide catabolites, dimethlysulphide or esters of lower fatty acids can also occur during spoilage of fish (Adeyemo and Foyle, 2022). NH_3 is produced the first day after slaughter during the autolytic breakdown of adenosine monophosphate to inosine monophosphate. It is also produced together with TMA during the anaerobic reduction of TMAO by *Shewanella putrefaciens* (Heising et al, 2012). An incraese in NH_3 content may reflect the decomposition of muscle since it is formed with the decomposition of proteins into amino acids.

The amount of TMA and TVBN contained in fish varies depending on the season and the region where the fish are caught, species, muscle type and processing techniques. A seasonal differentiation of spoilage patterns is reported during storage of sea bass (*Dicentrarchus labrax*), sea bream (*Sparus aurata*) and hake (*Merluccius merluccius*) (Orban et al, 2011).

TVBN legal or subjected rejection value is indicated as 35 mg/100 g by the EC Directive 95/149 (EEC, 1995). This limit is stated as same according to Sensory Properties Of Fishery Products And Total Volatile Basic Nitrogen Limits Communique No: 2012/73 by Ministry of Agriculture and Forestry for *Salmo salar*,

Merlucciidae family, and *Gadidae* family (Ministry of Agriculture and Forestry, 2011). TMA limit values are recommended between 5 mg/100 g and 10 mg/100 g in different studies (Malle and Poumeyrol, 1989; Souza et al, 2010; Ceylan, Sengor, and Yilmaz, 2017a). In fresh fish NH_3 is present in muscle at an average concentration of between 7-10 mg NH_3-N/100 g. It has been stated that fish have begun to have a bad odor when their level reached to 20-30 mg/100g (Heising et al. 2012). According to the Turkish Food Codex Regulation on Microbiological Criteria Draft (Ministry of Agriculture and Forest Food Control Laboratory Directorate, 2022) the histamine levels should not exeed 200 mg/kg in 9 random samples for fresh chilled fish products. Pseudomonas, H_2S-producing bacteria such as *Shewanella putrefaciens*) and *Brochothrix thermosphacta* can be the dominant bacteria at the end of the storage period for filleted fish products (Kyrana and Lougovois, 2002). However, according to Turkish Food Codex Regulation no limits are specified for microorganisms except *E. coli O157, L. monocytogenes, Salmonella spp., V.cholera,* and *V. Parahaemolyticus,* which should not be detected in fresh fish. In the Turkish Food Codex TMA, DMA, and TMAB limit counts have also not been specified. TMAB critical limit value of 6 log CFU/g is often used to determine the shelf life for fish products (ICMSF, 1986). On the other hand, aerobic total viable count limit is assigned between 6-7 log CFU g^{-1} depending on studies (Sullivan et al, 2020). In Table 1.1. some of the results were given for the parameters.

Marine diseases are common in the ocean and can reduce seafood's economic value by decreasing meat quality, increasing the marginal costs of harvest and processing, and diminishing biological productivity (Lafferty et al, 2015). Marine fish culture is dominated by Atlantic salmon (*Salmo salar*) led by Norway. Other economically important marine fish are gilthead seabream (*Sparus aurata*), and seabass (*Dicentrarchus labrax*). A few infectious diseases caused by bacteria are responsible of important economic losses in cultured fish worldwide. *Vibriosis, Photobacteriosis, Flexibacteriosis, Pseudomonadiasis, Streptococcosis, Mycobacteriosis* are some of the infectious diseases caused by bacteria in marine fish (Toranzo et al, 2005). According to TUİK data, seafood production in Türkiye reached 785.811 tons (13.708.550.105 Turkish Lira) in 2020 with 421.411 farming and 364.400 fishing. From that 201.157 tonnes were exported and 85.269 tonnes were imported in 2020.

European Sea bass (*Dicentrarchus labrax*) is a widely valued fish specie that is one of the major farmed fish species in Türkiye (Günlü and Koyun, 2013).

Table 1.1 : Some microbiological and chemical changes of various fish samples during storage.

	NH_3 (mg/100 g)	**TMAB (log CFU/g)**	**TMA (mg/100 g)**	**TVBN (mg/100 g)**	**Reference**
Dicentrarchus labrax (European sea bass)	<10 to 29 at 4 °C in 9 days	2.62 to 7.14 at 7 °C in 7 days	0.253 to 1.515 in 7 days	18.10 to 28.56 at 4 °C in 8 days	Heising et al. (2012), Ceylan et al. (2016), Najafi et al. (2022)
Sparus aurata (Sea bream)	1.16 to 4.91 at 3.8 °C in 9 days	2.19 to 8.18 at 4 °C in 11 days	0.19 to 8.54 at 4 °C in 11 days	19.00 to 51.65 at 4 °C in 11 days	Ceylan (2017; Ceylan et al. 2017a)
Merluccius merluccius (European hake)	-	>7 at 4 °C in 10 days	0 to >15 at 6-8 °C in 10 days	>20.00 to >35 at 6-8 °C in 13 days	Å Nia Baixas-nogueras et al. (2002); Fernández-Saiz et al. (2013)

Sea bass farming is comprised the biggest portion of the market in farming with an annual production of around 148.907 metric tonnes (TUİK, 2021). Since sea bass is consumed domestically and also exported in large quantities, it is very important to extend its shelf life, which is normally quite limited when kept refrigerated. Trout (144.182 tonnes) and sea bream are other main species (109.749 tonnes) in the Türkiye farming industry (TUİK, 2021). Therefore, in Chapter 3 and 4 sea bass and sea bream samples were chosen to be analyzed. Gadoid fish represent an important percentage of overall fish consumption in European countries. Within this group, hake is in great demand by consumers and has a worldwide distribution. Hake is among the most important fish species consumed in Europe, with a consumption per capita of 1.00 kg in 2018, equivalent to a 4 % share of the product's total apparent consumption. The most typical species are the European hake (*Merluccius merluccius*), which accounted for 66% of EU landings, and the Argentine hake (*Merluccius hubbsi*), Cape hakes (*Merluccius capensis, M. paradoxus*) are also landed (Opara *et al.*, 2022; Teixeira & Mendes, 2022). European hake, is of the highest commercial value in Spain, being preferred over other species of the genus *Merluccius* and other gadoids (Rodríguez et al, 2004). Moroever, its habitat is midwater or at bottom, chiefly 100–300. Serdaroğlu and Deniz (2001) have stated that deep fish products produce more TMA than others which is important quality indicator. Therefore, the *Merluccius* genus may produce more volatiles during spoilage. For the abovementioned reasons in Chapter 5 European hake (*Merluccius Merluccius*) was chosen to be analyzed.

In recent years, many new approaches have been presented to extend and predict the shelf life of seafood products. Nonthermal technologies such as cold plasma technology can be used (Liao et al, 2018; Ucar et al, 2021) for this purpose. Some other rapid and non-destructive techniques such as hyperspectral-imaging (HSI), have also gained interest due to their unique potential to monitor food quality and safety (Moosavi-Nasab et al, 2021). In the next sections, nanotechnological applications on seafood products will be discussed.

1.2.2 Electrospinning

Nanofibers are defined as cylindrical structures that generally have less than 1 μ size and not have pored structure (Ceylan et al, 2017b; Feng et al, 2017). Electrospinning is a method to produce nanofibers under a high voltage. An electrospinning system consists mainly of a power supply, a syringe pump, and a collector. In electrospinning, an electric field is applied to a polymer solution that flows between the needle tip and the conductor, and the polymer droplet is distorted into a conical shape through the internal electrostatic repulsion and external coulombic force. When the electric field reaches a critical value the electrically charged jet of polymer is ejected from the tip of the Taylor cone and directed toward the collector. As the jet is driven towards the collector, the excess electrical charges cause the bending motion of the jet, then, nanofibers are deposited on the collector with rapid evaporation of solvent and elongation of the jet. Parameters such as applied voltage, distance, and feed rate, can affect nanofiber morphology and diameter (Okutan et al, 2014; Wen et al, 2017; Isik et al, 2018).

Nanofibers can be used as antimicrobial layers by the integration of food-bioactive compounds such as essential oils (Rezaei et al, 2019). In this respect, trial patterns are established especially for prolonging the shelf life of seafood products. Various biopolymers (chitosan, zein, cellulose), reinforced with probiotics, essential oils, and plant extracts have been carried out in recent years for the application of nanofibers on fish meat surfaces to improve their quality (Ceylan et al, 2018b, 2018a; Mendes and Chronakis, 2021; Rodrigues Arruda et al, 2022).

1.2.3 Nanotechnology for active and smart packaging

Traditional food packaging is turning towards active packaging by integrating nanoscience to produce food packaging materials with improved functionalities.

Nanotechnology is an emerging science of developing and generating materials at the nano-level (1–100 nm) by manipulation of matter at the atomic scale. Nanomaterial-based nanocoatings are more advantageous than conventional packaging materials in providing better preservation and quality maintenance of seafood and aquatic products (Dar et al, 2019; Ashfaq et al, 2022). Therefore, active packaging has been used in recent years to prevent food spoilage by extending the shelf life. Indeed, nanomaterials possess unique characteristics that prolong freshness during storage and preserve foods from pathogens by improving the antimicrobial properties of packaging materials. Nanomaterials are applied as an additive and can be incorporated directly into food packaging material or embedded into food contact material. Further, the incorporation of antimicrobials in biopolymers has attracted attention (Göksen et al, 2020, Göksen et al, 2021; Sameen et al, 2021). The basic mechanism behind these compound's antimicrobial action is the increase in permeability of microbial cell membranes. This causes the loss of cellular ingredients (Omerović et al, 2021). Nanofibers (Altay and Okutan, 2015), NPs (Yilmaz et al, 2021), and nanoemulsions (Uçar, 2020; Cetinkaya et al, 2021a) are the main examples of nanostructures. NPs are solid carriers with a size range of 1−1000 nm, which are in different forms (Rezaei et al, 2019). Nanospheres are NP structures that can be also used to absorb compounds at their surface (Ahmed et al, 2019). The main advantage of applying NPs in seafood is to provide antimicrobial stability for the inhibition of foodborne pathogens (Wei et al, 2018a). The production of NPs enriched with various bioactive substances. As in nanofibers, chitosan is one of the main material used alone or in combination with other materials in the production of NPs (Zarei et al, 2015). The wet chemical method is also an example of NPs production (Rajar et al, 2021). Studies suggested that such silver and gold can present a better performance, and larger surface area and higher affinity with bacteria cells could be effective for chemical and microbiological preservation of fish fillets for long and short them of storage (Ayofemi Olalekan Adeyeye and Joshua Ashaolu, 2021). Chitosan-based nanomaterials, fenolic compounds, essential oils (such as thymol, luteolin, and fennel), and plant extracts (saffron, citrus) can be used for antimicrobial or antioxidant functions in nanomaterials (Ceylan, 2017; Bi et al, 2021; Babapour et al, 2022; Najafi et al, 2022). Biopolymer-based nanofibers reinforced with these materials demonstrated a broad range of antibacterial activity against fish spoilage bacteria such as *Pseudomonas fluorescens, Aeromonas hydrophila/caviae, Listeria innocua* which make them

important candidates for active packaging functions (Iturriaga, Olabarrieta and de Marañón, 2012). Generation of reactive oxygen species, disturbing the cell membrane permeability and inhibiting the enzyme activity are some of the mechanisms during the interaction of active packaging materials with these pathogens (Pandey et al, 2022) . When all these studies evaluated together, coating the fillets with nanofibers enriched with antimicrobial NPs agents and active compounds can be used to slow down the microbial, chemical, and physical deteriorations by taking advantage of the larger contact area feature of these functionalized nanofibers.

The usual method for measuring the TVBN level in fish involves several complicated steps and titrations which take typically four hours for one analysis. Conventional techniques are based on microbiological, chemical, or physico-chemical methods such as high-performance liquid chromatography or liquid chromatography-mass spectroscopy. But these methods can be complicated, slow, and expensive. Intelligent packaging can overcome some of these disadvantages (Chen et al, 2017; Gaudin, 2017; Meral et al, 2022). In an intelligent packaging system, a material is added to the packaging that interacts with the packaging environment and monitors the condition (storage time, temperature, shelf life, etc.) of the packaged food products. In this sense, the consumer is informed about the spoilage condition of the food product (Forghani et al, 2021). A fish freshness indicator can be considered as part of intelligent packaging, that uses metabolites as "information" to monitor the status of fish freshness. A gas sensor, and a communication device to transmit alarm output to the consumer can be required for smart packaging systems. These systems are portable, require small sample, selective response towards various analytes, are highly sensitive, and have good specificity over the traditional methods (Chen et al, 2017; Gaudin, 2017). In recent years, electrospinning has been utilized as a novel approach to the development of intelligent packaging systems. When fiber's diameter reaches nanometer size, surface area increases. High surface area and porosity lead nanofiber surface functionalization with NPs. These properties make nanofibers potential candidates for smart packaging applications. Furthermore, the high surface area may enhance the reactivity of the material and may speed up adsorption. Therefore, the possibility to fill this nanomaterial with gas or volatile and biochemical species may open methods (Mercante et al, 2017). Table 1.2 shows some examples of the electrospun nanofibers and films based colorimetric materials for the detection of

analytes in seafood. Colorimetric methods are suitable and versatile, while the assays can be performed in real-time without any interference in gas molecules concentration. The chemical species employed as active layers in gas sensors exhibit characteristic absorption in the UV/visible regions of the electromagnetic spectrum. Using electrospun biopolymers having the ability to absorb/emit light, or the functionalization of the nanofibers with active optical nanosystems are some of the ways to obtain optical sensors (Rozemarie Manea and Bertea, 2019). Metal NPs such as Au and Ag have also revolutionized the field of the colorimetric sensor system. The potential capability of functionalized metal NPs as an active probe for fish fillets needs more investigation. Although the conventional techniques are suitable for the detection of some volatiles, expensive cost and long analysis time limit their wide scope application. In contrast to such methods, colorimetric techniques are much preferred based on their simple procedure, cheaper and rapid analysis. For this reason, NPs can be used to detection of target analytes with sensor functions. All studies show that active packaging and intelligent packaging are the important global packaging approaches in the food market and will be dominant in the next few years.

Table 1.2 : Colorimetric nanofibers for detection of NO_2, volatile amines and biogenic amines and some applications on seafood samples.

Target analyte	Sensor material	Equipment	Matrix	Reference
Volatile amines (NH_3, triethylamine, aniline, ethylenediamine)	PVP/ZnO NF	UV/Vis spectrophotometry	Salmon	Bagchi et al. (2017)
Biogenic amines (Spermidine, putrescine, cadaverine, tyramine, triethlyamine)	Cellulose acetate NF	Canon EOS 550D camera eequipped with UV filter, Flame-S VIS-NIR spectrometer	Shrimp	Yurova et al. (2018)
Ethylenediamine vapor, volatile amines	PVA/Ag NF	Surface enhanced raman spectroscopy/ UV–vis spectroscopy	Shrimp	Marega et al. (2015)
TVBN	Cellulose acetate/alizarin NF	Colorimetric array (pH)	Rainbow trout fish	Aghaei et al. (2018)
NO_2	PVP/SnO_2/ Ag-Au NF	surface plasma resonance UV/vis/NIR spectrometer	-	Peng et al. (2018)
NH_3	PCL/anthocyanins	A smartphone-based visualization device	Shrimp	Liu et al. (2022)

1.3 Hypothesis

The main hypothesis of this dissertation is that zein nanofibers can be used as active packaging layer with the integration of gold nanospheres and gelatin nanofibers can be developed with plant extract, SnO_2, and gold NPs to predict fish spoilage by visual changes such as color, thermal behaviors or spectral chemical variations as smart packaging layer. In this context, 1) fish spoilage can be evaluated by dielectric properties, electrical conductivity, and surface tension 2) electrospinnability can be affected by electrical conductivity or dielectric properties of solution 3) integration of metal ions on nanofibers can be proved by infrared spectrums 4) aggregation characteristics, major axis values of nanofibers can be calculated by DLS measurements 5) chemical interactions between spoilage compounds and nanofiber can be detected 6) effect of NPs on nanofiber stability and absorption of volatiles can be evaluated by measuring band area ratios, and band distances with the help of programmes in spectrums 7) thermal resistance of nanomaterial can be interpreted with TGA and DSC 8) absorbed gases may generate stronger color changes when metal NPs integrated.

2. MONITORING MICROBIAL QUALITY OF SMOKED FISH PRODUCTS AFTER THEIR PACKAGES BEING OPENED AND PHYSICAL PARAMETERS OF FRESH FISH PRODUCTS DURING STORAGE[1]

2.1 Abstract

Smoked fish products are among consumers' favorites recently. However, once unpackaged, the microbial growth of smoked fish may rapidly increase. In this study, the microbial growth of in two different smoked fish products that are preferred by Turkish consumers were monitored at 0., 12., 24., 36., and 60. hour (h) periods. Although the samples was stored at refrigerator conditions of (4±1ºC); TMAB, TPB and TYM growth in smoked fish samples rapidly increased. Therefore, it is advised that smoked Norway Salmon (NS) and smoked Black Sea Salmon (BS) samples must be opened and stored at refrigerator conditions and should not be consumed after 36h post unpacking. That is because after 36 hours TMAB growth reached 5.95 logs CFU/g and 5.49 log CFU/g for smoked BS and NS respectively. On the other hand, TPB counts of BS and NS were determined as 6.02 log CFU/g and 6.11 log CFU/g respectively. TYM count of BS samples reached above 5 log CFU/g within 36h. While the TYM count of NS samples was still lower than 5 log CFU/g after 36h. Moreover, it was observed that a particular smoke aroma was lost in the packages, and the colour of some sample (which one) parts turned green after 24 hours. Once all results were evaluated, both samples' output suggested smoked fish be consumed within 24h post unpack. The findings of this study indicate that to delay the microbial spoilage in the smoked fish samples; a more functional package with properties of retaining the smoke flavor during shelf life should be opted for. In addition, the use of smart and/or active packaging applications that indicate the deterioration or delay the deterioration process should also be investigated.

[1] This chapter is based on the papers "Çetinkaya, T., & Ceylan, Z. (2019). An Observation of Microbial Quality Changes of Two Different Smoked Fish Products Stored at Refrigerator After Their Packages Being Opened. European Journal of Science and Technology, (17), 982-988." and "Çetinkaya, T., Altay, F. & Ceylan, Z. (2021). Determination of Fish Meat Quality Changes by Fast and Novel Methods During Storage Period. *Journal of the Institute of Science and Technology, 11* (3), 2030-2040."

Quality changes of three different fish species (local salmon: YS, sea bream: Ç, sea bass: L) were investigated at the initial, 2nd, and 4th days through the use of a set of physical parameters rarely studied and investigated by the literature. In this regard, the electrical conductivity value (mS cm^{-1}) of the samples was increased between 9.52% and 104% depending on the samples and storage. Surface tension values decreased with the storage period. In sea bream samples, this value declined rapidly from 42.56 mN m^{-1} to 16.20 mN m^{-1} on the second day of storage ($p<0.05$). The ε″ increased in all samples depending on the analysis time period. According to the sensory evaluation results, while the sea bream and sea bass samples are considered non-consumable as of the second day, the ε″ of these samples increased from 419.72 to 491.07 and from 408.21 to 430.7, respectively. However, no significant results were obtained with particle size (PB) and PDI values. Commonly used pH analysis results have been found to confirm these changes as pH values increased with storage times. In this context, the results of the current study have shown that the quality of rapidly perishable products can be successfully demonstrated with multiple and fast innovative analysis techniques. Furthermore, this novel study presents itself as an oriented for the seafood industry.

2.2 Introduction

Fish has an important place in human nutrition due to its nutritive value. Although seafood is consumed less in Türkiye compared to developed countries, fish and fish-based processed products are mostly preferred by consumers above other aquatic products (Ceylan and Unal, 2019a). On the other hand, processing methods and food preservation methods are also extremely important for public health. A processing method that is not carried out under appropriate conditions, may adversely affect the quality of products even when well preserved (Durlu-Özkaya and Cömert, 2008). Fish is considered among the healthiest food due to its living environment. Moreover, looking at the literature, fish meat is among the foodstuffs compared with breast milk. But fish meat is among the perishable seafood products (Külcü, 2017). In addition, more rapid changes may occur in the microbial or chemical quality of fish meat during processing (Ceylan et al, 2017a; Meral, et al, 2019b).

During the application of smoked technology, and because of the contact of emerged compounds in the incense content with food, these compounds can provide an antimicrobial effect on the product as well as give it a unique flavor (Ertaş, 1998).

Fish sell in fresh form. It also sells in processed, frozen, canned, and smoked forms. Fish is given the smoked aroma through a hot\cold smoking process (Yurchenko and Mölder, 2005). According to Stołyhwo and Sikorski (2005), the production conditions and smoke concentration in the smoked process may have a positive effect on human health as well as extend the shelf life of the product (Ertaş, 1998).

Smoked fish consumption in Türkiye is less than in other European countries (Ceylan and Ünal Şengör, 2015). However, it's consumption is increasing constantly as consumers have tried smoked fish. On the other hand, when buying smoked products, consumers pay attention to the expiry date on the label and observed that fish spoils faster than meat, microbial growth in it can increase rapidly from the moment it leaves the cold storage at 4 ºC.

Deterioration of fish may show itself in terms of color, consistency, odor, and taste which may affect the quality of the fish later than eliminate the possibility of its consumption afterwards. In general, deterioration in fish can be manifested by autolysis, oxidation, bacterial deterioration, and the combined activity of these factors (Küçüköner and Küçüköner, 1990; İnal, 1992). Bacteria belonging to the genus of *Bacillus, Clostridium, Escherichia, Flavobacterium, Micrococus,* and some yeasts in fish has been determined in fish products (Göktan, 1990). It has been indicated that *Enterobacteriaceae*, *Micrococcus*, *Lactobacillus*, *Vibrio*, *Coryneform* and *Streptococcus* bacteria can also be found in some fish originating from Norway (Ringø and Strøm, 1994). In addition to the studies mentioned above, many spoilage parameters in the fish meat are associated with microbial spoilage (Masette and Magnússon, 1999; Getu and Misganaw, 2015). In addition to the above-mentioned studies, many spoilage parameters in fish meat were associated with microbial spoilage. In addition, food-borne poisoning rates are at a level that cannot be ignored. For this reason, it is important to inform the consumers by revealing the microbial changes in commonly consumed products.

The quality and shelf life of food materials and their products are important for both the manufacturer and the consumer. For this purpose, especially microbiological

analysis methods such as TMAB are widely used. In addition, the sensory analysis also has an important place in the scientific field. It can even be associated with changes in microbial developments and changes in sensory characteristics (color, smell, texture, etc.) in most cases and studies (Bendini et al, 2007; Özogul et al, 2016; Ozogul et al, 2017). Moreover, chemical and physicochemical analyses such as TVBN or pH are also widely used to determine the quality of fish products (Ceylan et al, 2017b). Some physical analyzes such as texture and color are also used to determine the quality of fish meat (Ceylan and Meral, 2018). Moreover, depending on the type or species of most fish, limit values are also defined for both chemical and microbial analyzes. For example, there are available values such as 6-7 log CFU g^{-1} for TMAB or 30-35 mg/100g for TVBN. In sensory analysis, although there are different methods, in evaluations out of 10 or 9, in many studies, 5 and 4 points are accepted as limit values, respectively (ICMSF, 1992; Fan et al, 2009; Chotimarkorn, 2014; Ceylan et al, 2017b, Ceylan et al, 2018).

Fish meat can spoil more rapidly compared to butchery meat, due to reasons such as weak connective tissue, high water content, and softer internal organs (Külcü, 2017). To delay this spoilage, samples should be iced especially immediately after harvesting or fishing (Nair, 2002). Samples should also be kept in cold storage immediately after this process. Only after that, the products can also be shipped to factories for processing under their purpose. At this point, the products offered for sale as fresh can be kept in cold storage, and the products to be stored for long periods can be subjected to processes such as irradiation technology, sous vide, and modified atmosphere packaging (Gerdes and Santos Valdez, 1991; Díaz, Garrido and Bañón, 2011; Ceylan and Özoğul, 2019). Thus, the shelf life of the products can be extended in general to 4 days, depending on the storage and processing method 6 months or even up to a year. The above-mentioned analyzes are currently being performed to determine the changes that occur during storage and the shelf life. However, these methods are not efficient in terms of both time and cost. Especially in recent years, when the interest in the methods with a high benefit-cost relationship in fish meat preservation (nanotechnological) has increased (Ceylan, 2019), several methods are widely applied to examine changes in quality (Çetinkaya and Ceylan, 2020). For this purpose, depending on the changes in quality, changes in electrical conductivity value, differences in surface tension, dielectric loss factor, zeta potential, PB and PDI values

will be used in the food industry. According to Güzel and Bahçeci (2020); the electrical conductivity value can also be related to the protein concentration of the product. Surface tension is based on the principle of increasing the material surface by 1 cm^2 as a result of the force applied to a unit length. Surface tension is also known as surface-free energy (Tyson and Miller, 1977). At this point, Aydar and Bağdatlıoğlu (2014) stated that there is a relationship between oils and surface tension. Components of food may play a role in determining these values. In addition, it has been stated that there may be a relationship between the dielectric properties of the food and its moisture content (Komarov et al, 2005).

Electrical interactions in food systems can affect many factors such as determining the shelf life of food, or color and rheological properties (Cano-Sarmiento et al, 2018). In this respect, the evaluation of PS or zeta potential also emerges as an innovative approach. For a mono-disperse polymer such as a protein, the PDI value is defined as 1. Therefore, the PDI value of the solution obtained during storage in a protein-rich material should also be examined.

The main purpose of this chapter is to examine the development of TMAB, TPB and TYM in the smoked *Salmo trutta labrax* and *Salmo salar* products at certain hourly intervals, after unpackaged and stored under controlled conditions (4±1ºC) and to determine the changes in quality of fresh fish samples by revealing the changes in the electrical conductivity, surface tension, dielectric loss factor, PS, and PDI values. These studies on monitoring of microbiological quality of smoked fish products could be helpful on evaluating microbiogical quality of fresh fish fillets in Chapter 3 and Chapter 4. Furthermore, the outcome of the second part of this chapter which was related to the monitoring of dielectric loss factor of fresh fish filltes will be used as evaluating parameter for fresh fish fillets in Chapter 3 and Chapter 4.

2.3 Materials and Methods

2.3.1 Materials

For microbiological analysis, Black Sea salmon (*Salmo trutta labrax*) that contains salt and wood smoke, and “cold” smoked Salmon fish meat (*Salmo salar*), consisting of salt and wood smoke obtained with oak tree aroma, were used (n=3). They were purchased from the section offered in the cold fridge at 4ºC in a supermarket.

For physicochemical analysis, local salmon (YS), sea bream (Ç) and sea bass (L) samples were obtained from an international company. The samples were brought to Istanbul Technical University, Department of Food Engineering under cold storage and immediately stored at 10±2 ºC.

2.3.2 Methods

2.3.2.1 Microbiological analysis

TMAB, TPB and TYM counts were performed. 1 mL sample was taken from the dilution prepared from 10^1 to 10^8, and transferred into sterile petri dishes, after pouring PCA medium and shaking, the petri dishes were left to cool. The TMAB number was determined by incubating the petri dishes at 0, 12, 24, 36 and 60 hours for in an incubator set at 35 ºC (Memmert, D-91126, Schwabach FRG, Germany). To determine the change in TPB, petri dishes were incubated for 10 days in at 7 ºC. TMAB and TPB analyzes were performed according to the method of Maturin and Peeler (1988) in FDA (Food and Drug Administration) bacteriological analytical handbook. For the TYM count, Dichloran Rose Bengal Agar was poured into the medium. Similarly, 0.1 mL of the dilutions prepared from 10^1 to 10^8 samples were placed into the sterile dishes by spreading plate method. The petri dishes were incubated at 23 ºC for 5 days (Halkman, 2005).

2.3.2.2 Physicochemical analysis

PS and PDI values were performed using Zetasizer Nano ZS. Measurements were carried out with a 4.0 mV He-Ne laser (633 nm) at 25 ºC ambient temperature. HANNA HI 221 model pH meter was used for pH analysis. 1 g of each sample was taken, and 10 mL of distilled water was added to it and homogenized with a Silent Crucher S homogenizer (Heidolph Instruments) at 75 000 rpm for about 50 seconds, then the measurement was carried out by immersing the probe in the solution. For dielectric loss factor analysis, 1 g of each sample was homogenized with 10 mL of distilled water. Then prop (Agilent 5070E) was immersed in the prepared solution and the results were obtained by using the Network Analyser device under the conditions of 100 kHz-3 GHz. The values at 30 MHz frequency were evaluated. 1 g sample was homogenized with 100 mL distilled water for electrical conductivity analysis, and the values of the samples were measured in millisiemens centimeter^{-1} (mS cm^{-1}) using the

WTW LF95 device. For surface tension analysis 1:100 (w:v) samples were individually diluted, and measurements were performed in units of milliNewton meter^{-1} (mN m^{-1}) at 25 ºC using a tensiometer and PT 11 Wilhelmy plate 20003232 and Platinum-Iridium probe. In sensory analysis, 9 points were defined as the highest score, and 4 points were defined as the limit value that the product considered as non-consumable by panelists (Ceylan et al, 2018).

2.3.2.3 Statistical anaylsis

The obtained microbiological data were subjected to an ANOVA test and the differences in the samples during cold storage were evaluated statistically. The statistical software program JMP (SAS Campus Drive, USA Version 14) was used to reveal the statistically significant difference between groups and between storage hours (0., 12., 24., 36., and 60. hours). The statistical significance difference between groups and storage hours was revealed by Student's t-Test, and this statistical significance difference was found at $p<0.05$. The data obtained from the rest of the analysis were subjected to One-Way one-way ANOVA analysis in the JMP (SAS Campus Drive, USA Version 14) statistical software program, and the statistical differences that occurred during the storage of the samples were revealed with the Duncan multiple comparison test at $p<0.05$ significance level.

2.4 Results and Discussion

2.4.1 Microbiological analyzes

TMAB, TPB, and TMK results of Norwey Salmon and Black Sea salmon samples and their statistical interpretation are presented in Tables 2.1 and 2.2.

The TMAB (0. hour) load of two different processed smoked products was 3.29 log CFU/g and 2.93 logs CFU/g for NS and BS samples, respectively. In the literature, it was stated that smoking can be demonstrated by bactericidal and/or bacteriostatic activity on food material (Kolsarıcı and Güven, 1998). In other words, the fish smoking process is a factor that is lethal to the bacteria that may be present in fish meat earlier, or at least prevents the increase in the number of mesophile and psychrophile bacteria.

Table 2.1 : TMAB, TPB, and TYM changes in *Salmo salar* sample.

Sample	0.	12.	24.	36.	60.
TMAB	3.29 ± 0.02^{D}	4.04 ± 0.37^{C}	4.40 ± 0.11^{C}	5.49 ± 0.16^{B}	7.57 ± 0.03^{A}
TPB	3.49 ± 0.06^{E}	4.82 ± 0.13^{D}	5.70 ± 0.10^{C}	6.11 ± 0.03^{B}	7.58 ± 0.16^{A}
TYM	2.20 ± 0.28^{D}	3.04 ± 0.37^{C}	3.98 ± 0.04^{B}	4.37 ± 0.52^{B}	5.80 ± 0.13^{A}

$^{A, B, C, D, E}$ define the difference in NS samples is statistically significant depending on the storage time ($p<0.05$).

Table 2.2 : TMAB, TPB, and TYM in Salmo trutto labrax sample.

Sample	0.	12.	24.	36.	60.
TMAB	2.93 ± 0.29^{C}	4.67 ± 0.47^{B}	5.65 ± 0.49^{A}	5.95 ± 0.03^{A}	6.11 ± 0.06^{A}
TPB	3.26 ± 0.06^{C}	3.62 ± 0.54^{C}	5.20 ± 0.01^{B}	6.02 ± 0.23^{C}	6.65 ± 0.25^{C}
TYM	2.52 ± 0.35^{C}	3.16 ± 0.08^{BC}	3.28 ± 0.39^{B}	5.45 ± 0.21^{A}	5.57 ± 0.04^{A}

$^{A, B, C, D, E}$ define the difference in BS samples is statistically significant depending on the storage time ($p<0.05$).

In previous studies, fresh fish samples (sea bream 3.78 log CFU/g: Ünal Şengör et al. 2018), sea bass (2.92 logs CFU/g: (Ceylan et al. 2017b)), rainbow trout (3.11 log CFU/g: Meral et al. 2019b)) TMAB load is equivalent logarithmically with the initial TMAB load of the smoked products used in our study, thus, demonstrates the bactericidal and/or bacteriostatic effect of smoke. (Kaba et al, 2012) mentioned that the smoking process applied to fish may be effective in reducing the TMAB load. However, this study has revealed that the effects of smoke do not prolong the shelf life of the product very much and that the effects disappear quickly with the opening of the product package by the consumer. In fact, it was found that this value increased to 4.04 log CFU/g in NS samples at the 12. hour of storage and this difference was also statistically significant compared to the result of the previous analysis hour ($p<0.05$). Similar results were observed in the TMAB number of BS samples, where the bacterial load increased from 2.93 log CFU/g to 4.76 log CFU/g at the end of 12 hours ($p<0.05$). At the 24. hour of cold storage, the TMAB count of NS samples was evaluated as 4.40 log CFU/g and no statistically significant difference was found between the groups compared to the 12. hour ($p> 0.05$). On the other hand, the TMAB number of BS samples increased rapidly to 5.65 log CFU/g, and the difference between the results of the previous hour and the analysis was found to be statistically significant ($p<0.05$). Furthermore, while there was no statistical difference between the values reached for the BS samples at the later hours of storage (36. and 60. hours), the TMAB number of CA samples reached 6.11 log CFU/g at 60 hours. Compared to CA samples, it was found that the TMAB development continued rapidly and the number of TMAB reached 7.57 log CFU/g at the 60^{th} hour of storage. In addition, the TMAB load of this

product was found to increase at every hour of cold storage, and this increase was statistically significant in the results obtained at each analysis hour ($p < 0.05$). Accordingly, it can be concluded that the difference in microbial loads of the two products stems from the products themselves. In addition, the wall thickness of the product can be correlated with microbial quality. In the literature, Agbodaze et al. (2006) reported that wall thickness may be related to microbial quality. As can also be seen from Figure 2.1, both products have been identified as invisible, especially at 36 hours of cold storage. In this context, the increase in the number of TMAB has particularly affected the product as in smell and color.

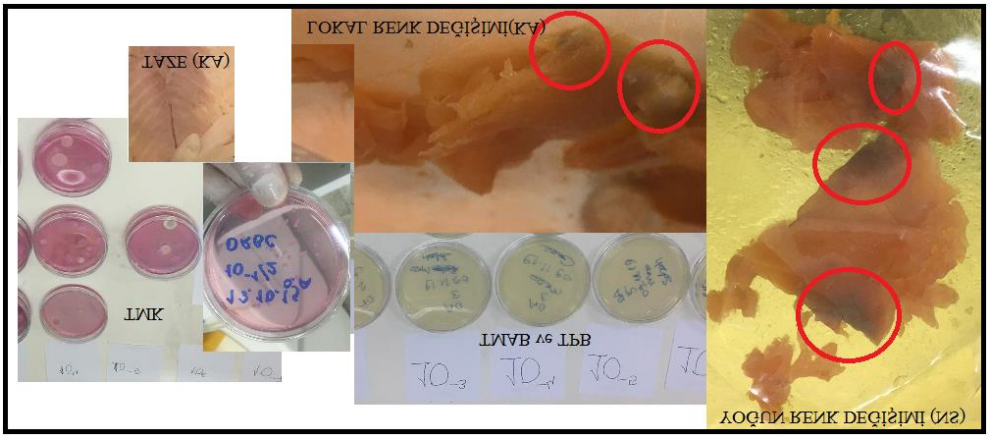

Figure 2.1 : Visual color changes in BS (middle) and NS (right) depending on microbial load.

Although ICMSF (1986) defined the number of mesophilic bacteria as 6 log CFU/g as the limit of the acceptability value after 36 hours when the fineness, color changes and odors of the products evaluated with a value of 5.95 log CFU/g in BS and 5.49 log CFU/g in NS. Therefore, it was concluded that after unpacking products can not be consumed. However, the rate of microbial increase for BS occurs particularly during 0 to 12 hours post unpacking, while the increase in microbial load at NS is relatively low (Figure 2.2).

The number of TPB in both products increased with storage time. According to Meral et al. (2019b), psychophilic bacteria which are responsible for the formation and deterioration of fishy odor can easily reproduce at cold storage temperature. In this context, when the results of the study were examined, the increase rate in the number of TPB of NS samples was statistically significant among all storage times ($p<0.05$). In particular, the rate of increase of the analysis results at the 24. hour of storage (5.70 log CFU/g) was found to be higher than other analysis periods when compared to the

initial hour (3.49 log CFU/g). Mesophilic bacterial load is lower in NS and BS samples compared to the initial psychophilic bacterial load. In other words, the TPB load is higher than TMAB. The reason for that could be the contamination of the raw material due to processing, sorting processes and sanitation conditions that cannot be performed under optimal conditions. Clark and Thatcher (1978) have also demonstrated that high psychophilic bacteria may occur in these cases.

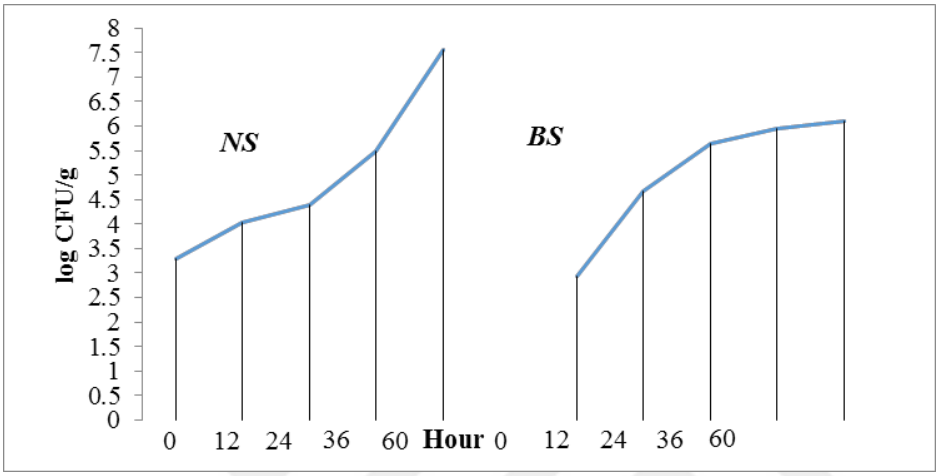

Figure 2.2 : Total mesophilic aerobic bacteria growth.

The increase in the number of psychrophilic bacteria in fish meat is also responsible for bad smell, bitter, ransit effects in meat (Jay, 2000). In this context as can be seen from Figure 2.3, the rate of increase in the number of TPB in BS samples is slower than NS samples. This may be related to the fact that the wall thickness of the product is higher than NS and the initial load is lower than NS samples. The results of the TPB study showed that, after opened and stored in the cold container, it is recommended that the consumer should consume products especially within the first 24 hours.

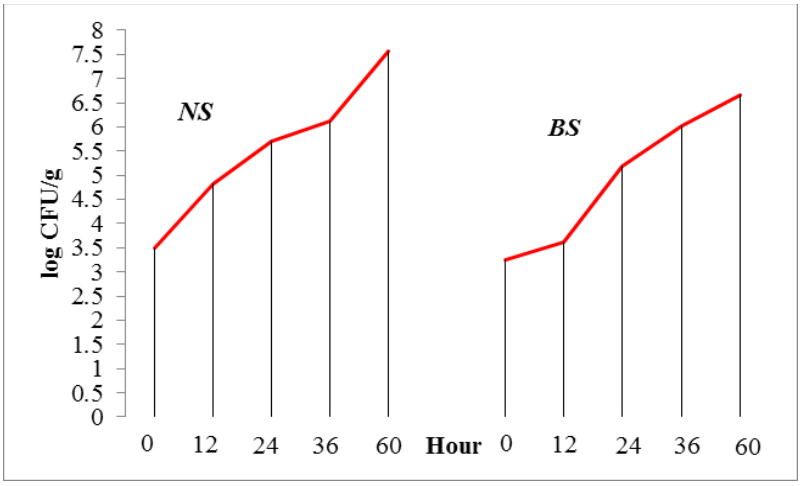

Figure 2.3 : Total psychrophilic bacteria growth.

Food and food materials are not sterile, so yeast and molds can be also found in foods up to 5 log CFU/g as stated by Stagnitta et al. (2006). When the results of the presented study were evaluated, TMAB and TPB count reached 7.57 and 7.58 log CFU/g and the TYM count was found to be 5.80 and 5.57 log CFU/g in the NS and BS groups, respectively, at the end of the 60^{th} hour.

Dutta et al. (2018) revealed that during the cold storage period the number of TYM in meat could increase smoked fish meat. In the same study, it was revealed that the consumption of smoked fish meat can cause significant health problems due to yeast-mold growth as well as bacterial growth, because of processes that are not carried out under fully controlled conditions. El-Lahamy et al. (2018) demonstrated that the smoked process can significantly reduce the yeast & mold content (from 2.30 log CFU/g to 1.0 log CFU/g) in addition to the already existing bacterial growth in fish meat. In this sense, in addition to the maximum number of TYM in NS and BS samples, the time zone with the highest rate of increase has been revealed by this study. As can be seen from these results and Figure 2.4, while a slower increase was detected in NS samples, a significant increase was observed in the KA samples especially between the 24th hour and 36th hour transition period of storage. In fact, this difference was found to be statistically significant ($p<0.05$). Furthermore, it is predicted that the amount of TYM in unpackaged samples that may vary depending on the differences in salt and smoke concentrations used in the products or how much the smoke can penetrate the meat. In this context, it has been demonstrated that the consumption of products, especially up to the 24th hour may be more appropriate to prevent the risk of YM that may transfer to the human body due to the consumption of an opened smoked fish product. Thus, reducing the potential health risks even more. From another point of view, in addition to the smoking methods introduced by (Ceylan, Unal Sengor & Yilmaz, 2018d), with the nano-encapsulated liquid smoke format, controlled release and the possibility of contacting the smoke with a larger surface on the fish meat were provided. Thus, as can be seen from the study results presented here, the effectiveness of the smoke disappears quickly after the package is opened. However, while the nano-encapsulated material can provide a longer lasting flavor to the consumer, it can also provide the opportunity to limit the development of TYM in the longer term.

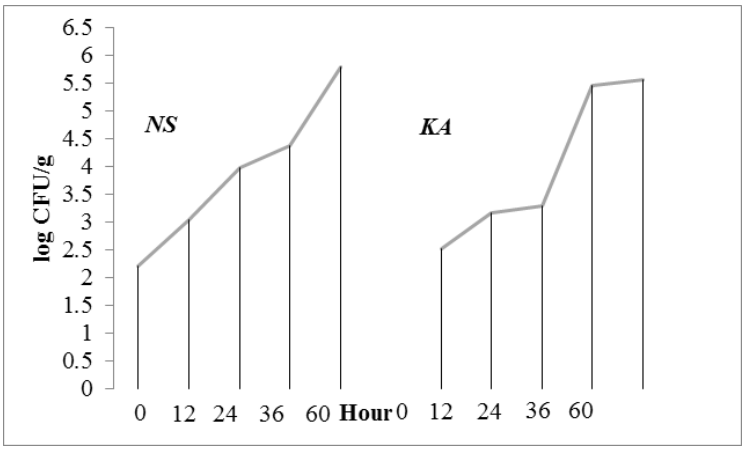

Figure 2.4 : Total yeast and mold growth.

2.4.2 Electrical conductivity

Electrical conductivity values are presented in Figure 2.5. The initial conductivity values of the YS, Ç, and K samples were found as 0.21±0.006, 0.24±0.0, 0.233±0.0 mS cm^{-1}. In parallel with the increase in storage period, the conductivity value of YS samples increased to 0.23±0.006 on the 2nd day (increase: 9.52%). Similarly, an increase was also detected for Ç (increase:16.66%; $p<0.05$) and L (increase:20.00%; $p<0.05$) samples values. When Ç and K samples are considered non-consumable on the 2nd day of storage in terms of sensory scores. The above-mentioned values can be accepted as the values to spoil product reach. However, on the 4th day of storage 48.57% increase was observed in YS samples compared to the 2nd day of storage ($p<0.05$). Foods are known to conduct electricity. Unlike metals, charge carriers in foods are ions rather than electrons. In normal applications, ions carry charges while the ion mass moves along the electric field.

The concentration and mobility of ions determine the electrical conductivity (Zhang, 2007). There may be several reasons for these differences in electrical conductivity values of the products. The first of these is the differences between the initial qualities of the products and the other can be considered as the nutritional composition of the products (Jha et al, 2011; Kaya and İçier, 2019). As it is known, changes/destructions may occur in the structure of fats as well as proteins with spoilage. It has been demonstrated in previous studies that there may be a relationship between conductivity value and protein content or percentage. Moroever, Souza et al. (2010) found that the conductivity value in meat samples increased over time. The reason for this has been described as the damage to the cell membranes over time and the increase in ion release

(Pliquett et al, 2003). These results show that the electrical conductivity value should be widely used in scientific studies and food sector in determining the quality.

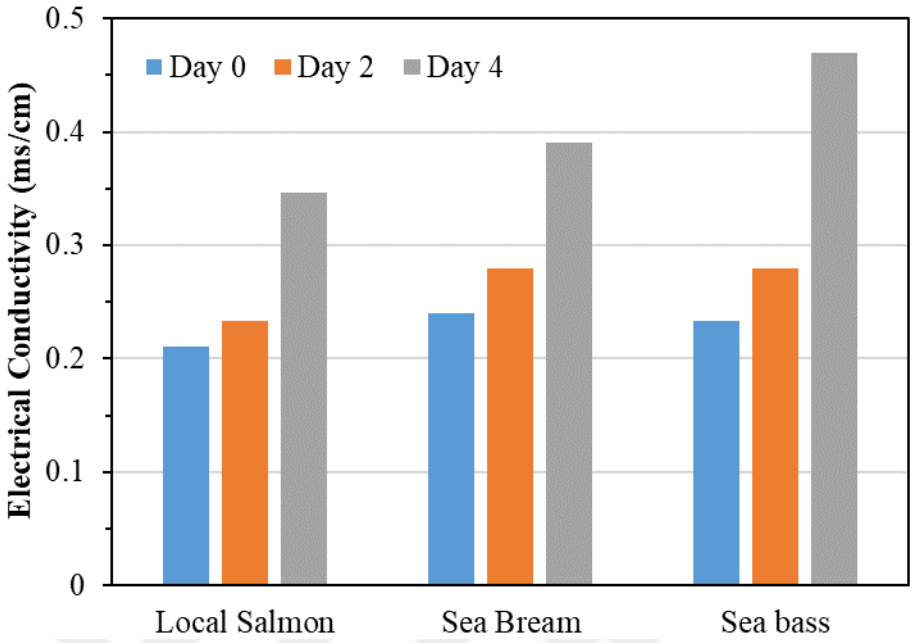

Figure 2.5 : Changing electrical conductivity values in YS, Ç and L samples depending on the storage days.

2.4.3 Surface tension

Surface tension values and changes are given in Fig. 2.6. Initial surface tension values of YS, Ç, and L meat samples were determined as 38.22, 42.56, 37.57 mN m^{-1}, respectively. Medina et al. (2009) defined the surface tension value as 60.64 mN m^{-1} in their study on the surface of Norwegian salmon. In addition, they stated that the adhesion property, has an important function in determining the surface tension.

At this point, Michalski et al. (1997) stated that on the adhesion value, structures such as the protein of fish meat and fat carbon hydroxides also play an important role on the adhesion mechanism of meat. As it is known, the increase in storage time significantly affects the quality of fish oils due to oxidation. Proteolithic activity, on the other hand, may cause the degradation of proteins in fish meat, which may also cause fish to deteriorate (Sriket, 2014; Zhang et al, 2019). Besides, adhesiveness value may vary depending on storage. Moreover, according to Dunnewind et al. (2004) it has been stated that there may be a relationship between adhesion value and sensory characteristics in foods. The interrelated scientific statements given above reveals that surface tension can be considered as an important quality parameter. The result of this study also confirms these chain quality parameters. Along with the changes in sensory

qualities, surface tension values decreased from 38.22 mN m^{-1} to 21.71 mN m^{-1} in YS samples. It was determined that the values of the Ç samples are decreased from 42.56 mN m^{-1} to 25.23 mN m^{-1} on the last day of storage, while the surface tension values of L samples decreased from 37.57 mN m^{-1} to 17.56 mN m^{-1}. As a result, it has been revealed that the surface tension analysis can be evaluated as an important and fast quality parameter in the analyzed fish samples.

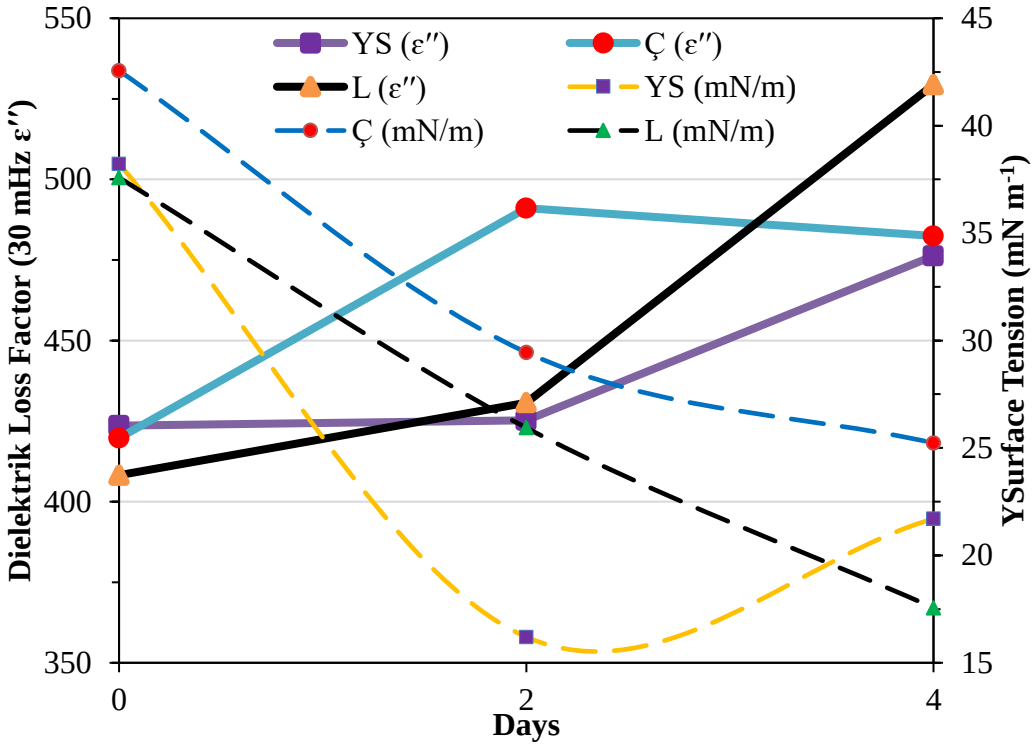

Figure 2.6 : Dielectric loss factor at 30 MHz frequency showing an increasing trend depending on storage days and surface tension values showing a decreasing trend in YS, Ç and L samples.

2.4.4 pH

Changes in pH values are presented in Table 2.3. With the conversion of glycogen to lactic acid, the pH value may decrease for a short time after hunting. However, depending on the increase in storage time, an increase in the pH value of fish meat can be observed and this value is associated with freshness (Abbas et al, 2008; Ceylan et al, 2018). In the presented study, the initial pH values of YS, Ç and L groups were determined as 6.38, 6.27, and 6.36, respectively. On the 2nd day of storage, the highest increase rates were found in L samples (5.34%), while the lowest increase was found in domestic salmon (1.25%) samples. On the last analysis day, while pH value was determined as 6.81 in Ç samples, L and YS samples were found to have lower values

compared to other groups. Kayim and Can (2010) determined the pH value of fishtail as 6.8 on the last analysis day in their study. They associated this increase in pH value with the increase of bacterial metabolites in the spoiled fish. In this study, although the rates were different, it was found that the pH values of YS, Ç and L samples increased depending on time.

Table 2.3 : pH changes in samples during storage periods.

Sample	Initial	2th Day	4th Day
Local Salmon	$6.38^{c} \pm 0.03$	$6.46^{b} \pm 0.03$	$6.51^{a} \pm 0.01$
Sea Bream	$6.27^{c} \pm 0.02$	$6.51^{b} \pm 0.02$	$6.81^{a} \pm 0.02$
Sea Bass	$6.36^{c} \pm 0.01$	$6.70^{b} \pm 0.03$	$6.76^{a} \pm 0.01$

a, b, c letters indicate the statistical difference between analysis days. ($p<0.05$)

2.4.5 Dielectric loss factor

The ε″ describes the ability to radiate energy in response to an applied electric field or various polarization mechanism. Thus, energy absorption is affected, and heat is usually appeared Sosa-Morales et al. (2010). Water content is one of the main factors affecting the dielectric properties of foods, in other words, their low or high ε″ (Tıraş et al, 2019). The three different food products examined in the study are seafood, and it is known that the moisture content of seafood is higher than most foods. ε″ results for Y, Ç and L samples are given in Figure 2.6. The initial ε″ values of the analyzed samples were found between 423.59 and 408.21. Due to the increase in storage, while the dielectric loss factor increased from 423.59 to 476.27 in YS samples, this change was defined 12.4% as a percentage. Moreover, it was determined that this rate of increase was (29.68%) higher in sea bass samples. During shelf life, moisture losses may occur in samples. This situation may have been related to the increase in dielectric loss factor values. Water can be removed from the food automatically during its shelf-life period, and it can also be removed from the food through treatment by heat. Another expression of this situation can bee seen in a study by Cao et al. (2019). The ε″ value of fish surimi gels increased from 29.61 to 42.50 at different temperatures (from 20 ºC to 90 ºC). Microwave treatment (heat treatment) performed in this study caused the removal of water and the ε″ value increased by a great rate of approximately 43.53%. In our study, it was found that the ε″ factor value increased depending on the deterioration. In fact, the percentage difference between fresh and stale products has reached up to 29.68%. In this context, L samples gave the most active result for this method in the rapid detection of deterioration in the presented study.

2.4.6 Particle size and polydispersity index

PS and PDI changes for the samples were also examined (Table 2.4). There was no significant relationship between PS values. Similarly, although the PDI values of the samples varied between a maximum of 1 and a minimum of 0.5, a value change related to deterioration was not detected.

Table 2.4 : Particle size and polydispersity index changes during storage period.

Sample	Initial	2th Day	4th Day
	PB (dnm)/PDI	PB (dnm)/PDI	PB (dnm)/PDI
Local Salmon	4814^{c} / 1^{a}	7951^{b} / 1^{a}	11136^{a} / 0.5^{b}
Sea Bream	7091^{a} / 0.8^{b}	7173^{a} / 1^{a}	2696^{b} / 1^{a}
Sea Bass	1223^{b} / 1^{a}	980.8^{c} / 0.78^{b}	4291^{a} / 1^{a}

$^{a, b, c}$ letters indicate the statistical difference between analysis days (p<0.05).

2.4.7 Sensory analysis

Sensory analysis interpretations and results are given in Table 2.5. All products have been stored within the range of 10 ± 2 ºC. The initial quality of the products (YS, Ç and L) was defined as 9 points out of 10 points (p>0.05). The initial quality of the raw material plays a key role in the degradation rate (Huss, 1994). Depending on the storage temperature being kept higher than 4 ºC, on 2nd day of storage, sensory scores of YS samples were decreased to the mean general acceptability value of 4.5 (p<0.05), while samples C and L were <4 points received (p>0.05).

Table 2.5 : Sensory scores and observations during storage periods.

Sample	Initial	2nd Day	4th Day
Local Salmon Scores	9^{a}	4.5^{b}	1.5^{c}
Observations	Vivid color	Water/oil release, medium odor, softening, soggy, discoloration	Insects on sample
Sea Bream Scores	9^{a}	2^{b}	0.75^{b}
Observations	Tough structure, vibrant color	Very heavy odor, water release, deterioration in structure, completely dull eyes, distinct color change	Redness of the eyes
Sea Bass Scores	9^{a}	1^{b}	0.55^{b}
Observations	Tough structure, vibrant color	Much heavier odor, water release, deterioration in structure, eyes completely dull, artificial appearance, significant color change	Redness of the eyes

According to these results, YS samples were below the sensory acceptability value, while the other two samples are considered non-consumable as of the 2nd day. Some of the most important criteria determining the sensory quality or differences in fish and products derived from fish are defined as fish species and natural flora in meat (Berik and Kahraman, 2010). Quality changes occurring in the rapidly deteriorating product were identified by fast methods (dielectric properties, electrical conductivity, etc.).

2.5 Conclusion

Despite the low consumption of fishery products in Türkiye, it is known that the interest in processed fish products has increased in recent years. In this context, smoked products are also widely preferred. Sometimes the consumer eats some part of the product and puts the rest of the opened product in the refrigerator for later consumption. In this context, it is unaware how and how much microbial development occurs in the product. In addition, the visual changes seen depending on the sensory analysis days are shown in Figure 2.7, Figure 2.8, and Figure 2.9.

Figure 2.7 : Visual photographs of local salmon samples on day 0, 2, and 4.

In this study, the microbial change of smoked fish products being sold in gross markets was monitored at 0., 12., 24., 36, and 60. hours. As a result, the TMAB development of NS samples increased especially at the 36th hour of storage compared to hour 0. TPB growth at the 24th hour and the increase in the number of TYM almost doubled the initial load logarithmically at the 36th hour of cold storage. In BS samples, TMAB

development nearly doubled compared to the initial load at 36 hours. The TPB growth and TYM growth more than doubled compared to the initial load, especially at 36 hours of storage. Once all results were evaluated, it was concluded that both samples should not be consumed after the 36th hour.

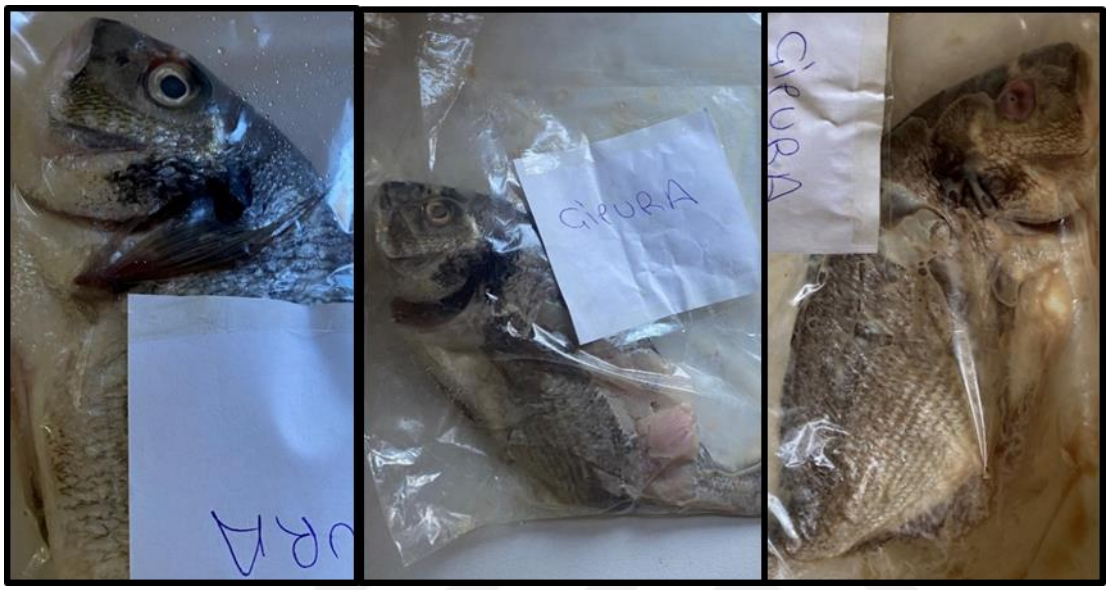

Figure 2.8 : Visual photographs of sea bream samples on day 0, 2, and 4.

It is recommended that the best consumption time is within the first 24 hours after opening the package. In addition, after this time interval, the smoked product aroma vanishes quickly from the product and the product has already lost its properties.

Commonly used pH analysis results have been found to confirm these changes as pH values increased by increasing storage times. The pH, electrical conductivity, and dielectric loss factor values in the meat samples of the L, Ç, and YS samples increased depending on the storage time. However, the surface tension values of the samples decreased. Sensory losses were observed in the study, and changes were determined in accordance with the above-mentioned analyzes. With this study, it was found extremely important to examine food materials such as fish, which are valuable in terms of nutritional content but can experience rapid quality losses.

Figure 2.9 : Visual photographs of sea bass samples on day 0, day 2, and day 4.

3. ZEIN NANOFIBERS CONTAINING Au NANOSPHERES AS ACTIVE COATING LAYER USED FOR FRESH FISH (*DICENTRARCHUS LABRAX*)[2]

3.1 Abstract

The development of Au-zein-based nanofibers (AuZ-Nm) was successfully carried out by using the electrospinning method. The average diameters of Au were found as 161 ± 45 nm within zein nanofibers (530 ± 377 nm). The nanofibers were used to delay the TMAB growth in the skinless fish fillets stored at 4 ± 1 °C. Besides control samples, dielectric values (ε′ and ε″) of the skinless fish fillets treated with AuZ-Nm were revealed. During the 8-day-storage, sensory changes in the samples treated with AuZ-Nm were determined. The microbiological test demonstrated that the use of AuZ-Nm limited the TMAB growth up to ~1 log CFU/g ($p<0.05$). ε′ values of the fish samples treated with AuZ-Nm (changes from 76.47 to 54.29) were more stable as compared to untreated fish samples ($p<0.05$). The changes in ε″ for control and nanotreated samples were 86.94% and 77.92%. The overall acceptability of the nanotreated samples was higher than the control samples. The stability of dielectric properties, limitation of microbiological spoilage, and also delaying of sensory deterioration of the fish fillets could be provided by using AuZ-Nm. In this context, the use of Au-zein-based nanomats in the present study with the results could play a guiding role for further seafood applications.

[2] This chapter is based on paper "Çetinkaya, T., Ceylan, Z., Meral, R., Kılıçer, A., & Altay, F. (2021). A novel strategy for Au in food science: Nanoformulation in dielectric, sensory properties, and microbiological quality of fish meat. Food Bioscience, 41, 101024."

3.2 Introduction

Food preservation methods have been used for a long time to provide longer shelf life for food materials. Especially, for highly perishable seafoods, the limitation of rapid microbiological growth like TMAB growth is a crucial issue for consumer health and providing food safety in the food industry (Ceylan, 2019). For this aim, food additives, different food packaging applications, and irradiation technology in the seafood industry are widely used (Arvanitoyannis and Tsarouhas, 2010; Bouletis et al, 2017; Olatunde and Benjakul, 2018; Gokoglu, 2019). The preservation steps are very important for fish and seafood due to their highly perishable natures. Fish has weak connective tissue and higher water content (Kiessling et al, 2006; Silva et al, 2008; Ceylan et al, 2020), so these properties could make it highly perishable. So, the above-mentioned preservation methods are a kind of necessity for fish preservation. Moroever, to reveal the quality changes in foods, some analyses (TMAB growth and TMA etc.) giving results in a larger period are widely used. However, rapid detection methods are gaining much more importance recently. In this sense, the dielectric properties of foods giving rapid results and comments related to food spoilage should be searched for especially highly perishable foods (Sosa-Morales et al, 2010). In this sense, dielectric constant and dielectric loss factor values can be adapted in order to reveal the quality changes in foods. The dielectric properties of cereal grains and oilseeds, bakery products, dairy products, poultry products, fruits, and vegetables were reviewed. Furthermore, dielectric properties can reveal the quality changes of fats and oils during the processing, and storage periods (Bogale Teseme and Weldemichael Weldeselassie, 2020). The dielectric properties of foods are related to moisture content, storage period, and temperature, which can be highly important for fish and fish products.

In terms of food preservation and rapid detection of quality changes of foods, novel approaches are gaining much more importance, so researchers are applying or integrating some new systems in order to delay the rapid spoilage of food products. In this sense, it has been seen that nanotechnology application has an effective role in delaying microbiological spoilage, chemical deterioration, and physical and sensory deterioration in foods. Particularly, different kinds of (bio)polymers, bioactive materials (thyme, curcumin, and carvacrol so on), bacteriocin (nisin), probiotic bacteria (*L. rhamnosus* and *L. reuteri*, etc.) were used in order to fabricate

nanomaterials that would be able to provide food safety (Ceylan et al, 2017a; Ceylan et al, 2019; Meral et al, 2019; Yilmaz et al, 2019). Besides food safety, the obtaining of nano-functional foods and how to use the nanomaterials for essential amino acids (Ceylan et al, 2017a) and fatty acids (Ozogul et al, 2017a; Uçar, 2020) in foods has been recently studied. Nanofibers, nanoparticles, nanoemulsions, nanocapsules, or nanoencapsulated materials that provide a larger contact area on the surface of the food were successfully used to provide seafood safety and seafood quality (Ceylan *et al.*, 2018c; Yazgan, Ozogul & Kuley, 2019; Cetinkaya *et al.*, 2021b). In order to produce nanofibers, different methods could be used but one of the most effective methods is defined as electrospinning which provides a process utilized to produce nano-scale materials with average diameters to nanometer range using a high-voltage power supply unit (Park, 2011). As could be seen from the mentioned studies, nanotreatment, and nanocoating applications have been effectively used. Recently, the use of alternative materials in nanotechnology defines an important issue. Ag NPs are widely used in different kinds of food and packaging applications (Carbone et al, 2016; Gallocchio et al, 2016). In addition to Ag, Au NPs in different dimensions and shapes possess antibacterial properties against both Gram-positive and Gram-negative bacteria. Furthermore, Au known as a valuable mine, can interact with bacteria and overcome the resistance mechanisms of bacteria (Zheng et al, 2017; Borzenkov et al, 2020; Okkeh et al, 2021). In this regard, it can be evaluated for seafood products.

The main objectives of the present study were three-folds. First, it was to effectively fabricate electrospun zein nanofibers containing Au and to characterize their morphology. The second was to delay the microbiological spoilage of fresh sea bass fillets by applying electrospun zein nanofibers containing Au onto them as an active packaging layer. The third was to monitor the dielectric and sensory properties of control and nanocoated fish fillets during eight days of storage at 4 °C.

3.3 Material and Method

3.3.1 Material

The graphical abstract of the present study is summarized in Figure 3.1. Zein from maize, molecular weight (Mw) ≃22–24 kDa, was obtained from Sigma-Aldrich Inc. Gold (Au) Nanospheres, (NanoXact, 0.05 mg/mL) was obtained from nanoComposix. Technical ethanol (96%) was provided by Aven Chemical. Throughout all

experiments, distilled water was used. Fish samples (*Dicentrarchus labrax*) were purchased from an international supermarket.

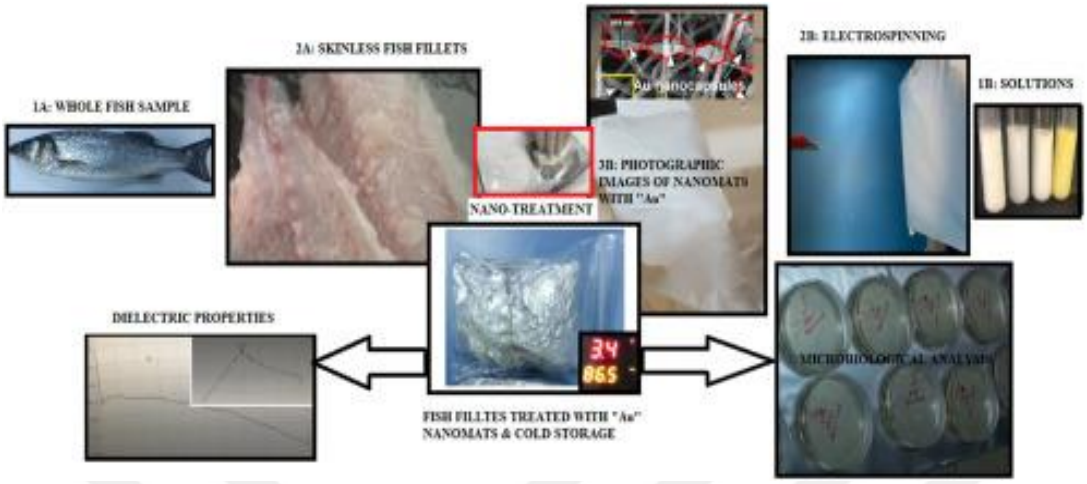

Figure 3.1 : Application of zein nanofibers containing Au as active packaging layer. (Based on paper; Çetinkaya, T., Ceylan, Z., Meral, R., Kılıçer, A., & Altay, F. (2021). A novel strategy for Au in food science: Nanoformulation in dielectric, sensory properties, and microbiological quality of fish meat. Food Bioscience, 41, 101024).

3.3.2 Method

3.3.2.1 Electrospinning process

Ethanol/water (80/20 v/v) solution was used for dissolving zein at a concentration of 30% w/v. 2 mL ethanol solution, 0.5 mL liquid gold nanospheres, and 0.75 g zein powder were mixed and then obtained feed solution was blended for 20 min at 600 rpm using a magnetic stirrer. The electrospinning unit basically consisted of a syringe pump unit, an external high-voltage supply, and a spinneret (18 G needle). The feed rate was 0.8 mL/h and the distance from the spinneret to the collector plate was 15 cm and the applied voltage was 20 kV.

3.3.2.2 SEM

Morphologies of electrospun nanomats were examined under low vacuum in a field emission scanning electron microscope SEM at different magnifications with a working distance of 8 mm. An accelerating voltage of 5 kV was determined for obtaining secondary electron images (Ceylan et al, 2018b). The average diameters of electrospun nanostructures were obtained by using 50 different measurements (n = 50).

3.3.2.3 Application of electrospun nanomats onto fish samples and their storage

The given methodology below related to nanotreatment of fish fillets was applied as stated by Ceylan (2019). Whole fish samples with high quality were filleted and then the skin of the filleted samples was removed. Skinless fish fillets were treated and wrapped with electrospun nanomats with Au. The samples were stored at (4 ± 1 °C) cold storage conditions. Fish samples treated with Au-nanomats and untreated fish samples were analyzed for each analysis period (1, 2, 3, 4, 7, and 8^{th} days).

3.3.2.4 Microbiological analysis

TMAB count was determined as stated by the (FDA, 2001). For each treatment, 10 g of the sample was homogenized for 2 min in a stomacher with 90 mL peptone water obtained from 0.1% peptone from meat. Serial dilutions from 10^1 to 10^7 were prepared. Diluted samples were placed on PCA and then incubated at 35 °C for 48 h (n = 12).

3.3.2.5 Measurements of dielectric properties

1 g of each sample was homogenized with10 mL of distilled water for 50 s with a homogenizer (Silent Crucher S) at 75 000 rpm. The ε′ and ε″ of samples were determined by using a Network Analyzer (Agilent Technologies) equipped with a probe (Agilent 507E) at 3 GHz frequency and room temperature (n = 10).

3.3.2.6 Sensory evaluation

Sensory quality changes were assessed by ten panelists who had experience with fish quality. Sensory evaluation was applied in a wellventilated room and the samples were presented on the white ground with random code. The panelists separately assessed samples from each other on the 1, 2, 3, 4, 7, and 8^{th} days of the cold storage period. The color, texture, and odor properties of the samples (C: Control and fish samples treated with AuZ-Nm), were defined by panelists. 5 out of 10 points were accepted as the limit value for the rejection (Ceylan et al, 2018a).

3.3.2.7 Statistical analysis

Collected data were subjected to analysis of variance (ANOVA) to detect the growth of TMAB, sensory quality, ε′, and ε″ changes of fish fillets treated with AuZ-Nm and untreated samples for the experimental period. GraphPad Prism software was utilized to reveal significant differences between groups. Once a significant ($p<0.05$) main

effect was obtained, the mean values of the samples were further analyzed using Tukey's multiple-range comparison test.

3.4 Results and Discussion

3.4.1 Morphology of electrospun nanomats

SEM images of the AuZ-Nm are presented in Figure 3.2. SEM images defined morphology and average diameters of the materials indicate the efficiency of the electrospinning process, especially for the microencapsulation and nanotechnology studies as stated by (Torres-Giner et al, 2008; Ceylan et al, 2017c) . The obtained images showed the formation of beadless electrospun zein nanomats with Au.

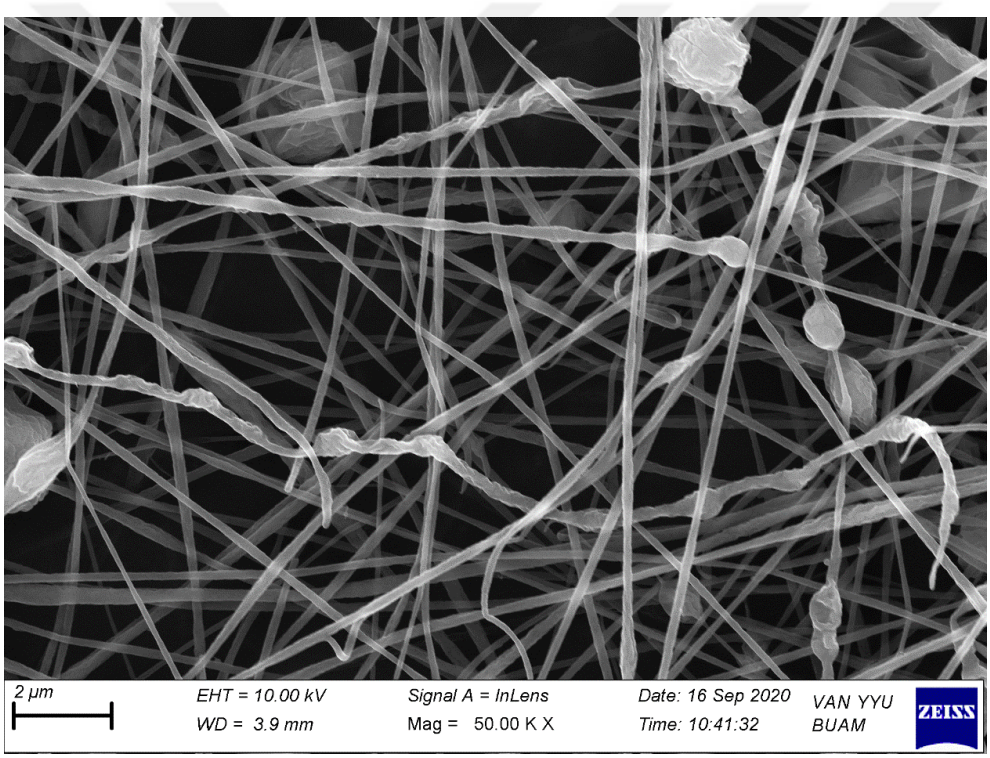

Figure 3.2 : SEM images of integrated Au within zein nanomats.

In the present study, the average diameter of integrated Au was defined as 530 ± 377 nm within zein nanomats having 161 ± 45 nm. Au nanostructures within electrospun zein were successfully observed in the SEM images. The use of different materials in nanotechnology applications may occur with different morphological structures. For instance, while the average diameter of nisin and curcumin nanofibers was determined 128.98 nm, poly(e-caprolactone)-based nanofibers had a 130-nm diameter (da Silva et al, 2015). Moroever, big diameters such as 330 nm or 640 nm were reported depending

on the use of material types such as chitin, chitosan, and PLGA (Jayakumar et al, 2009; Mehrasa et al, 2015; Ranjbar-Mohammadi et al, 2016; Ceylan et al, 2020b). Another study revealed that the molecular weight of the material could play an important role to obtain smaller size nanomaterials having different properties (Schiffman and Schauer, 2007). In the current, the integration of Au integration within zein provided an antimicrobial activity on the growth of TMAB in fish fillets during cold storage conditions.

3.4.2 Microbiological analysis

The results of TMAB growth coated with nanofibers and uncoated fish fillet samples are presented in Table 4.1. The raw material TMAB load of fish fillets was defined as 3.70 ± 0.07 log CFU/g. The initial TMAB load of fish meat samples depends on fish species, processing conditions, contamination, environmental factor, and slaughter method. Oğuzhan and Angiş (2012) stated that the TMAB count of fish raw material was 3.12 log CFU/g while that of different fish species was determined as 4 log CFU/g (Taşkaya et al, 2017). Sea bass fillets treated with electrospun nanofibers containing Au had the same TMAB count with the initial value of the samples on the first analysis day of the experimental period at 4±1 °C. Similarly, nanocoating such as nanofibers could decrease the initial TMAB load of fish meat samples (Ceylan et al, 2018b).

In the current study, control group samples had a higher TMAB count (4.11 log CFU/g) than the group treated with electrospun mats with Au, during the initial period. On the 2nd day of storage, fish fillets treated with electrospun mats had the lowest TMAB count (3.88 log CFU/g) which is statistically significant (p<0.05). The differences between the groups were defined as 19.07%. On the 3rd day of the experimental period, similar differences in percentages (21.64%: 4.89 to 4.02 log CFU/g) were obtained between the two groups. The difference between the two groups on the 4th day was found as 0.79 log CFU/g. With the increase in storage period, the TMAB load of control group samples was more rapidly increased as compared to the fillets treated with AuZ-Nm. In addition, at the end of the storage period, the TMAB counts of the group treated with electrospun mats with Au and control group samples were determined as 6.14 CFU/g and 7.06 CFU/g, respectively (p<0.05). The treatment of electrospun mats with Au presented better preservation in terms of microbiological stability as compared with control group samples. Saleh et al. (2016) revealed that in

terms of the elimination of fish disease outbreaks, nano Au and Ag had antimicrobial properties.Thirumurugan et al. (2013) reported, the antibacterial activity of nisin was successfully increased with the use of Au NPs. *Micrococcus luteus*, *E. coli*, *Bacillus cereus*, and *Staphylococcus aureus* (food spoilage microorganisms) were determined as the most sensitive bacteria samples against bacteriocin and Au NPs combinations. Besides given in vitro studies above, the antibacterial activity of Au NPs with different particle sizes in vitro was effectively checked by reporting the growth curves of *E. coli* and *S. aureus* (Zhu et al, 2020). Also, the treatment of fish fillets with nanoemulsion limited the growth of food-borne pathogens and spoilage bacteria (Ozogul et al, 2020). With the current study, the use of electrospun mats with Au delayed the rapid TMAB growth in fish meat stored at 4 °C.

The comparison of results from Chapter 2 (Table 2.1 and Table 2.2) for microbiological quality of smoked fish products with the results of microbiological quality of fresh fish fillets (Table 3.1) revealed that the process of smoking decreased the initial TMAB load. However, after open the package, the TMAB values of the smoked fish increased more (Chapter 2) compared to the values for fresh fish fillets (Chapter 3), suggesting that active packaging layer for the fish products may be helpful for keeping microbial stability during storage. Apparently, the Au loaded zein nanofiber mats as active packaging layer for fresh fish fillets (Table 3.1) provided lower TMAB values compared to the values of smoked fish products after their packaging being opened (Chapter 2, Table 2.1 and Table 2.2).

3.4.3 Dielectric properties

The initial ε′ value was 76.47 for fresh fish. Basaran et al. (2010) revealed that the ε′ of salmon muscle was 77.61 at 20 °C and 27 MHz. In the same study, the ε′ of trout muscle was found to be 83.64 (at 20 °C and 27 MHz). The differences between the two species were probably due to the fat content found in fish flesh. Because it is known that high-fat content gives a lower dielectric constant due to the hydrophobicity of fat molecules (Li et al, 2019). Similarly, our results were consistent with the results conducted by Basaran et al. (2010). On the 1st day of storage, ε′ value was determined as 71.16 for sample C, it was found to be 76.40 for the sample treated with electrospun mats with Au, which is close to the initial ε′ value of fish. ε′ values for samples C and Au fluctuated during storage. While the ε′ values of both samples decreased until the

8th day of storage, they increased again on the last day of storage (Table 3.1). The loss of water during storage affecting the dielectric properties of food might be decreased the ε′. It is stated the moisture content is a main dominant factor in the values of ε′ because the dielectric constant of water is about 80. Due to the presence of dipole moments that cause polarization, the ε′ of water is high at 25 °C (80) (Krishnaswamy and Orsat, 2015). It was determined that there were statistically significant differences between groups during the storage period ($p<0.05$). ANOVA results revealed that on the 1st, 2nd, and 4th days of storage, nano-application had a significant effect ($p<0.05$) on the ε′. However, no significant differences between the groups were found on the 3rd, 7th, and 8th days of storage. Although the ε′ value gradually decreased until the 8th day of storage and it was increased again on the 8th day of storage, the decline was lower in the Au nanomats samples and the decrease in the initial ε′ value was less in the samples treated with Au nanomats. On the 1st day of storage, the change in the initial value of ε′ was 6.48% for sample C, and 0.10% for sample Au nanomats. On the 7th day of storage, a 34.53% decline was recorded for the control group according to the initial ε′ value, while this decrease was less than 30% in the samples treated with Au nanomats. As can be seen from the results, it was determined that the two samples showed similar behavior. However, the ε′ of the samples treated with Au nanomats remained more stable than the control group. It is due to the presence of Au in the electrospun mats. Krishnaswamy and Orsat (2015) demonstrated that the dielectric properties of Au NPs were similar to the dielectric properties of water. They stated that the ε′ for AuNP ranged between 78.71 and 40.41 and between 80.77 and 36.99 for water (200 MHz-20 GHz).

The initial ε″ value was 11.64 for the fresh sample. From Table 3.1, it could be seen that the ε″ values of the two groups decreased until the 7th day of storage, at the 7th and 8th days of the storage period, the ε″ values of fish samples were again increased. The ε″ for control samples ranged from 10.38 to 1.52 and ε″ for samples treated with Au nanomats ranged from 11.34 to 2.57.

Table 3.1 : TMAB and dielectric properties of control and fish samples treated with Au nanomats.

Microbial and dielectric properties	Initial	Sample	Storage Days					
			1st	2nd	3rd	4th	7th	8th
TMAB	3.70±0.07	C	4.11±0.00^{aC}	4.62±0.04^{aC}	4.89±0.57^{aBC}	4.94±0.04^{aBC}	5.70±0.00^{aB}	7.06±0.13^{aA}
		Au	3.70±0.15^{aC}	3.88±0.02^{bC}	4.02±0.02^{aC}	4.15±0.04^{bC}	4.86±0.06^{bB}	6.14±0.02^{bA}
ε’	76.47±1.94	C	70.28±1.50^{bA}	71.51±0.43^{bA}	70.02±0.39^{aA}	53.94±1.03^{bB}	50.07±2.60^{aB}	75.19±0.59^{aA}
		Au	76.40±0.38^{aA}	76.39±0.45^{aA}	72.97±3.86^{aA}	59.68±0.07^{aB}	54.29±0.41^{aB}	73.07±0.91^{aA}
ε’’	11.64±0.12	C	10.38±0.01^{bA}	8.66±0.43^{bA}	8.44±2.83^{aA}	1.52±0.22^{bB}	6.92±1.20^{bA}	8.49±0.33^{bA}
		Au	11.34±0.24^{aA}	10.85±0.43^{aA}	10.16±1.17^{aA}	2.57±0.93^{aB}	9.06±0.84^{aA}	10.95±0.05^{aA}

$^{a-b}$ Within each column, different superscript lowercase letters show differences between treatment groups for same storage day ($p<0.05$). $^{A–C}$ Within each row, different superscript uppercase letters show differences between the storage days within same analysis group ($p<0.05$). C: Control (Fillets uncoated); Au: samples treated with zein nanomat containing Au.

On the 8th day of storage when the fish fillets were accepted as unfit for consumption, the ε″ was determined to be 8.9 for the control group and 9.06 for the Au nanomats samples. In Chapter 2, it was reported that ε″ values taken at 30 MHz increased with storage. It appears that dielectric factors may vary with frequency, and type of fish and fish composisitin depending on caught season.

The ε″ is defined as a measure of a molecule's polarizability and electrical energy storage ability. ε″ is a term related to the energy absorption and propagation of electromagnetic energy from a field (Bircan and Barringer, 2002). Many factors affect the dielectric properties of a substance. Water and salt are the most important food components affecting the dielectric properties of food products (Isik et al, 2018). A change in the molecular structure of the substance may result in a change in its dielectric properties. It is also reported that the physical state of the food affects its dielectric properties. There are several studies revealing that the ε′ and ε″ changes as a result of the heating of gluten proteins-starch mixtures, denaturation of whey proteins, and gelatinization of starch (Bircan and Barringer, 2002). In the current study, the results showed that ε′ and ε″ values of fish samples firstly decreased probably due to the decrease in water content during storage. It is known free and bound water influences the dielectric properties and then ε′ and ε″ begin to increase. Changes in dielectric properties could be attributed to microbial deterioration. Because dielectric measurements have been used as a quality indicator in fish samples because it indicates the rate of deterioration (Zhuang et al, 2007). Lougovois et al. (2003) found a positive correlation between sensory flavor scores reflecting the measure of fish freshness and dielectric properties. As shown in Table 3.1, the TMAB load of fish fillets increased during storage. It is known that the integrity of the muscle tissue is disrupted by microbial deterioration. In addition, proteolytic enzymes degrade proteins. The degradation of collagen causes tissue changes in the muscle. It is suggested that meat tenderization is a result of the disintegration of collagen fiber because of enzymatic degradation and lactic acid produced during post-mortem anaerobic glycolysis (Masniyom, 2011). In the current study, the increases in the ε′ and ε″ were probably caused by the charged free amino acids resulting from the degradation of proteins (Fernandes, 2016) and also disruption of tissue integrity caused by microbial deterioration (Meral et al, 2019; Ceylan et al, 2020b). Although fluctuations in the ε′ and ε″ occurred during storage, these changes were lower in the samples treated with

Au nanomats. As a result, for further studies, it can be claimed that fish fillets treated with Au nanomats will have a lower microbial load and can be heated more easily during microwave heating.

3.4.4 Sensory evaluation

Table 3.2 shows the sensory changes for the samples. In this sense, being observed that the changes in microbiological quality and dielectric loss factor of fish samples had a good relationship with the sensory deterioration in the all samples. Furthermore, while sensory score (from 10 to 5: acceptable limit value) declined at the same time TMAB growth in control group samples was increased, especially, ε″ in C samples continuously decreased. On the other hand, higher ε″ values as compared to C samples were obtained in the fish samples treated with Au nanomats. Furthermore, by an increase in storage period, fishy-odor in control group samples was more rapidly determined while the nanotreated samples had a better sensory quality ($p<0.05$). Nanotechnology applications in fish processing are used for providing stronger color and aroma (Sharma and Ahmad, 2013). In addition, nanostructures such as nanoemulsions, nanoparticles, and nanofibers can be utilized to limit rapid sensory deterioration (Chellaram et al, 2014; Ozogul et al, 2017b). For instance, nanoemulsions based on essential oils suppressed the fishy odor and provided a positive effect on the sensory quality of rainbow trout samples stored at 4 °C (Durmus et al, 2019). Moroever, sea bass fillets treated with commercial oils such as sunflower, canola, corn, olive, soybean, and hazelnut, had better sensory quality (Özogul et al, 2016). In another study, skin brightness and slime, flesh-texture, odor, and also the color of the untreated sample were found to be higher than those of sea bass samples treated with nanoemulsions (Yazgan *et al.*, 2017). With the current study, sensory deterioration in fish fillet samples treated with Au nanomats was successfully limited. Therefore, especially, costly seafood like caviar could be preserved by using Au nanomats instead of chemical-based food additives. In terms of sensory quality, this may be a guiding role for further studies regarding seafood products.

Table 3.2 : Sensory evaluation of control and fish samples treated with Au nanomats.

Paremeter	Initial	Sample	Storage Days					
			1st	2nd	3rd	4th	7th	8th
Color	9.78±0.33	C	9.62±0.19^{aA}	9.10±0.16^{aB}	8.48±0.63^{aC}	7.54±0.35^{aD}	2.66±0.38^{aE}	1.90±0.23^{aE}
		Au	9.74±0.09^{aA}	9.48±0.28^{bA}	9.08±0.23^{bA}	8.36±0.36^{bB}	6.66±0.92^{bC}	4.30±0.37^{bD}
Texture	9.72 ± 0.42	C	8.98±0.33^{aA}	8.18±0.31^{aB}	6.20±0.41^{aC}	5.56±0.81^{aC}	3.80±0.60^{aD}	1.98±0.63^{aE}
		Au	9.32±0.25^{aA}	8.56±0.36^{bB}	7.80±0.32^{bC}	6.96±0.59^{bD}	6.20±0.52^{bD}	4.52±0.28^{bE}
Odor	9.70 ± 0.46	C	9.62±0.11^{aA}	9.22±0.13^{aB}	8.50±0.44^{aC}	6.18±0.28^{aD}	3.50±0.27^{aE}	2.00±0.35^{aF}
		Au	9.64±0.22^{aA}	9.40±0.16^{aA}	8.84±0.09^{aB}	7.56±0.59^{bC}	6.38±0.33^{bD}	4.06±0.58^{bE}
Overall Score	9.58.0.27	C	9.22±0.42^{Aa}	8.46±0.19^{aB}	7.22±0.16^{aC}	6.26±0.15^{aD}	4.48±0.2^{aE}	2.92±0.23^{aF}
		Au	9.44±0.18^{aA}	9.30±0.16^{bA}	8.9±0.25^{bA}	8.44±0.23^{bB}	6.74±0.71^{bC}	4.12±0.98^{bD}

a-bWithin each column, different superscript lowercase letters show differences between treatment groups for same storage day (p<0.05). A−C Within each row, different superscript uppercase letters show differences between the storage days within same analysis group (p<0.05). C: Control (Fillets uncoated); Au: samples treated with zein nanomat containing.

3.5 Conclusion

Au-zein-based nanomats were successfully fabricated by using the electrospinning method. TMAB results revealed that the use of 530- nm-Au nanomaterial within zein nanomats having 161 nm average diameters was effective in order to limit the growth of TMABc (~1 log CFU/g) in the fish fillets. Being revealed that the stability of dielectric properties (change in ε″: 86.94% and 77.92%), which can change depending on the increase in the storage period, could be provided by using Au-zein-based nanomats. Also, the rapid changes (up to 50%) in the sensory characteristics of control group samples were reported. Above all, the current study clearly revealed that Au-zein-based nanomats could be covered in seafood materials stored at cold storage conditions.

4. ZEIN NANOFIBERS CONTAINING Au NANOSPHERES AS ACTIVE COATING LAYER USED FOR FRESH FISH (*SPARUS AURATA*)[3]

4.1 Abstract

The fabrication, deep characterization, and nanocoating effect of zein nanofibers produced with Au nanospheres were studied. Zein solution containing ethanol:liquid gold nanospheres (80:20 v/v) was prepared to produce biopolymer based nanofibers. ε′, ε″, and loss tangent (ε″/ε′) values of the feeding solution were evaluated at 300 and 3000 MHz, and the electrical conductivity of the solution was determined (808.67 ± 2.082 μs/cm). A smooth structure of the Au-zein nanofibers was collected by SEM. DLS measurements (translational diffusion coefficient, hydrodynamic radii, PDI, major axis) and zeta potential were done by dispersing nanofibers in ethanol or water. The stability of nanofibers dispersed in ethanol was higher (+41.73 mV) compared to that of dispersed in water (+5.1 mV). Chemical characterization by FTIR approved the molecular interaction of the zein-Au through a N-Au coordination bond and electrostatic interactions. The Au-zein nanofibers nanocoating in fresh sea bream fillets reduced 17.8% of TMAB compared to the uncoated group ($p<0.05$) after 8 days of observation. The highest changes in ε′ for uncoated (57.65%) and coated samples (14.84%) during storage showed the positive impact of nanofiber treatment. These results indicated that zein nanofibers with Au nanospheres could be potentially used as an antimicrobial layer for seafood products.

[3] This chapter is based on paper "Cetinkaya, T., Wijaya, W., Altay, F., & Ceylan, Z. (2022). Fabrication and characterization of zein nanofibers integrated with gold nanospheres. *LWT*, 155, 112976."

4.2 Introduction

The enrichment of food matrices with carotenoids, antioxidants, probiotics, bioactive and antimicrobial compounds have gained more interest in recent years. Spray-drying, spray-cooling, fluid-bed coating, extrusion, and emulsification followed by solvent evaporation are some of the example methods that are available for the encapsulation of these compounds within a wall material (García-Moreno et al, 2018; Wei et al, 2018; Mendes and Chronakis, 2019). Although spray drying is one of the most widely used techniques, it requires heating and the size of the encapsulates obtained in this process is large (10–100 μm). Emulsification-evaporation, emulsification followed by solvent evaporation, is another common method for preparing NPs <500 nm (Wei et al, 2018). Electrohydrodynamic methods such as electrospinning and electrospraying are emerging as alternative nanoencapsulation techniques, since they are cost-effective and functional nanofibers, nanocapsules, and NPs with very low size can be produced (García-Moreno et al, 2018; Mendes and Chronakis, 2019; Miguel et al, 2019). In this respect, nanotechnology applications related to the food industry and food science are becoming people's next-generation food applications. For example, nanofibers that integrated with curcumin (Meral et al, 2019) or nanoprobiotics (Ceylan et al, 2018a) successfully limited the microbial growth in fish meat and effectively improved the acceptability during cold storage. In the last decade, emulsification systems like nanoemulsions have been also utilized in order to inhibit pathogenic microorganisms, which could be host in fresh or processed fish fillets (Meral et al, 2019b). So, some coating treatments, could be called nanocoating (<1000 nm) as well, have been newly applied for fish meat products.

Biopolymer-based nanostructures have an important role in delaying microbiological spoilage, physical and chemical deterioration in seafood. Zein is non-toxic, widely available, and biocompatible plant protein and biodegradable polymer extracted from corn. So, more researchers have been attracted to investigate the functionalities of zein-based nanofibers (Turasan and Kokini, 2017; Aman Mohammadi et al, 2021; Ansarifar and Moradinezhad, 2021). In addition to nanofibers, zein-based NPs have been also employed to encapsulate bioactive ingredients such as antioxidants, ω-3 fatty acids, and carotenoids (García-Moreno et al, 2018; Wei et al, 2018, Wei et al, 2020). For example, the bioavailability of folic acid, vitamin D_3, curcumin, resveratrol, and beta-carotene can be improved using zein-based nanomaterials (Kasaai, 2018; Afonso et al,

2020; Silva et al, 2021). Green tea catechins have been also effectively encapsulated in zein NPs with a mean diameter of 157 nm by electrospraying. Bhushani et al. (2017) expressed that the encapsulated green tea catechins were more stable under in vitro gastrointestinal stability and easier to permeate when compared with controls. So, a similar concept can be applied to zein based nanofibers to improve the functionalities of nanomaterials.

The use of antimicrobial agents or NPs to enhance the physical, chemical, and antimicrobial properties of zein-based materials has received great interest in recent years (Moradkhannejhad et al, 2018; Aytac et al, 2020). In addition, zein can be used to encapsulate metallic NPs as they act both as reducing as well as capping agents and provide chemical stability (Mahendia et al, 2010). Zein-Au complex NPs have been proven to improve the mechanical, functionality, and degradability of Au NPs (Puthiyaveetil Yoosaf et al, 2019; Turasan et al, 2019).

A material's dielectric property is an important parameter to determine its molecular structure. A change in the dielectric properties of the material may be related to a change in molecular structure. A dielectric material (host material) containing filler particles with sizes of 10–100 nm in a well-dispersed state constitutes a nanodielectric system (Krishnaswamy and Orsat, 2015). Zein, is a dielectric material in which NPs can be dispersed. In this respect, zein solution with NPs can be considered a nanodielectric system. ε' is defined as material's ability to store electrical energy. ε'' is defined as an index of the energy dissipation characteristics (Icier and Baysal, 2004; Krishnaswamy and Orsat, 2015). The chemical composition of the material, water, salt contents and other minerals affects dielectric properties. Organic components make the sample dielectrically inert (Sosa-Morales et al, 2010). Generally, Au nanospheres are obtained by the reduction of Au salts by using reducing agents like PVP. Therefore, it can be important to know ε'' values of the feeding solution. Another dielectric value is the $\varepsilon''/\varepsilon'$, which is related to the material's ability to penetrate and dissipate electrical energy as heat (Krishnaswamy and Orsat, 2015).

During cold storage maintaining the quality of seafood products is important. It is clear that microbial growth of fish is related to the deterioration of chemicals in fish. So, chemical, physical, microbiological, or sensory analyzes can be conducted to predict fish deterioration. Since seafood is dielectrically active, knowledge of dielectric properties, is also essential for the investigation of fish quality (Nguyen, Ahmad &

Jayanath, 2020). Dielectric properties can be considered a fast and non-invasive way to monitor different parameters of seafood (Franceschelli et al, 2021). The dielectric properties of fish muscle may alter during storage as tissue components degrade over time. In this regard, changes in the dielectric properties of seafood products can also be used for the evaluation of their spoilage degree (Sant'Ana et al, 2011; Çetinkaya et al, 2021).

Pure Au is safe to eat and has been used as a food decoration in the food industry. Au (E175) is approved as a food additive in the European Union (Panyala et al, 2009; EFSA ANS Panel, 2016). In 2016, the EFSA Panel stated that no data on subchronic, chronic toxicity, or genotoxicity of elemental Au are available. In the same report it has been indicated that the daily mean intake of Au from the regular diet can be estimated to be in the range of 0.01 μg/kg bw/day to 0.02 μg/kg bw/day. Dietary exposure to the food additive and the regular diet would lead to a mean intake for children from 0.03 to 0.10 μg/kg bw/day. On average, dietary exposure from the food additive would represent around 30% of the total exposure (from both the food additive and the regular diet) (EFSA ANS Panel, 2016). In this respect, there is growing interest in the investigation of Au metal by nanotechnological applications due to its biocompatibility, ease of surface functionalization, and optical properties. Au particles can be synthesized in different dimensions and shapes such as nanoflowers (Penders et al, 2017), nanotubes (Liu et al, 2020), nanostars (Lin et al, 2021), nanocapsules (Singh et al, 2018), nanorods, nanocages, and nanospheres (Cobley et al, 2011). According to recent studies, Au in different morphologies showed antibacterial properties (Zheng et al, 2017; Borzenkov et al, 2020; Wang et al, 2020; Okkeh et al, 2021; Omerović et al, 2021). It has been stated that an increase in the membrane tension of bacterial cells was caused by the adsorption of Au NPs leading to mechanical deformation of the membrane, and eventually cell rupture and death (Linklater et al, 2020; Okkeh et al, 2021). Boatemaa et al. (2019) reported the detection and inhibition of *S. typhi* strains via Au NPs with a size of 40–60 nm. Although NPs within the size range of 80–100 nm are unable to freely translocate across the bacterial cell membrane, they still can inactivate bacteria (Okkeh et al, 2021). The ultra-small Au nanoclusters with a size smaller than 2 nm can easily traverse into the cell wall pores to kill bacteria (Zheng et al, 2021). Suganya et al. (2017) reported the antibacterial and antibiofilm potential of zein with Au NPs (50–80 nm along with

different shapes, such as nanospheres and nanoplates), by microtiter plate and agar well diffusion techniques. They have indicated that the presence of zein molecules enhances the binding capacity between Au NPs and outer membrane components of gram-positive (*B. pumilus* and *B. subtilis*) and gram negative (*S. sonnei* and *P. aeruginosa*) bacteria. In this way, Au NPs create electronic effects due to their size, and reduced surface area, then penetrate inside the bacteria to cause cell death.

These above-mentioned studies showed that Au NPs could be ideal materials to prevent microbial growth in seafood products. However, as stated before antibacterial mechanism action for Au depends on its size and bacterial strain to which they are applied. So, the integration of Au nanospheres with a size of 15 nm inside wall materials, could be an effective way to inhibit microbial spoilage in fish meat. The goal of the present study was to fabricate zein-Au nanofibers conjugate and to investigate its functionalities on sea bream fillets. Electrical conductivity and dielectric values (i.e. ε', ε'', $\varepsilon''/\varepsilon'$) of the zein-Au solution were investigated to evaluate the effect of incorporated Au nanosphere on its electrospinnability. Produced nanofibers were characterized by their zeta potential, hydrodynamic radii, PDI, molecular, and morphological properties. Finally, microbiological deterioration using specific parameters such as TMAB counts and dielectric changes on sea bream fillets was investigated to determine the coating effect of Au integrated zein nanofibers.

4.3 Material and Method

4.3.1 Material

Zein (purity of 98%), was purchased from Sigma-Aldrich Inc. Au nanospheres (15 nm, NanoXact, 0.05 mg/mL in water) coated with PVP were kindly received from NanoComposix Inc. PCA was purchased from Merck & Co., Inc. Technical ethanol (96%) was obtained from Aven Chemical. Distilled water was used throughout all experiments. Gilthead sea bream samples (*Sparus aurata*) were purchased from Metro market (Istanbul, Türkiye), filleted and deskinned.

4.3.2 Method

4.3.2.1 Feed solution properties

Ethanol-liquid Au nanosphere solution (80:20 v/v) was used for dissolving zein at a concentration of 30 g/100 mL. The mixture was blended for 30 min at 600 rpm using a stirrer to obtain a feed solution. The electrical conductivity of the solution was measured according to the methodology described by Dias Antunes et al. (2017). Measurement was done in triplicate with a unit of microsiemens/centimeter (μs/cm) using WTW LF95 electrical conductivity meter (Wissenschaftlich-Technische Werkstatten GmbH & Co.) at 22 °C. ε′, ε″ and loss tangent (tan δ = ε″/ε′) values of the solution were obtained as the methodology described by Krishnaswamy and Orsat (2015), using Network Analyzer instrument (Agilent Technologies) with Agilent 85070E Option 030 dielectric probe kit. Measurements were conducted in triplicate and were investigated at 300 MHz and 3000 MHz frequencies. Software graphs for ε′, ε″, ε″/ε′, and cole-cole values are also provided in Appendices (Figure A1, Figure A2, Figure A3, and Figure A4).

4.3.2.2 Electrospinning process

The electrospinning process was utilized with Inovenso NE100 (Istanbul, Türkiye) equipped with a syringe pump unit, and an external high-voltage supply (Nanofen, Ankara, Türkiye). The solution was electrospun at a 0.8 mL/h feed rate with an applied voltage of 6 kV and an 18 G needle was utilized. The distance between the aluminum foil covered on the collector and needle was arranged as 15 cm.

4.3.2.3 Structure of nanofibers

The morphology of zein nanofibers integrated with Au nanospheres was examined using FE-SEM under low vacuum with 50.000 times magnification with a working distance of 8 mm. An accelerating voltage of 10 kV was used for obtaining secondary electron images. The nanofiber diameter distribution was obtained by measuring 50 random nanofibers with the Image J program. Moroever, TEM images were presented in Appendices (Figure A5, Figure A6).

4.3.2.4 Zeta potential and dynamic light scattering measurements

The zeta potential and DLS measurements of zein nanofibers integrated with Au nanospheres were performed using Malvern Zetasizer Nano equipment. Distilled water or ethanol was used as a dispersant as performed by Dede and Altay (2021). Nanofibers were dispersed at 0.1 g/100 mL in ethanol using Silent Crusher S (Heidolph Instruments, GmbH & Co. KG) and in water by magnetic stirrer for 60 s and 180 s, respectively. Then, dispersions were filtrated through a Whatman® Schleicher & Schuell filter paper (Grade 595 ½, 90 mm diameter). The methodology of zeta potential and translational diffusion coefficient was modified from Okutan et al. (2014). Filtrated dispersions were analyzed using a scattering angle of 173°. Zeta potential analysis was done in disposable folded capillary cell DTS1070 (Malvern Panalytical Inc.). The hydrodynamic radius and PDI analyses were developed from the methodologies of Chen et al. (2021) and Saunders et al. (2015). Measurements were performed by dropping filtrated samples in disposable cuvettes.

4.3.2.5 FTIR spectroscopy

The infrared spectrum was obtained at a 4/cm resolution with IRAaffinity-1 FTIR spectrometer (Shimadzu Corp., Tokyo, Japan) equipped with single reflection ATR. Measurements were done by accumulating 10 scans. The nanofiber sample was measured in transmission mode and the measurement was recorded in the range of 600–4000/cm at room temperature.

4.3.2.6 Coating of fish fillets with nanofibers

After the production of nanofibers on aluminum foil, deskinned sea bream fish fillets were treated and coated by rubbing the samples to nanofibers according to the methodology described by Meral et al. (2019b). Thus, the zein nanofibers integrated with gold nanospheres were absorbed by the surface of the fish flesh. Control samples were not coated with nanofiber (untreated). Then, untreated and nanocoated samples were stored at 4 ± 1 °C and analyzed on initial, 1, 2, 3, 4, 7, and 8th days.

4.3.2.7 Microbiological analysis

TMAB count was determined according to FDA standard protocol (Maturin and Peeler, 2001). For each treatment, 10 g of the sample was homogenized for 2 min in a stomacher (IUL Instruments, Barcelona, Spain) with 90 mL peptone water obtained

from 0.1 g/100 mL peptone from meat. Serial dilutions from 10^1 to 10^7 were prepared. Diluted samples were placed on PCA and then incubated at 35 °C for 48 h (n = 12).

4.3.2.8 Dielectric properties of fish samples

Dielectric analyses of fish samples were performed from a methodology described by Çetinkaya et al. (2021). 10 mL of distilled water was added to 1 g of each sample, and the mixture was homogenized for 50 s with Silent Crusher S homogenizer at 75000 rpm. Network Analyzer (Agilent Technologies) with a 200 mm probe (Model/Part Number 85070-20037) used to determine ε′ and ε″ at 300 MHz and 3000 MHz frequencies, respectively.

4.3.2.9 Statistical analysis

Collected data was evaluated using IBM SPSS Statistics 28.0 (IBM Corp.) program to determine solution properties, the TMAB, ε′, and ε″ differences of nanocoated and uncoated group samples during the 8-day storage period. The mean values of the samples were then analyzed using Tukey's multiple range comparison tests, whereas a significant ($p<0.05$) the main effect was found.

4.4 Results and Discussion

4.4.1 Feed solution properties

The fabrication, characterization, and surface coating of zein nanofiber containing Au nanospheres is shown in graphical the abstract (Figure 4.1). The electrical conductivity, i.e. ε′, ε″, and ε″/ε′, of the feeding solution is given in Table 4.1. The electrical conductivity of the feed solution was found to be 808.67 ± 2.082 μS/cm. Wang et al. (2019) reported a higher electrical conductivity (1.43 ± 0.01 mS/cm) of zein (30 wt%) in water/ethanol (30/70 v/v). Liquid Au nanosphere in zein solution might decrease the solution's electrical conductivity, leading to a decrease in the number of soluble species with charge-carrying ability, likely because of the interaction of Au nanospheres with zein. The electrospinning process requires the transfer of electrical charge to the polymer droplet at the injection needle to the elongated fluid jet. The conductivity of the feed solution indicates the capacity of electrons to move in the solution. Therefore, electrical conductivity may influence the

electrospinnability of the feed solution (Okutan et al. 2014; le Corre-Bordes et al, 2018; Moradkhannejhad et al, 2018).

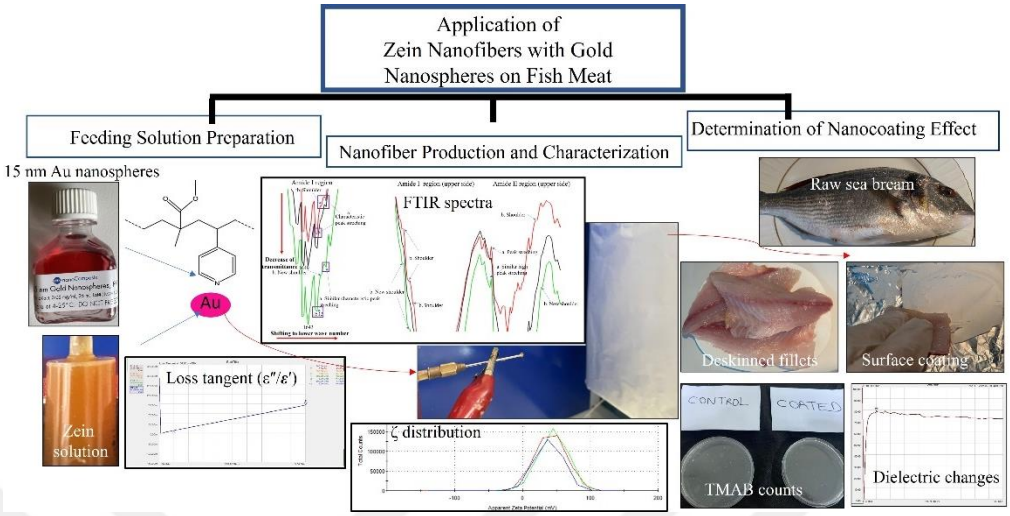

Figure 4.1 : Gold nanosphere loaded zein nanofiber application processes along with solution preparation, nanofiber characterization, and surface coating application. (Based on paper; Cetinkaya, T., Wijaya, W., Altay, F., & Ceylan, Z. (2022). Fabrication and characterization of zein nanofibers integrated with gold nanospheres. LWT, 155, 112976).

Electrical conductivity value can be evaluated as an essential parameter for the formation of bead-free fibers. A high conductivity (>10 mS/cm) of feeding solution may result in a necklace, beaded, nonuniform, ribbon-like and branched jet formation. For example, the soy protein isolate solution showed electrical conductivity of 13.06 ms/cm but did not form nanofibers due to instability in jet formation (Seethu et al, 2020; Aslaner et al, 2021). So, a low electrical conductivity is preferable for nanofiber formation since the feeding solution is subjected to weaker electrical forces (Moradkhannejhad et al, 2018). An increase in the conductivity of the solution could increase beading because of more stretching of the polymer jets, which tends to produce thinner nanofibers (Moradkhannejhad et al, 2018; Aslaner et al, 2021; Facchi et al, 2021). However, the 16% pullulan feed solution had a very low conductivity (0.06 mS/cm) that was not able to form desirable nanofibers (Seethu et al, 2020). These studies suggested that electrical conductivity depends on polymer concentration and type, affecting the nanofiber structure. In the current study, homogenized beadfree Au-zein nanofibers produced by the feeding solution that has an electrical conductivity of 808.67 ± 2.082 μS/cm.

The ε′, ε″, and ε″/ε′ of solutions may depend on factors such as water content, frequency, temperature, chemical composition, and the structure of the material (Icier and Baysal, 2004; Sosa-Morales et al, 2010; Samuel and Trabelsi, 2012). Moroever, the size and concentration of metal NPs remarkably affect the dielectric properties of polymer/metal materials (Zare and Shabani, 2016). In this regard, the dielectric properties of the feed solution influenced the structure and diameter of the nanofibers. Electrospinning of feed solution with higher ε′ would give a stronger jet split capability in the high electric field (Jørgensen et al, 2015; Mendes and Chronakis, 2019). Therefore, a feed solution with relatively high ε' can facilitate the formation of thin fibers (Facchi et al, 2021). Pure water shows a relatively high ε′ of 80.4 at 20 °C due to the presence of dipole moments. Thus, H+ and OH− bonds in water tends to polarize, with the influence of an applied electrical field. The ε′ for Au NPs by the Turkevich method ranges from 78.71 to 40.41 (Krishnaswamy and Orsat, 2015). Zein solution containing ethanol/liquid Au nanospheres (80/20 v/v) showed in line ε′ values, i.e. 78.64 ± 0.115 and 76.92 ± 0.075. These values were slightly lower than ε′ of water. Nguyen et al. (2020) reported that the higher concentration of proteins resulted in the reduction of available moisture content, where the ε′ was also decreased. Table 4.1 shows that the higher frequency of 3000 MHz resulted in higher dielectric properties than that obtained at a lower frequency of 300 MHz. The frequency dependency of dielectric properties was in accordance with previous studies (Krishnaswamy and Orsat, 2015; Isik et al, 2018). Krishnaswamy and Orsat (2015) stated that the ε″ and ε″/ε′ increased with an increase in frequency (200 MHz–20 GHz) which could also increase charge mobility within the polymer matrix and ion diffusion in the direction of the electric field.

Table 4.1 : Electrical conductivity, ε′, ε″, and ε″/ε′ values of zein solution containing ethanol/liquid Au nanospheres (80/20 v/v).

Electrical Conductivity (μs/cm)	808.67 ± 2.082	
Dielectric Properties	**300 MHz**	**3000 MHz**
Dielectric constant (ε′)	78.64 ± 0.115	76.92 ± 0.075
Dielectric loss factor (ε″)	1.06 ± 0.057	11.08 ± 0.057
Loss tangent (ε″/ε′)	0.0135	0.145

4.4.2 Morphology of nanofibers

SEM image of zein nanofibers integrated with Au nanosphere is shown in Figure 4.2. The average diameter of zein nanofibers was 438 nm. The minimum and maximum fiber diameters were 85 nm and 789 nm, respectively. Figure 4.2 shows that Au nanospheres are well distributed on the surface of fibers. Yilmaz et al. (2016) successfully produced curcumin-loaded zein nanofibers (less than 350 nm in diameter) and did not find a remarkable morphological difference between zein and curcumin-loaded nanofibers. It has been reported that conductivity and fiber diameter showed an inverse relationship, where lower conductivity of feeding solutions produced thicker diameter fibers owing to decreasing electrostatic force and jet elongation. The electrospinning of solutions that had a high electrical conductivity resulted in a smaller fiber formation (Uygun et al, 2020; Aslaner et al, 2021) because of high stretchability (Facchi et al, 2021). Thus, the higher diameter of zein-Au nanofibers (438 nm) could be attributed to the presence of the Au nanosphere which reduced the electrical conductivity properties in the feeding solution.

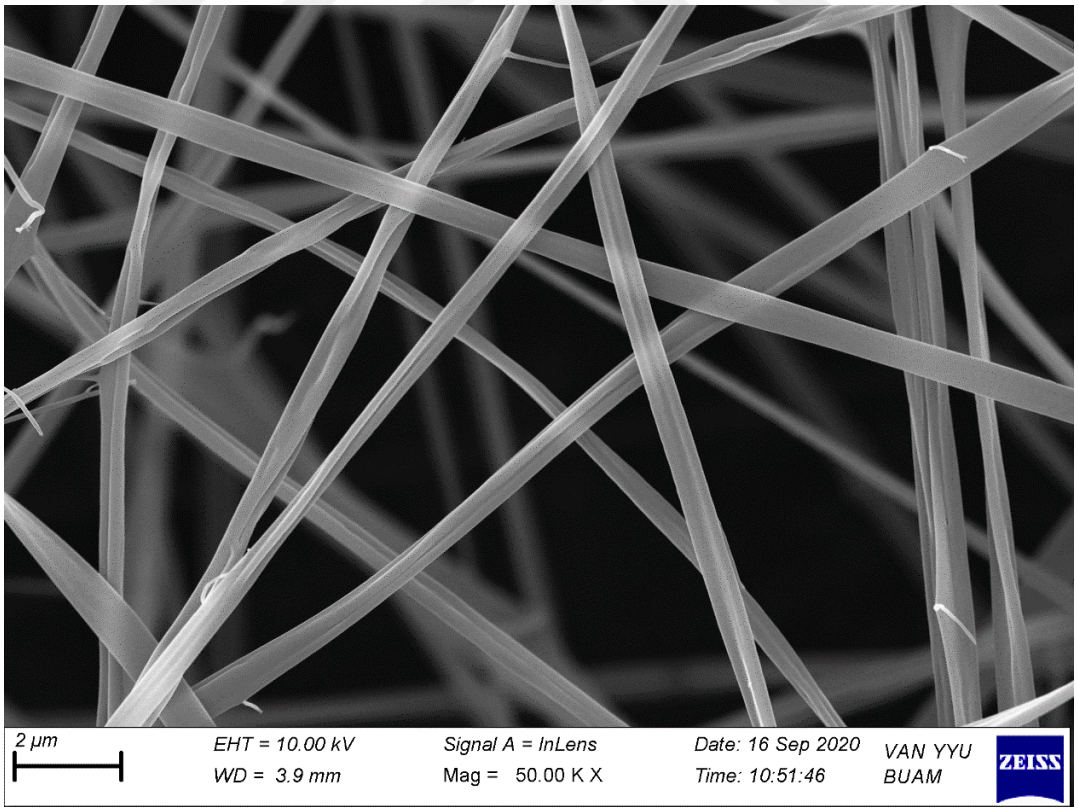

Figure 4.2 : SEM image of zein nanofibers integrated with Au nanospheres.

4.4.3 Zeta potential and dynamic light scattering measurements

The stability of electrospun nanofibers was evaluated by zeta potential measurements. Dispersions with zeta potential values above +25 mV or below −25 mV can be considered a stable colloidal dispersion (Okutan et al. 2014). Nanofiber dispersed in ethanol showed a relatively high zeta potential, i.e. +41.73 ± 3.1 mV, indicating the nanofibers can be well dispersed for a relatively long time. However, changing the solvent to water reduced the value to +5.1 ± 2.49 mV, indicating the occurrence of particle-particle attractive interactions leading to aggregation since zein is a hydrophobic protein (Table 4.2). According to Yilmaz et al. (2016) zeta potential values of 2.5% and 5% curcumin-loaded zein (based on the weight 30% zein powder) nanofibers were calculated as −24.1 ± 2.44 mV and −29.8 ± 2.16 mV, respectively. It has been reported that more negative charges were carried out by increasing curcumin concentration in zein nanofibers (Yilmaz et al, 2016). We observed a similar phenomenon in that the opposite charge of zein and Au particles resulted in attractive interactions between zein and Au nanospheres, suggesting an increase in of the thickness of a charged layer the nanofiber surface due to increasing positive charge.

PDI of zein/Au complexes in ethanol, i.e. 0.36, and in water, i.e. 0.22, showed a multimodal size distribution. Similarly, the PDI of zein dispersions was earlier found to be in the range of 0.25–0.64 (Giteru et al, 2021). The multiple modal peaks could be attributed to the size difference between zein particles and Au nanospheres (15 nm). This size distribution could confirm the existence of supramolecular nanostructures in dispersion (Chen et al, 2021).

Table 4.2 : Zeta potential, translational diffusion coefficient, hydrodynamic radius, polydispersity index, and major axis values of dispersed (0.1 g/100 mL) electrospun zein nanofibers.

Parameter	Dispersed in ethanol	Dispersed in water
Zeta potential (mV)	+41.7 ± 3.1	+5.1 ± 2.5
Translational diffusion coefficient (D) ($\mu m^2/s$)	1.85 ± 0.09	2.03 ± 0.03
Hydrodynamic radius of aggregated nanofiber (nm)	221 ± 9.94	242 ± 3.03
Polydispersity index of aggregated nanofiber	0.36 ± 0.02	0.22 ± 0.01
Calculated major axis for nanofiber in a solvent (nm)	693.07	629.78

Data represent average amounts ± standard deviations of three replications.

The translational diffusion coefficient of complex nanofibers in water and ethanol dispersions was 2.03 $\mu m^2/s$ and 1.85 $\mu m^2/s$ respectively. The results indicated that the sample dispersed in the ethanol had a 9.73% lower translational diffusion coefficient than the one dispersed in water. Monaghan and White (1936) showed that slightly decreased mobility of red cells by adding proteins indicated absorbed water molecules (or hydrated) on the surface of red cells. Moroever, Isik et al. (2018) stated that a higher diffusion coefficient indicated a higher mobility of the polymer in the suspension. So, high mobility might indicate low absorption of ethanol (or water) on the surface of a polymer in the suspension. Similarly, the lower translational diffusion coefficient of zein nanofibers in ethanol may indicate higher water absorption on the surface of nanofibers compared to zein nanofibers in water. Hydrodynamic radii of nanofibers dispersed in water and ethanol were 242 ± 3.03 nm and 220.5 ± 9.94 nm respectively. The lower hydrodynamic radii of nanofibers in ethanol may be attributed to the hydrophobic character of zein. Zhong and Jin (2009) reported that the size of zein-based NPs is typically found between 100-200 nm. It was observed that the increase of zein NP diameter was followed by decreasing ethanol concentration. In this regard, larger particles would be formed with a relatively high-water concentration. Moroever, shear rate and polymer concentration may also affect the particle size (Zhong and Jin, 2009). It should be noted that the values of hydrodynamic radii obtained from the DLS are not the nanofiber diameter. This is due to the fact that the hydrodynamic radius measurement from DLS follows the theory of Brownian motion and calculates the hydrodynamic radius assuming a spherical particle (Pecora, 1985; Saunders et al, 2015). Despite the inaccuracy of the hydrodynamic radius measurement for fiber suspensions in ethanol or water, the values can provide a notion regarding the relative extent of aggregation since the solution ionic strength and polymer type may affect the aggregation state (Saunders et al, 2015).

To calculate the major axis for nanofiber in water and ethanol solvents, at first F_D value was measured. Equation (4.1) was given below:

$$F_D = log\rho + 0.312 + \frac{0.565}{\rho} - 0.1/\rho^2 \quad (4.1)$$

The equation was provided for long rods from Supporting information (Arenas-Guerrero et al, 2018). (ρ) is the length to diameter ratio of the cylindrical-shaped

particle. According to Yabuki et al. (2017), the length of short nanofibers from cellulose acetate with silica particles was 52.4-15.3 μm. If the length would be taken as 52.4 μm, the aspect ratio (length/diameter) would be ~120 when considering the average diameter of zein nanofibers was 438 nm. On the other hand, Iwamoto et al. (2014) prepared cellulose nanofibers with aspect ratios varying from 30 to 300. These aspect ratios were reported for nanofibers as it is, not in a solution. So, the aspect ratio of zein nanofibers with Au was taken as 200 to calculate F_D which was found as 2.62. After calculating F_D, then the major axis of nanofibers (L) in a solvent was calculated by using the following equation (4.2):

$$D = \frac{k_B T}{3\pi\eta L} F_D \tag{4.2}$$

D is the translational diffusion coefficient obtained from DLS measurement, kB is the Boltzman constant (1.38 x 10^{-23} kg m^2/s^2.K), T is the temperature (25 °C + 273.15 = 298.15 K), η is the viscosity of ethanol (0.8911 × 10^{-3} Pa.s) Tanaka et al. (1977) or water (0.8937 × 10^{-3} Pa.s) Perry (1950) at 25 °C. Using equation (4.2), major axis values were calculated as 629.78 nm and 693.07 in water and ethanol solvents, respectively (Table 4.2).

4.4.4 Molecular characterization by FTIR spectroscopy

The infrared spectrum of gold nanosphere, pure zein nanofiber, and zein nanofiber containing Au nanospheres is shown in Figure 5.3. The -OH stretching vibration was observed around 3291 cm^{-1} and C-H stretching from CH_2 and CH_3 functional groups was revealed at 2873, 2956, and 2928 cm^{-1}.

The characteristic peak observed at 1643 cm^{-1} (amide I) is related to the C=O stretching of peptide chain, while 1537 cm^{-1} (amide II) was related to the N-H in-plane vibrations. 1236 cm^{-1} (amide III) and 1444 cm^{-1} were related to C-N stretching vibrations. These results were in accordance with previous studies (Dashdorj et al, 2015; Yilmaz et al, 2016). The amplitude of the peak with wavenumber between 3400 and 3200 cm^{-1}, representing mainly OH groups observed in the spectrum. For zein-based materials, 1538–1546 cm^{-1} for N–H, 1649–1653 cm^{-1} for C=O, and 1428–1451 cm^{-1} for C–N has also been previously observed (Dashdorj et al, 2015; Yilmaz et al, 2016; Pérez-Guzmán and Castro-Muñoz, 2020). It can be seen from Figure 4.3 that the spectrums of pure zein nanofiber and zein nanofiber with Au showed a similar

trend. However, with a closer look, important differences were more clearly determined (Figure 4.4 and Figure 4.5). For example, after the encapsulation of Au nanospheres, similar characteristic high C=O stretching peaks were observed at 1643 cm^{-1} and 1632 cm^{-1} with a decreased transmittance (a). This could be attributed to the interaction of amide functional groups with Au nanospheres.

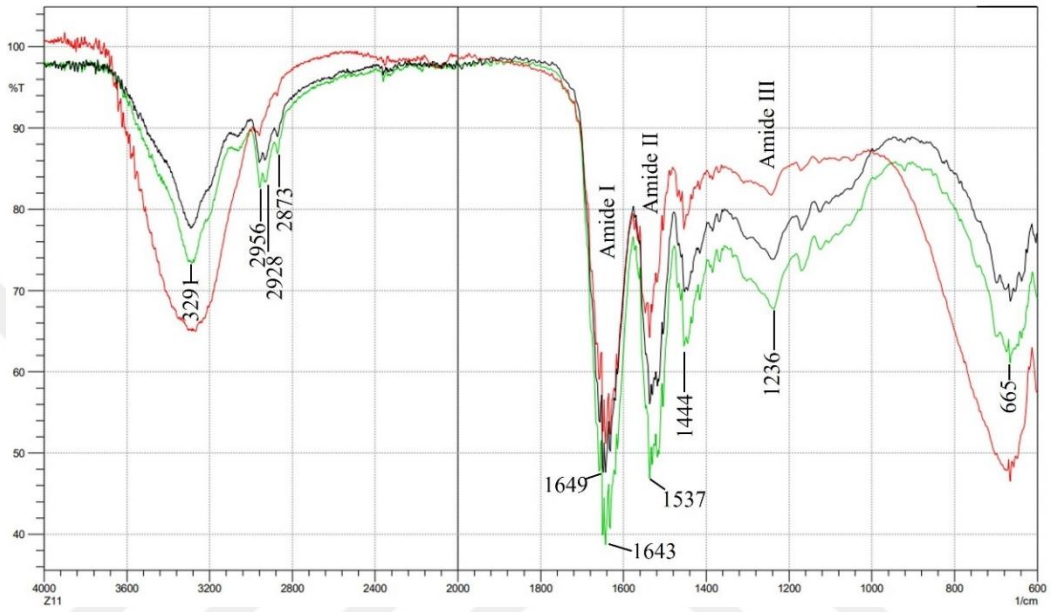

Figure 4.3 : FTIR spectrum of gold nanosphere (—), pure zein nanofiber (—), and zein nanofiber integrated with gold nanospheres (—).

Similarly, in a study by Puthiyaveetil Yoosaf et al. (2019), these peaks were observed at 1638 cm^{-1} for zein film with Au NPs and at 1644 cm^{-1} for gold nanoparticle caped zein ligand. Authors stated that decreasing of C=O peaks attributed to the distribution of charge on –N–C=O moiety (Puthiyaveetil Yoosaf et al, 2019). In amide I and amide II region, new shoulders (b) were observed with C=O carbonyl stretch vibrations. These shoulders were detected in Au nanosphere spectrum but not in pure zein.

N-H functional groups play an important role in the stabilization of zein nanofibers. Dias Antunes et al. (2017) have stated that lower wave numbers in amide regions show better structural stability, with an increased hydrogen bonding interaction occurring at the N-H group. As can be seen from Figure 4.4, a decrease of transmittance and shifting (from 1649 cm^{-1}–1643 cm^{-1}) in N-H vibration was observed for the spectrum of zein nanofiber with Au, compared to pure zein nanofiber. These differences could be attributed to increasing molecular weight after the attachment of Au nanospheres to

nitrogen atoms which also affected the vibration intensity of the N-H bond (Wei et al, 2009).

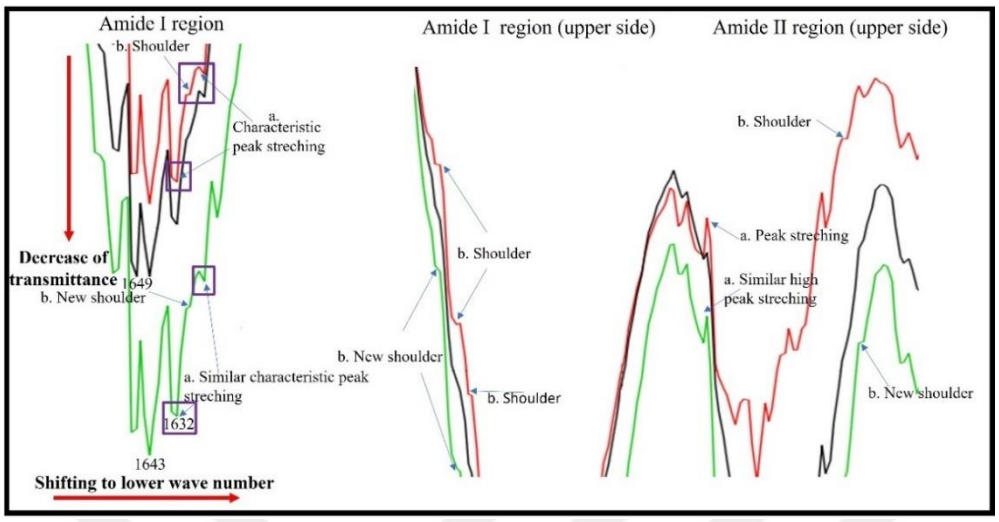

Figure 4.4 : Enlarged peak assignments of gold nanosphere (—), pure zein nanofiber (—), and zein nanofiber integrated with gold nanospheres (—) in amide I and amide II regions.

Figure 4.5 shows that there were disappeared bands for pure zein (c, d, e), which changed to the stretching peaks with cleaving and elongation for zein nanofiber with gold. For example, bands at 1452 cm^{-1} and 1447 cm^{-1} appeared as stretching peaks at 1454 cm^{-1} and 1445 cm^{-1}, respectively.

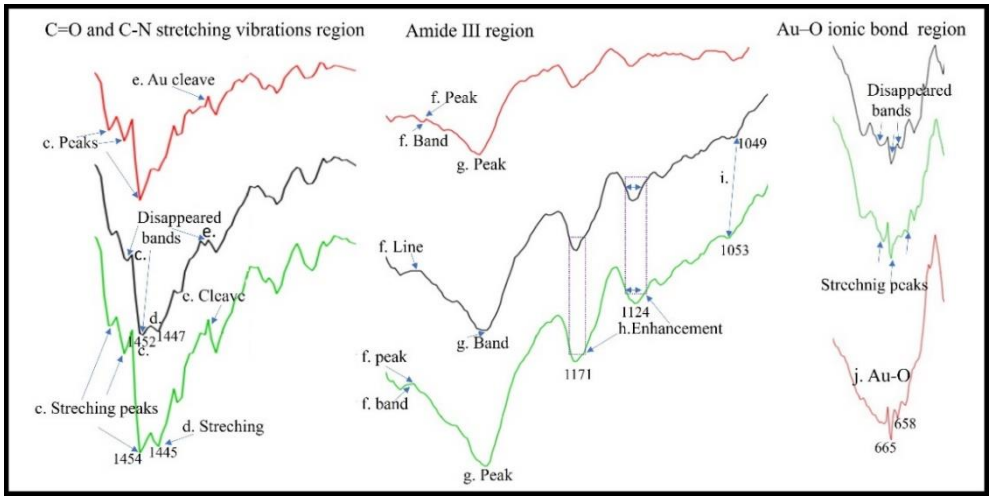

Figure 4.5 : Enlarged peak assignments of gold nanosphere (—), pure zein nanofiber (—), and zein nanofiber integrated with gold nanospheres (—) between 1500 cm^{-1}-600 cm^{-1}.

In previous studies, a band around 1297 and 1303 cm^{-1} was observed for Ag loaded zein materials which were thought to be generated by the newly formed Ag–N coordination bonds (Zhang et al, 2010; Dashdorj et al, 2015). In this sense, a band at

1308 cm^{-1} (f) and a stretching peak at 1300 cm^{-1} (g) may indicate possible Au-N interaction.

An enhancement in the signal at 1171 cm^{-1} and 1124 cm^{-1} (h) was detected corresponding to carbonyl group. These changes indicated the reduction of the Au ions which was coupled to the oxidation. The low oxidation process proved that Au nanospheres were successfully attached to the zein nanofibers. The results were in accordance with the previous study (Chandran et al, 2006). C-N stretching amine was observed at 1049 cm^{-1} for pure zein and shifted to 1053 cm^{-1} for zein with Au nanospheres (i). Suganya et al. (2017) produced zein-coated Au NPs and stated that 1096 cm^{-1} indicated the C-N stretching of amine. For gold spectrum peaks observed at 665 cm^{-1} and 658 cm^{-1} (j) might indicate the vibration frequency of Au–O ionic bond groups. These peaks were also observed in zein nanofiber with gold spectrum. Furthermore, a narrowing band was detected at 670 cm^{-1} after integration. These trends were previously observed by Gharibshahi et al. (2017) who detected Ag-O ionic bond at 513 cm^{-1}.

All above-mentioned findings approved the binding between gold ion and zein molecules, which promotes integration of the Au nanospheres to the zein nanofibers.

4.4.5 Effect of nanocoating on fish fillets

4.4.5.1 Microbiological analysis of fish fillets

The results of TMAB growth in uncoated and nanofiber coated fish fillets are shown in Table 4.3. The initial TMAB count of sea bream fillets was 3.80 ± 0.18 log CFU/g. Nanocoated samples showed a lower TMAB count than that of uncoated samples after storage. Overall, the coated fish fillets showed a remarkable reduction of TMAB counts, i.e. 5.60 CFU/g, compared to that of the uncoated samples. The microbiological data were in line with recent studies, where the inhibition of rapid TMAB growth in sea bass fillets could also be obtained by nanocoating the fresh fish samples with electrospun zein mats containing Au nanospheres (Çetinkaya et al, 2021b). TMAB counts showed the impact of zein-Au nanofibers coating to inhibit the deterioration of fish fillets. There are various mechanisms which Au NPs show an antimicrobial property, i.e. interaction with the bacterial cell wall, prevention of biofilm formation, production of reactive oxygen species, and inducing leakage of intracellular components (e.g., interactions with DNA and/or proteins) (Okkeh et al,

2021). The antimicrobial mechanism depends on the shape and size of the nanomaterial. Penders et al. (2017) showed that the antibacterial action of Au-nanoflowers is associated with high-aspect ratio spikes and pillars, triggering local stress on the bacterial cell wall, and resulting in membrane rupture. Nanofibers formed by other biopolymers such as chitosan interacts with the bacterial cell wall, this interaction occurs through cationic amine groups with anionic binding sites of bacterial cell walls, which damages the bacteria membrane (Arkoun et al, 2017; Mohamady Hussein et al, 2021). Furthermore, strong adhesion of Au-zein nanofibers to the membrane due to the coupling of gold/amine groups might lead to a synergistic effect in the deformation of bacteria cells.

Fish fillet's surface efficiently absorbed the nanofibers due to its relatively high moisture content. The gold nanospheres slowly interacted with the outer membrane of bacteria over time, causing an increase in membrane permeability and leakage of intracellular constituents, which could damage the cells.

The comparison of results from Chapter 2 (Table 2.1 and Table 2.2) for microbiological quality of smoked fish products with the results of microbiological quality of fresh fish fillets (Table 4.3) revealed that the process of smoking decreased the initial TMAB load. However, after open the package, the TMAB values of the smoked fish increased more (Chapter 2) compared to the values for fresh fish fillets (Chapter 4) as in Chapter 3, suggesting that smoking process of fish works duing storage without opening its package. This result leads to that active packaging could be used for keeping TMAB load low. It appears that the Au loaded zein nanofiber mats as active packaging layer for fresh fish fillets (Table 4.3) resulted lower TMAB values compared to the values of smoked fish products after their packaging being opened (Chapter 2, Table 2.1 and Table 2.2).

4.4.5.2 Dielectric properties of fillets

Table 4.3 shows ε′ and ε″ values of nanocoated, and uncoated fish fillets. On the initial day, ε′ value was 75.60. Similarly, the ε′ value of the seabass fillet was found as 76.47 at 3000 MHz (Çetinkaya et al, 2021b). On the 1st day, there was a slight increase in ε′ values, i.e. 77.87 and 78.80 for the uncoated and nanocoated groups, respectively. The nanocoated samples showed a higher ε′ in first 3 days than that the uncoated samples.

Table 4.3 : TMAB, ε′-dielectric constant, and ε″-dielectric loss factor results of nanofiber coated and uncoated fillets.

	Group	Initial	1st	2nd	3rd	4th	7th	8th
TMAB	U	3.80±0.18	3.92±0.09^{aA}	4.38±0.23^{aAB}	4.68±0.14^{aB}	4.85±0.22^{aB}	5.72±0.14^{aC}	6.81±0.16^{aD}
	AZN		3.85±0.18^{aA}	4.02±0.05^{bA}	4.26±0.21^{aAB}	4.43±0.15^{bB}	4.67±0.05^{bB}	5.60±0.06^{bC}
ε′	U	75.60±4.64	77.87±0.72^{aA}	75.94±4.63^{aA}	71.73±3.70^{aA}	119.18±21.98^{aB}	64.46±4.53^{aA}	76.08±3.92^{aA}
	AZN		78.80±0.62^{aA}	77.75±0.47^{aA}	77.38±0.64^{aA}	75.58±3.42^{aA}	64.38±1.25^{aB}	74.77±0.81^{aA}
ε″	U	10.55±0.71	11.22±0.30^{aA}	9.90±1.20^{aAB}	10.46±3.70^{aAB}	8.47±0.52^{aB}	9.79±0.40^{aAB}	10.68±0.47^{aAB}
	AZN		11.62±0.42^{aA}	11.14±6.06^{aA}	11.20±0.29^{aA}	9.89±1.1^{aA}	10.24±0.2^{aA}	10.41±0.50^{aA}

$^{a-b}$ Within each column, different superscript lowercase letters show differences between treatment groups for same storage day (p<0.05). $^{A–D}$Within each row, different superscript uppercase letters show differences between the storage days within same analysis group (p<0.05). U: Uncoated samples; AZN: Samples treated with zein nanofibers containing gold nanospheres.

Wang et al. (2008) observed an increase in ε′ at 27 MHz (from 97.8 at 20 °C to 149.6 at 120 °C) and at 40 MHz but decreasing at 433 MHz (from 60.4 at 20 °C to 56.7 at 120 °C). Fluctuation was observed in terms of ε′ values, since ε′ values were decreased on 2nd and 3rd day of storage for nanocoated and uncoated groups. However, a significant reduction of ε′ values was observed for the uncoated group. Çetinkaya et al. (2021b) stated that fluctuations might occur in ε′ and ε″ during the storage of fish fillets. In Chapter 2, it was reported that ε″ values taken at 30 MHz increased with storage. It appears that dielectric factors may vary with frequency, and type of fish and fish composisitin depending on caught season. The dielectric properties of foods could be affected by the degree of water binding with constituents of the food (Samuel and Trabelsi, 2012). Li et al. (2019) reported that moisture content is the most influential factor on the dielectric properties of fish meat. In this regard, the decreased ε′ was attributed to the loss of water, as it might affect the dielectric behavior. The lowest ε′ values were observed on the 7th day. Significant differences (p<0.05) between storage days were observed on the 4th day of storage for the uncoated group (119.18) and the 7th day for the nanocoated group (64.38). The initial ε″ value was 10.55 for the fresh fillet. The ε″ for the uncoated samples and nanocoated samples ranged from 11.22 to 8.47 and 11.62 to 9.89, respectively. Results showed that fluctuations of ε′ and ε″ were higher for uncoated group, suggesting a stabilization effect of nanocoating on shelf-life. Similarly, Çetinkaya et al. (2021b) proposed that the stability of dielectric properties can be provided by functional antimicrobial nanofibers.

4.5 Conclusion

The fabrication, characterization, and application of zein-Au electrospun nanofibers were successfully reported in this study. The dielectric properties and electrical conductivity of feeding solutions composed of Au nanospheres and zein strongly affected the formation and properties of zein-Au nanofibers. Zeta potential and DLS measurements were applied as a useful approach to characterize nanofibers. The monitoring dielectric loss factor of fresh fish fillets for evaluating its quality (Chapter 2), was used in this Chapter. The aggregation behavior of nanofiber samples in ethanol or water was successfully determined. FTIR data showed the interaction of amide functional groups between zein and Au suggesting the stabilization of the Au nanospheres by zein. The zein nanofibers integrated with Au nanospheres improved

surface coating properties and reduced TMAB (17.8%) after 8 days of storage. The functionalities of zein-Au nanofibers in the reduction of TMAB were also affected by dielectric properties of fish fillet coated by nanofibers, where a change in ε′ and ε″, i.e. 14.84% and 10.14%, respectively, in the coated group were lower than that of an uncoated group, i.e. 57.65% and 19.72%, respectively. This study will set light on further applications of Au-zein-based nanofibers as edible antimicrobial preservatives in the seafood industry.

5. GELATIN NANOFIBERS CONTAINING BLACK ELDERBERRY, Au, AND SnO_2 AS SMART PACKAGING LAYER USED FOR *MERLUCCIUS MERLUCCIUS* FILLETS

5.1 Abstract

After being caught, fresh fish products have been transferred to the wholesale fish market, gross markets, and/or bazaars. The transportation procedures may take time and may affect the freshness of products as generally there is no preservation method applied. Furthermore, especially in public markets such as seafood markets, wholesale fish markets, and bazaars, these products are being sold at room temperature. In rural areas, public hawkers (traveling salesmen) have been still selling these products on streets without interfering with temperature settings. In this sense, products may spoil with time and consumers may have concerns about whether the products they buy have high quality and are acceptable. Furthermore, internal cleaning, fish head cutting, and deboning processes have been applied indoors haus at room temperature. Therefore, it is important for consumers to predict the quality of fresh fish products before they cook or fry them. In this sense, in this study, it is aimed to determine the shelf life of fresh Hake fish fillets by the color-changing properties of gelatin-based nanofibers. For this purpose, a smart electrospun gelatin-based layer was produced using BE extract, SnO_2, and Au nanopowders. Four different nanofiber samples were prepared, and SEM images confirmed the formation of continuous ultrafine fibers with smooth surface for the control sample and nanoparticle-integrated surfaces for other samples. Differences between nanofibers were evaluated in terms of thermal stability, and chemical composition in the initial hour and after the 30^{th} hour storage of hake fish at 20±2 °C. FTIR spectrums indicated disappeared bands, shiftings, and new peaks, suggesting strong bonding interactions between gelatin and other compounds. Furthermore, a new approach was developed by using the values of transmittance ratios to evaluate nanofiber stability. Shifting in DSC involved the formation of new chemical bonds. DSC and TGA results indicated that the addition of NPs contributed to the thermal stabilization of the gelatin chain with interactions. *L*, *a*, and *b* values of

nanofibers were also measured during storage. A rapid color change occurred within the first 6 hours after exposure to volatiles with the highest difference in *L* (52.29%) of GLESA ($p<0.05$). An increase in the pH and TMA values of the samples during the storage was attributed to the production of volatile and nitrogenous compounds. This study showed that the absorption of volatiles on nanofibers that are produced by the deterioration of fish can be examined by spectroscopic, thermal, and colorimetric measurements. The results of this chapter indicated that gelatin nanofiber reinforced with BE extract and NPs can be applied for smart packaging layer in seafood products.

Keywords: functional nanofiber, smart packaging, tin dioxide, gold nanopowder, plant extract, nanofiber stability, volatile compounds

5.2 Introduction

Hake fish (*Merluccius Merluccius*) is a high-value seafood that is generally consumed in European nations. According to research, it has a water content of 65–80%, pH between 6–7, and non-protein nitrogen between 9-18% which is a highly perishable aquatic product and may spoil rapidly due to biochemical and microbial breakdown mechanisms depending on processing and storage (Rey et al, 2012; Fernández-Saiz et al, 2013; Otero, Pérez-Mateos & López-Caballero, 2017; Sullivan et al., 2020).

The use of indicator materials to track changes in the quality of seafood products is an indispensable part of the application of intelligent packaging materials (Kim et al, 2022). Gelatin is formed by partial the degradation of collagen and has been used as a functional bio-polymer in food packaging materials since it has non-toxicity, biocompatibility, and biodegradability. The translucent character of gelatin film facilitates the color recognition of the pH-responsive indicator materials. On the other hand, gelatin based materials have high brittleness caused by dehydration of the 3D structure of molecular crystallite (Zheng et al, 2022). To overcome the brittleness, the addition of other polymers or plasticizers has been used as an alternative method. For instance, it has been stated that the pH-responsive colorimetric indicator film made of haskap berries extract and fish gelatin has lower brittleness, due to the intermolecular H bonds (Liu et al, 2019). In another study by Rawdkuen et al. (2020), it has been stated that butterfly pea anthocyanins had high pH-sensitivity with wide color ranges, which were strongly suitable to determine the changes in food quality. Blueberry and

blackberry pomace extracts were also used as possible indicator sensors for easy and rapid detection of food quality degradation (Kurek et al, 2018).

Berry extracts such as blueberry and mulberry are commonly used for intelligent packaging. They generally have a higher content of anthocyanins than other fruits, flowers, or vegetables. For instance, cyanidin compounds reported as major anthocyanin in BE samples (*S. nigra*) are mostly in glycoside form and afford intense reddish-purple hues, that facilitate the visual perception of pH-dependent color change (Mikulic-Petkovsek et al, 2014; Neves et al, 2022). Other anthocyanidin derivatives such as peonidin, petunidin, and malvidin attribute magenta or purple colors due to the presence of methoxy substituents (Neves et al, 2022). Therefore they can be used to functionalize electrospun nanofibers. Nanofibers that have different morphologies and structures improve mechanical and thermal, and barrier properties for food packaging materials (Nikolic et al, 2021). In this sense, gelatin-based nanofibers are promising for smart packaging applications. The degree of fish spoilage is increased with an increase in the number of bacteria, causing the release of more volatiles such as NH_2 or H_2S. Therefore, changing color values of the nanofibers could be correlated with the absorption of amines, aldehydes, or other volatiles by metallic NPs (Naghdi et al, 2022). Recently, metal oxides have been extensively investigated and applied as sensing materials for gases such as CO_2, NH_3, H_2S, H_2O, DMA, and TMA that are released during spoilage (Nikolic et al, 2021). SnO_2 has a lower wall thickness compared to other nanostructure types as it has a hollow nanostructure. The resistance of this metal oxide changes more dynamically along with the thickness of the generated surface depletion layer. Oxygen molecules can easily permeate and adsorb on their surface because of their porous and polycrystalline structure. The catalytic effect of metal NPs allows for an increase in the amount of adsorption and desorption of gas molecules, and the variation of resistance is also amplified. These properties lead to an enhanced sensing performance of SnO_2 hollow nanostructures with the metal NPs such as Au (Cai et al, 2021). In this respect, gelatin nanofibers can be functionalized with metal-based nanostructures to have better gas-sensing properties.

Microorganisms utilize various compounds to produce volatiles such as organic acids, ethanol, and ethyl esters (Parlapani et al, 2014). Spoilage occurs with the microbial decomposition within a fish muscle and the production of bacterial metabolites cause biochemical changes. Although spoilage compounds may not reach a high level

enough to cause detectable changes by FTIR, some compounds such as TMA, esters, ketones, and aldehydes, may be determined or may show slight intensity changes in spectrums (Sone et al, 2011). In a study by Saraiva et al. (2017), FTIR was used to predict the freshness of salmon fillets by chemometric approaches. Furthermore, in a study by Raba et al. (2015) coffee oils induced significant spectral alterations in some regions which are determined by the absorbance ratios. Changes contributed to the primary and secondary oxidation processes of the lipid fraction (Raba et al, 2015).

The spoilage of seafood is often accompanied by the formation of nitrogenous gases and changes in pH caused by the degradation of proteins and lipids with microorganisms and enzymes' action. Protein degradation leads to the formation of NH_3 and amines, which increase also the pH. Alterations in the quality can therefore be monitored by measuring pH during storage (Alizadeh Sani et al, 2022). Increases in the TMA and pH value of fish muscle during storage have been reported to indicate the accumulation of NH_3, TMA, and other nitrogenious compounds, mainly generated with bacteria (Mendes et al, 2021).

These above-mentioned studies revealed that nanofibers incorporated with functional nanoparticles could be ideal materials to predict spoilage in seafood products. The main aim of the present study was to produce and investigate various gelatin-based nanofibers with nanomaterials for smart packaging functionalities. Chemical deterioration in European hake fillets was examined with TMA, TVBN, and pH analyses. Fabricated nanofibers were deeply characterized in terms of spectroscopic, thermal, and color changes to have information about volatile gas functions.

5.3 Material and Method

5.3.1 Material

Gelatin Emprove (1.04078.1000), was purchased from Merck. BE (*Sambucus nigra*) powder extract (12% UV, Lot: NBE20200820) was kindly received from Nante Kimya ve Ambalaj San. Tic. Ltd. Şti. Gold (III) chloride hydrate ($HAuCl_4$) received from Sigma (Product number: 50790; Lot: BCCB3763). SnO_2 was provided from ITU Chemical and Engineering Faculty, Deparment of Metallurgical and Materials Engineering. European hake (*Merluccius merluccius*) was purchased from

international supermarket (Istanbul, Türkiye). Skin and bone of fish was removed, and skinless fillet divided in portions.

5.3.2 Method

5.3.2.1 Synthesis of liquid nanoparticles and nanopowders

Firstly, liquid gold nanoparticles and dried gold nanopowders were produced from gold salt, $HAuCl_4$. Gold nanoparticle and nanopowder fabrication methodologies were modified from a study reported by Rajar et al. (2021). The liquid Au nanoparticles were produced by reducing the $HAuCl_4$ in a sodium borohydride ($NaBH_4$) aqueous solution. 0.3% of PVP was used as a capping agent. Firstly, it was prepared the $NaBH_4$ aqueous solution of 0.001 mol/L concentration in 30 ml of water. This mixture was kept on stirring for about 10 min. The 60 µL of PVP solution was added to the solution of $NaBH_4$. Then, 30 µL of $HAuCl_4$ solution was added drop by drop (33.98 mg/L). The solution was kept at 450 rpm stirring until the pink colored Au NPs appear. Then necessary amount was mixed with acetic acid (1:1 w/w) to prepare solvents (GL, GLE, GLES, GLESA). Approximately 2.5 Liter of liquid Au NP solution was prepared to obtain Au nanopowders. Au NPs were added to glass Petri dishes, placed in a water bath, and dried at 100 °C. This procedure was repeated until all liquid had evaporated. Au nanopowders were collected by scraping glass Petri dishes with a stainless-steel spatula. Then necessary amount was added to the gelatin solution to fabricate GLESA nanofibers.

5.3.2.2 Preparation of the feeding solutions and electrospinning process

1:1 w/w acetic acid: liquid Au nanoparticles were used as a solvent to dissolve gelatin. The solution was blended approximately for 30 min at 600 rpm using a magnetic stirrer at 40 °C. The first solution contains only 20% gelatin and 80% solvent which is control (GL). Other solutions were prepared under the same conditions containing 20% wt. gelatin, with the addition of mentioned compounds in Table 5.1. Electrospun nanofibers were fabricated by Inovenso NE100 equipment with a pump (New Era Pump Systems, Inc.), and a voltage supply (Nanofen, Türkiye).

Table 5.1 : Compositions of feeding solutions.

Sample	Gelatin (%)	Black Elderberry Extract (%)	SnO_2 (%)	Au nanopowder (%)	Solvent* (%)
GL	20	-	-	-	80
GLE	20	10	-	-	70
GLES	20	10	5	-	65
GLESA	20	10	5	2	63

* Contains 1:1 w/w acetic acid: liquid gold nanoparticles. Gold nanoparticle concentration in water is 33.98 mg/L.

Electrospinning was performed with a 17 G needle, at 10 kV voltage, and 0.7 mL/h feed rate. The collector was covered with white silicon-based paper. Needle-collector distance was kept at 10 cm.

5.3.2.3 Application of nanofibers to fresh fish fillets

Electrospun fibers were used to monitor quality changes during a 30-hour storage period. The European hake fish meat was divided into portions of 10 g and was arranged in a Petri dish (60 mm×15 mm). Petri dishes were sealed with a PVC film. Then, produced nanofiber samples (GL, GLE, GLES, GLESA), were carefully removed from the baking paper and deposited into circle shapes, folded into a semicircle shape, and placed on the PVC film. The PVC-sealed and semicircle nanofiber placed Petri dishes with fish fillet samples were stored at 20 °C ± 2.

5.3.2.4 Morphology of electrospun samples

The morphology of produced nanofibers were examined by SEM (FEI, Inspect S50, Hillsboro, OR USA) with an EDS (Energy Dispersive X-ray Spectroscopy) detector under 10^{-2} Pascal (distance of 9 mm). 20 kV accelerating voltage was applied to obtain the images. Team Prime (EDAX Inc V4.1) software was used for elemental analysis. The minimum, maximum, and average diameter of nanofibers were obtained with selected 50 random nanofibers using the Image J program.

5.3.2.5 FTIR spectroscopy

Data were collected at a 4/cm resolution with Perkin Elmer Spectrum Two Spectrometer (Lambda 25, Waltham, MA) equipped with a diamond ATR device. The nanofiber samples were examined in transmission mode in the range of 4000–650 cm^{-1}. Measurements were done in two different storage periods (the initial hour and

the 30th hour). During storage, volatile gases produced by fish were absorbed on nanofibers and a second measurement was done at the end of the storage (30th hour).

The transmittance ratio method is developed with the inspiration of Moharam and Abbas (2010) and Raba et al. (2015). After the selection of bands, areas in the bands were calculated using Origin, Version 2022b (OriginLab Corporation, USA), ratios named TI (1590-1485/3700-3090), TII (1485-1425/3700-3090), TIII (1070-950/3700-3090), TIV (1585-1480/3700-3115), TV (1480-1420/3700-3115), and TVI (1045-950/3700-3115). Image J program used for distance measurements in bands. The scale was set as 33.1034 pixels/cm at 187% magnification (Distance in pixels: 864; Known distance: 26.1 cm). The band beginning transmittance (T_0)-band ending transmittance (T_e) were selected between 3700-3090 cm^{-1}, 3000-2900 cm^{-1}, 1430-1360 cm^{-1}, 1260-1210 cm^{-1}, and 1180-1130 cm^{-1} for distance calculations.

5.3.2.6 Thermal properties of nanofibers

Thermal behavior nanofibers on the initial and 30th hour were evaluated by using a DSC (144 Q10, New Castle, USA). 5 to 10 mg of sample was weighted in aluminum pans and pressed after putting a lead on it. As a reference pan an empty one was used. Data were recorded at a range of 10 °C-300 °C, with a heating rate of 20 °C/min under a nitrogen atmosphere (20 mL/min). Melting temperature (T_m) and the enthalpy of melting (ΔH_m) was calculated based upon the measuring peak begin-end temperatures by TA Instruments Universal Analysis 2000 software. Thermogravimetric analyses of nanofibers were performed using Shimadzu TG-60WS equipment on initial and 30th hour. Samples were heated a rate of 10 °C/min using approximately 15 mg of the sample under flowing air (50 ml/min), where the temperature varies between 15-630 °C.

5.3.2.7 Colorimetric measurements of nanofibers

The color of nanofibers was evaluated using a chromameter (CR-400, Konica Minolta Sensing Inc., Japan) equipped with an 8-mm head. A white calibration plate (CR-A43, Konica Minolta Sensing Inc., Japan) was used for calibration. The total color difference (ΔE) was calculated using equation (5.1):

$$\Delta E = \sqrt{(\Delta L)^2 + (\Delta a)^2 + (\Delta b)^2} \quad (5.1)$$

Where ΔL, Δa, and Δb differences between the color value of the control nanofiber and test nanofibers as stated by Kim et al. (2022). The color was expressed in *L, a,* and *b*. The *L* indicates the lightness of the samples, which range from 0 (black) to 100 (white), the *a* represents redness (+) and greenness (-), and the *b* represents yellowness (+) and blueness (-).

The colorimetric response of the nanofibers toward NH_3 and TMA was measured by the methods of Mohseni-Shahri et al. (2023) and Jang et al. (2023) with modifications. Different concentrations of NH_3 (0.05 M and $3.9.10^{-5}$ M) and TMA solutions (0.05 M 78.10^{-5} M) were poured (80 mL) into the glass bottles. A glass with a center gap immersed inside the solutions and nanofibers (2×2 cm^2) were placed on a glass with a 1 cm distance above the solution for 30 min. Then, every 4 min *L, a, and b,* parameters of the nanofibers were measured triplicate at room temperature and photographic images were recorded by smartphone having 3024x4032 pixels and 72 dpi.

For real sample analysis, color values were measured at different positions on each nanofiber sample in triplicate on the initial, 3rd, 6th, 24th, and 30th hours.

5.3.2.8 Physicochemical analysis of fish samples

TVBN was applied according to the study published by Najafi et al. (2022). The TVBN analysis was done by using 0.1N NaOH for titration. The TVBN was calculated as mg/100 g using the following equation (5.2);

$$\text{TVBN}\left(\frac{\text{mg}}{100}\text{g sample}\right) = \frac{(V_1 - V_0)\times 0.14\times 2\times 100}{M} \qquad (5.2)$$

Where: V_1 is the volume of titration of the sample (ml of 0.1 N NaOH), V_0 is the volume of titration of control (withiout sample), M is: Weight of fish sample (10 g). For TMA analysis, 10 g of homogenized fish sample was added to 10% TCA solution and then filtrated. 1 mL formaldehyde, 3 mL KOH, 10-mL toluene, and 4 ml of the filtrate were put into tubes and the tubes were shaken. The upper phase was taken to another test tube and then 0.02% picric acid was added into the same tube in a ratio of 1:1 (Ceylan *et al.*, 2017a). Absorbance values were measured at 410 nm by SP-3000 plus (Optima Inc. Japan). The TMA amounts of fish meat samples were measured as mg/100 g. pH values were determined by homogenizing samples with deionizing water (1:10). The results were measured by using a probe with triple results.

5.3.3 Statistical analysis

Data values were conducted using IBM SPSS Statistics program to determine differences during the 30-hour experimental period. One-way analysis of variance (ANOVA) was performed, and mean values of the samples were further analyzed using Tukey's multiple range comparison tests (p<0.05). Data values were presented as mean ± standard deviations.

5.4 Results and Discussion

5.4.1 Morphology of nanofibers

SEM images of nanofiber samples are shown in Figure 5.1. The average diameter of pure gelatin nanofibers was 81.4±22.9 nm without any beads.

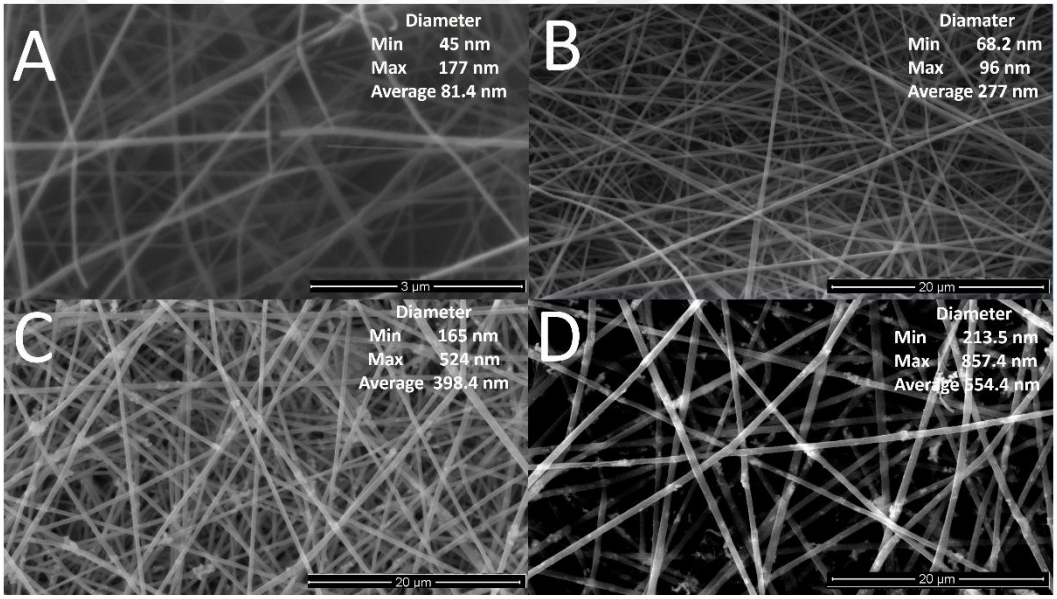

Figure 5.1 : SEM images of (A) GL; (B) GLE; (C) GLES; (D) GLESA nanofibers.

With the addition of BE extract, the diameter increased to 277.2±77.2 nm still with smooth formation. The addition of anthocyanins into the solution, increases the viscoelasticity of the polymer jet, making the stretching of fibers more difficult, thereby increasing the average diameter (Sun et al. 2014; Prietto et al. 2018). Therefore, higher average sizes are attributed to the incorporation of BE inside nanofibers. The average fiber diameter increased (398.4±73 nm) and new structures have been observed with accumulation after the addition of SnO_2. Similarly, Cai and Park (2020) observed several agglomerated bumps on the SnO_2 nanowire surface.

Furthermore, as can be seen from Figure 5.2A, when these structures integrated on the surface of some parts, these parts enlarged.

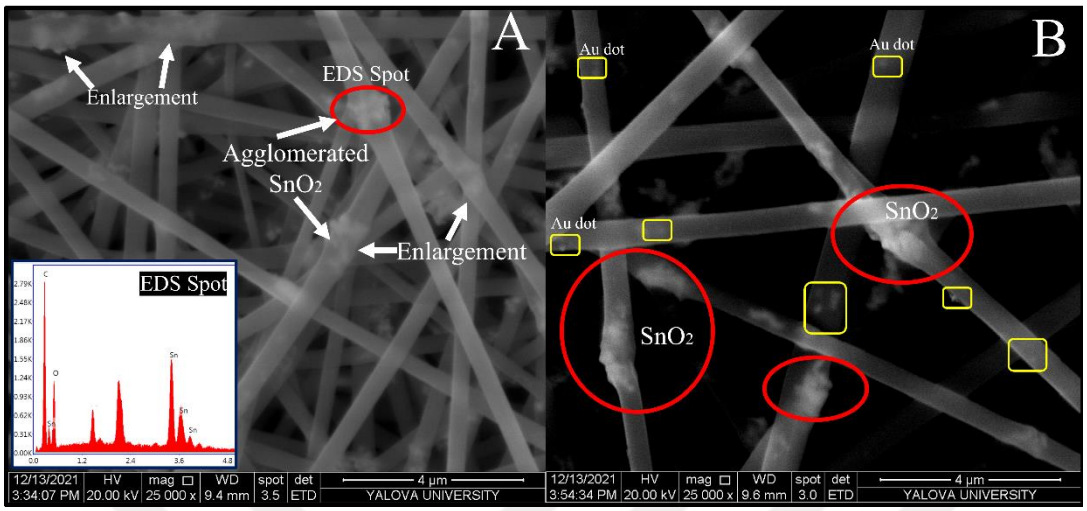

Figure 5.2 : SEM images of (A) GLES, and (B) GLESA nanofibers show differences after the incorporation of metals into gelatin. Inset (A): EDS elemental mapping of chosen spot for GLES sample.

This may show that SnO_2 nanoparticles are both encapsulated inside the nanofiber and attached to the surfaces. Shavisi and Shahbazi (2022) studied the mean diameters of chitosan-gum Arabic and chitosan-gum Arabic+*Rosa damascene* extract nanofibers. They have indicated that the larger diameter of *Rosa damascene* extract added nanofibers (725.39±0.46 nm) compared to the neat ones (300.12±0.25 nm) may be attributed to the change of electrical conductivity, viscosity, and surface tension of the solution. The EDS analysis also confirmed the attachment of SnO_2 to the nanofibers (Figure 5.2A). Carbon and oxygen are the main components of the nanofiber because they are present in proteins, polysaccharides, and anthocyanins (Alizadeh Sani et al, 2022). Chosen EDS spot exhibited four Sn peaks and one oxygen peak for GLES, proving that those peaks correspond to the structure of SnO_2. Morphology of GLES sample after absorption of volatiles presented in Appendices (Figure B1, Figure B2). Mallakpour and Madani (2015) indicated that functional agents significantly change the morphology of metallic NPs. So, although there are fiber formations in Figures, the homogenized structure is broken, and luminous SnO_2 NPs dissipated all over the material. When we look closer at the GLESA sample, the addition of Au nanopowders increased the average size up to 554±107.5 nm. Although it may be hard to separate Au clusters and the SnO_2 grains from the SEM images, we can see from Figure 5.2B that many well-dispersed small dots were observed on the surface of the GLESA

samples. These small dots may be attributed to the Au nanopowders since they are attached in a different form (possessed a spherical shape and discontinuous) to the nanofibers.

5.4.2 FTIR spectrums

5.4.2.1 Initial nanofiber properties

As can be seen from Table 5.2, the main functional groups for gelatin and BE are amine groups and OH^- groups. The vibrations/spectral positions of amine groups and OH^- groups may change with the interactions with other substances. Duymuş et al. (2014) examined BE extract and stated that polyphenols and anthocyanins are the main components. Anthocyanin compounds may also have, groups of alkanes, aromatic groups, and pyran rings (Espinosa-Acosta et al, 2018; Cabrera-Barjas et al, 2021). In particular, anthocyanin compounds have absorption in the 3400-3100 cm^{-1} (OH), 2900-2840 cm^{-1} (C-H aliphatic), 870-675 cm^{-1} (C-H aromatic), and 1660 cm^{-1} (C=C aromatic) (Wahyuningsih et al, 2017). 1160-900 cm^{-1} is attributed to the C-O stretching vibration of the sugar moiety of the glycosides and the aromatic C-O stretching. C-O stretch and C-O-H bending of phenols, ether, esters, alcohols, and carboxylic acid can be also detected between 1400-1150 cm^{-1} (Westfall et al, 2020). Looking closer at Figure 5.3, there are many differences between spectrums such as shiftings, ascending/descending, and broadening in intensities, splittings, and new bands. Differences between spectrums of GL, GLE, GLES, and GLESA in regards to shifting wavenumbers and peak assignments were detailly explained in Table 5.2.

After the encapsulation of BE, the determined changes in the position of the peaks at ~3299-3282 cm^{-1} and ~1642-1525 cm^{-1} for GLE, GLES, and GLESA suggested that the O–H groups in the anthocyanins formed H bonds with the N–H and O–H groups (proteins of gelatin). These changes may prove the H bond between gelatin, BE, SnO_2, and Au molecules. Intramolecular interaction and H bonding between extracts, metals, and biopolymers have been previously confirmed (Cabrera-Barjas et al, 2021; Duan et al, 2021; Alizadeh Sani et al, 2022b, Alizadeh Sani et al, 2022a). Between 3300 and 3100 cm^{-1} intensities are increased and broadening is observed after the addition of SnO_2 and Au nanopowder. A peak at 3067 cm^{-1} for GL disappeared and broadened for the GLES spectrum.

Table 5.2 : Transmittance wavenumbers and peak assignments of initial nanofiber sample spectrums.

Wavelength GL (cm^{-1})	**Wavelength GLE (cm^{-1})**	**Wavelength GLES (cm^{-1})**	**Wavelength GLESA (cm^{-1})**	**Responsible functional groups***
3282.1	- 3298.5	- 3287.5	- 3286.5	υ(NH), υ(−OH) Amide A υ(−OH)
3067.5	-	- Shoulder	- Shoulder flattening	υ(−OH) υ_{OH}(Sn-OH)
2938.8	- 2928.6	- 2932.2	- 2928.6	υ(CH) Amide B υ(CH) (attributed to -CH_2 and -CH_3 stretching vibrations)
2877	2877 (shoulder)	2877 (shoulder flattening)	2877 (shoulder)	υ(CH) (attributed to stretching vibrations of −CH_3 and CH_2 aliphatic groups)
1632.8	-	-	-	υ(C=O) Amide I
	1642	1634.9	1641.8	υ(C=C) and υ(C=O) aromatic rings, υ(NH) of carboxylate groups
1525	- 1541.2	- 1537.7	- 1537	δ(NH), υ(CN) Amide II υ(C=C) of aromatic rings
1445.8	-	-	-	δ(C−H) asymetric stretching vibrations of CH_2 groups, υ(C=O), COO symmetric stretching
	1450.7	1450.6	1450.4	(C=C) of aromatic rings, (C-H) aromatic groups
1403.3	-	-	-	δ(N–H), υ(CN), υ(C–O)
	1407.3	1407.3	- 1405.3	υ(C–O) Au-O streching, υ(C–O)

Table 5.2 (continued): Transmittance wavenumbers and peak assignments of initial nanofiber sample spectrums.

Wavelength GL (cm^{-1})	Wavelength GLE (cm^{-1})	Wavelength GLES (cm^{-1})	Wavelength GLESA (cm^{-1})	Responsible functional groups*
1333				
	1335.9	1335.5	1333.9	
1238.8	-	-	-	υ(C–O-C) asymmetric Scissoring plane vibration of phenol ring
	1242.7	1242.5	1242.7	
-				
	1205.1	1203	1201.1	
1163.4	-	-	-	
-	1151.2	1151	1151.8	
1081.5	1079.2	1078.7	1079.2	υ(C–O)
1030.6				
	1027.1	1024.8	1026.5	υ(C−O−C) esters, δ(C-H) (ortho)
921.6	-	-	-	δ(C-H) (ortho)
	929.5	928.9	931.5	υ(C-H) (ortho)
874	-	-	-	υ(C-H)
	854.2	854.2	856.1	υ(C-H) phenol ring symmetric stretching
-	763	763	759	υ(C-H) phenol ring deformation

*Some functional groups were compiled from; (Amalric-Popescu and Bozon-Verduraz, 2001; Espinosa-Acosta et al, 2018; İnal and Mülazımoğlu, 2019; Westfall et al, 2020; Cabrera-Barjas et al, 2021; Fang et al, 2021) υ: stretching; δ: bending.

The disappeared band and appeared in the new shoulder around 3067 cm^{-1} may be attributed to the fundamental vibration of υ_{OH}(Sn-OH) (Amalric-Popescu and Bozon-Verduraz, 2001; Korotcenkov et al, 2011). This shoulder flattened after the addition of Au nanopowders.

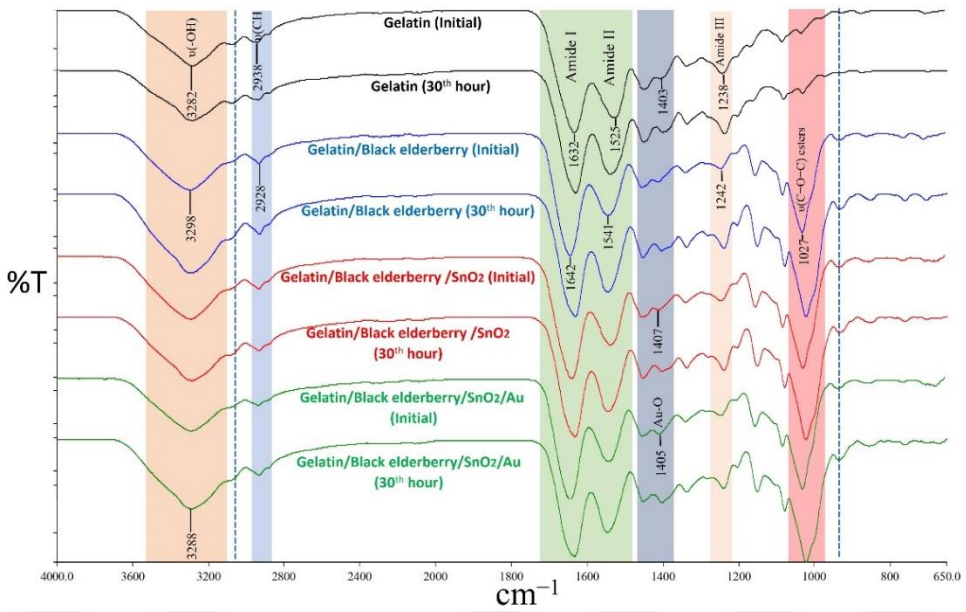

Figure 5.3 : The infrared spectrums of GL, GLE, GLES, and GLESA nanofiber samples on initial and 30th hours. Spectrums shifted vertically for clarity.

The intensity in the region between 1700-1500 cm^{-1} was also changed. The reason may be attributed to C=C stretching vibrations of anthocyanins (Cabrera-Barjas et al, 2021). Furthermore, compared to GLES, the peak intensity at 3300-3100 cm^{-1} and 1670-1610 cm^{-1} attenuated and widened for GLESA, suggesting H bond interaction between Au nanopowders and other components (Wu et al, 2019). Asymmetrical C–H tension bands of $–CH_2$ groups at 1446 cm^{-1} for GL, moved to 1450 cm^{-1} for GLE, GLES, and GLESA and became broadener with weaker intensities, which may be attributed to change in C-C aromatic ring vibrations (İnal and Mülazımoğlu, 2019). The band at 1407 cm^{-1} for GLES, moved to 1405 cm^{-1} for GLESA and showed enhancement of intensity which became wider with the presence of O-C-O and Au-O bonds. The changed intensity of bands between 1050-950 cm^{-1} and 860-840 cm^{-1} could be attributed to the presence of an aromatic ring in ortho substitution (C-H). Furthermore, a specific high absorption peak at 1078 cm^{-1} in the spectrum of GLE, GLES, and GLESA was attributed to the C–O stretching vibration of polyphenols or proanthocyanin. Similarly, Cabrera-Barjas et al. (2021) observed increased intensity of bands between 1200-700 cm^{-1} for nanofibrous β-chitin films integrated with BE.

Other differences in spectrums were splitting, cleaves, new bands, and shoulders. There was a peak at 1541 cm^{-1} for GLE (Figure 5.4C). After the integration of SnO_2 into the material, this peak moved to 1537.7 cm^{-1}, and split which was shown in partially enlarged drawing one. This splitting was disappeared after Au nanopowder

added to the material (GLESA). It is also important to note that splitting at 1634.9 cm^{-1} for the GLES spectrum observed, which was not seen for the GLE spectrum as can be seen in partially enlarged drawing two. These splitting may be attributed to Sn-O bonds. After combination with Au, the Sn-O bond disappeared and changed to Au-Sn-C carbon skeletal vibrations and/or stretches (Křenek et al, 2012).

Stabile peaks for GLE, GLES, and GLESA spectrums exactly at 1450 cm^{-1} showed aliphatic, aromatic groups (C-H), plane deformation peaks of methyl and methylene groups with reduction processes that prove the incorporation of BE extract (Bankar et al, 2010). Detected shoulder around 950 cm^{-1} for GL disappeared for GLE, GLES, and GLESA. One new band was determined at 763 cm^{-1} for GLE after the encapsulation of BE which could be corresponded to the C-H stretching vibrations from anthocyanins. Cabrera-Barjas et al. (2021) also located bands between 850 cm^{-1} and 700 cm^{-1} for pure BE extract. Shifted band for the GLE spectrum between 860-840 cm^{-1} may correspond to the phenol ring C-H deformations (Espinosa-Acosta et al, 2018). A high stretching band at 707 cm^{-1} was also detected. This band disappeared after the integration with SnO_2 for the GLES spectrum (Figure 5.4A). New vibration peaks were observed between the 700-650 cm^{-1} region, which can be attributed to Sn-C carbon skeletal vibrations or stretches (Křenek et al, 2012). Furthermore, in a study by Chung et al. (2014), it has been indicated that the peaks at wavenumbers between 680-660 cm^{-1} are associated with Sn–O-Sn bond vibration streches. In this respect, these newly formed vibration peaks may also correspond to Sn-O bonds for the GLES spectrum. GLESA spectrum indicated that an extra vibration band with splitting appeared in this range after Au nanopowder addition, proving increasing the stability of material with an Au-O bond (Panicker et al, 2020). Cleaves between 680-670 cm^{-1} for the GLES spectrum, formed one stretching band with increased intensity when gold NP is introduced into the material (GLESA) probably because of the Au-OCO bonds (Korotcenkov et al, 2011; Panicker et al, 2020). Cetinkaya et al. (2022) characterized zein nanofibers loaded with gold nanospheres and stated that 670-650 cm^{-1} might show the vibration frequency of Au–O ionic bonds. Moroever, Ivanovskaya et al. (2021) indicated that wavenumbers of Sn-O vibrations in SnO_2 increased between 692-676 cm^{-1} when colloidal Au is introduced into SnO_2.

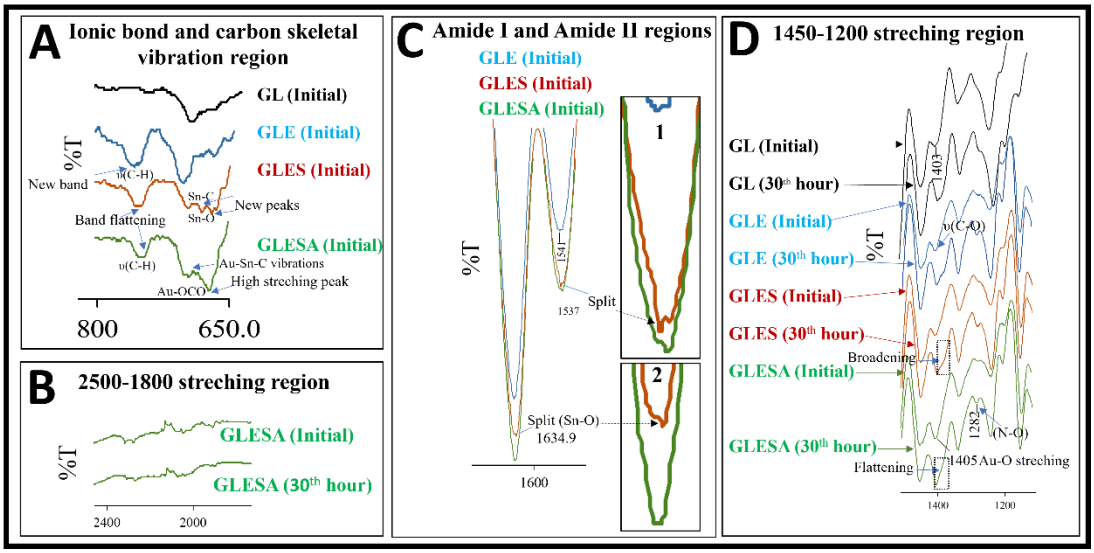

Figure 5.4 : Enlarged peak assignments of GL, GLE, GLES, and GLESA nanofiber sample spectrums. (C1 and C2; partially enlarged drawings). Spectrums shifted vertically for clarity.

5.4.2.2 FTIR measurements of nanofibers after absorption of volatiles

As can be seen from Figures 5.3 and 5.4, and Appendices (Figure B3, Figure B4), after absorption of volatiles, the transmittance differences were observed between 1500-1000 cm^{-1}. The reason could be attributed to the increase in the concentrations of non-protein nitrogenous constituents and ethyl esters as a result of autolytic or microbiological proteolysis (Sone et al, 2011; Saraiva et al, 2017; Fengou et al, 2019).

The absorption of these compounds may be also associated with peak intensity changes in C-H and N-H bonds, in the spectral regions of 2995–2860 cm^{-1} and 1750–1705 cm^{-1}, respectively (Govari et al, 2021). Biochemical composition changes in the flesh due to early autolytic degradation, pH or water activity can be observed because of the growth of spoilage bacteria (Tito et al, 2012). The initial spectrum for GLESA revealed that there is a band between 2010-1990 cm^{-1}. After outgassing, with the appearance of nitrogen compounds, this band changed to several peak intensities (Figure 5.4B) which may indicate that these compounds are weakly adsorbed on Sn/Au nanostructures (Amalric-Popescu and Bozon-Verduraz, 2001).

It has been stated that hake fish species have high water content (~80%) (Otero et al, 2017). Comparing Fig. B.3 and B.4, an increase in intensities for O-H stretches after storage, was most likely due to water molecules since the humidity of nanofibers increased with the water loss of the fillets (Socrates, 2001; Saraiva et al, 2017; Fengou et al, 2019).

The H_2S-producing bacteria (typical of *Shewanella Putrefaciens*) produce sulfur compounds resulting in the spoilage of hake fish (Fernández-Saiz et al, 2013; Sullivan et al, 2020). In this context, 1390-1370 cm^{-1} may indicate molecular absorption of Sulphur compounds, on oxygen atoms of SnO_2 for the GLES spectrum. The oxygen capable to form a coordination link with SnO_2 is created by the removal of H atoms from OH groups. As can be seen from Figure 5.4D, shoulder at 1390-1370 cm^{-1} attributed to the Sulphur compounds vibrations, became broader when SnO_2 added, then after integration of Au nanopowders, this shoulder flattened/disappeared (Berger et al, 1996; Ivanovskaya et al, 2021).

The adsorption peaks of N-O (1290-1170 cm^{-1}) appeared and weak broadening was observed in H-O (1710-1600 cm^{-1}) for the GLESA spectrum after exposure to volatiles. Wang et al. (2001) previously studied the reacted products of NH_3 gas on the SnO_2 material surface. They have stated that after the decomposition reactions of NH_3, end products (NO_2 and H_2O) may occur. Therefore, intensity changes of the N-O and H-O bands in present spectrum may indicate the presence of NO_2 and H_2O. After outgassing and then absorption of gases, compared to initial spectrums, a loss of transmission is observed at 1180 cm^{-1} and a weak shoulder near 1120 cm^{-1} is detected. This fall of transmission is ascribed to the produced free electrons upon outgassing (Amalric-Popescu and Bozon-Verduraz, 2001).

Values of band area ratios were examined to evaluate the stability of nanofiber samples (Table 5.3).

Table 5.3 : Measured band area ratios of GL and GLESA nanofibers on inital and 30^{th} hour.

Transmittance Band Area Ratio	Sample	Initial	After absorption (30^{th} hour)
TI ($T_{1590\text{-}1485}/T_{3700\text{-}3100}$)	GLESA	0.1121±0.004	0.1143±0.002
TII ($T_{1485\text{-}1425}/T_{3700\text{-}3100}$)	GLESA	0.0833±0.002	0.0845±0.001
TIII ($T_{1070\text{-}950}/T_{3700\text{-}3100}$)	GLESA	0.1197±0.004	0.1199±0.005
TIV ($T_{1585\text{-}1480}/T_{3700\text{-}3115}$)	GL	0.0604±0.002	0.0750±0.001
TV ($T_{1480\text{-}1420}/T_{3700\text{-}3115}$)	GL	0.0564±0.003	0.0734±0.002
TVI ($T_{1045\text{-}950}/T_{3700\text{-}3115}$)	GL	0.2003±0.002	0.1843±0.003

On the initial hour and 30^{th} hour, transmittance band area ratios were closer for the GLESA spectrum (1.90%, 1.47%, and 0.27% difference for TI, TII, and TIII respectively). However, for GL, the difference was calculated as 24.28%, (TIV) 30.29% (TV), and 8.72% (TVI) respectively. In a study by Cakmak-Arslan (2022), the

effect of frying on different oils was examined by calculating the area ratios of FTIR bands. Heating the oils caused increased ratios of 3475/2854 cm^{-1} and 1744/2854 cm^{-1} bands, suggesting different thermal stabilities. Moroever, it has been stated that functional groups such as amines prevent the aggregation of the NPs by electrostatic or Van der Waals interactions and enhance stability (Singh et al, 2020). In this sense, the lower difference for GLESA band areas may indicate the higher stability of the nanofiber sample that contains Au nanopowders.

Microbial metabolites (amides, amines, ethyl esters, aldehydes, and ketones) have been associated with the metabolic activity of specific spoilage microorganisms (Parlapani et al, 2014; Parlapani et al, 2017; Fengou et al, 2019; Govari et al, 2021). In this sense, changes in intensities with the storage may be related to the production of free amino acids, non-protein nitrogenous constituents, peptides, and other volatile compounds in fish fillets. Therefore, the band distances were compared to reveal the relationship between spoilage and produced metabolites. The values on the initial hour and after absorption for the GLESA spectrum were presented in Table 5.4.

It should be noted that transmittance peak intensity differences appeared to increase after storage. Higher differences in N-H, C-N, and Au-O stretching regions (T_{1430}-T_{1360}: 35.54%) and N-O stretching regions (T_{1180}-T_{1130}: 27.50%) could be attributed to strong absorption of volatile amines, NH_3, and nitrogenious compounds, generated from hake fish that contains approximately 9-18% non-protein nitrogen (Sullivan et al, 2020). Furthermore, Saraiva et al. (2017) observed wavenumbers linked to volatile amides and amines and stated that their communality value is higher than for other wavenumbers.

All afore-mentioned results prove that specific spectral changes may be responsible for the absorption/attachment of water molecules and volatile compounds to the functional nanofibers during the storage period.

Table 5.4 : Some of the band transmittance distance values of GLESA nanofiber sample on initial and 30th hour measurements.

T_0-T_e	Initial	After absorption (30th hour)
T_{3700}-T_{3090}	4.17±0.032	4.56±0.015
T_{3000}-T_{2900}	0.51±0.025	0.51±0.01
T_{1430}-T_{1360}	1.64±0.01	1.21±0.01
T_{1260}-T_{1210}	1.27±0.02	1.44±0.012
T_{1180}-T_{1130}	2.00±0.025	2.55±0.015

5.4.3 Thermal characteristics of nanofibers

5.4.3.1 Differential scanning calorimetry

The DSC thermograms of electrospun nanofibers are shown in Figures 5.5 and 5.6. DSC curves showed endothermic peaks (Li et al, 2021; Zhang et al, 2021). T_m value corresponds to the polymer network destruction (Zhang et al, 2021). The T_m peak of GL nanofibers appeared around 110 °C which was in accordance with the previous studies (Morsy, 2022; Linh et al, 2010). Doping the gelatin fibers with the BE extract resulted in a shift in T_m (to ~144 °C). Similarly, İnanç Horuz and Belibağlı (2018) found that after the addition of carotenoid extract into the gelatin nanofibers, T_m increased to higher temperatures.

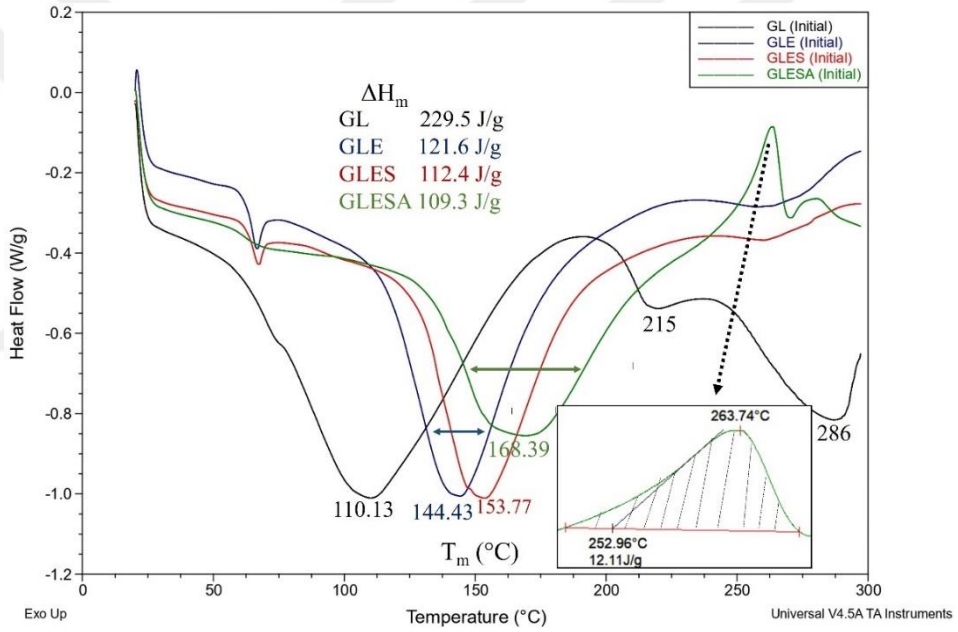

Figure 5.5 : DSC curves of GL, GLE, GLES and GLESA nanofiber samples on the initial hour.

The thermograms of GLE samples indicated that the extract was in the amorphous state in gelatin nanofibers with good incorporation and without crystallization. T_m results from the breakage of H bonds of the triple-helix structure (Morsy, 2022). BE extract increased the T_m owing to the fact that the enhanced H bonding and hydrophobic interaction could affect the stability of the triple helix structure in the polymer. After the addition of SnO_2 and Au nanopowder, the T_m peak of GLES and GLESA samples shifted to 153.77 °C and 168.39 °C respectively. Shen et al. (2021) stated that the amino groups of proline and the OH^- groups of hydroxyproline in gelatin can form H bonds with other additives such as natamycin. Therefore, the formation of

H bonds (ortho, phenol ring symmetric stretchings, etc.) between gelatin, BE extract and nanopowders may cause the improvement of the regularity and compactness of polymer chains. The formation of the cross-linking bonds between the components restricts the mobility of polymer chains, causing enhanced thermal stability (Amjadi et al, 2020). Furthermore, Rath et al. (2016) reported the nanoencapsulation of ZnO NPs in the gelatin nanofibers affected the thermal stability due to cross-linking of ZnO NP to polymer chains. The intensity of the T_m melting transition peaks in the DSC curve of GLES was reduced and became broader when the Au nanopowder was added to the material. In summary, these changes and shiftings may indicate the formation of the new ionic bond complexes as approved by FTIR spectrums.

An endothermic peak at about 215 °C was detected for GL curves, which also appeared at about 210-225 °C in previous studies (Song et al, 2008). This can be the decomposition temperature since ~225 °C is characteristic of gelatin powder (Song et al, 2008; Li et al, 2021). The formation of strong and compact network structures could increase the decomposition temperature of the nanofibers (Lin et al, 2018) An extra endothermic peak around 286 °C for GL. Song et al. (2008) observed a similar broad endotherm (275-300 °C) on the electrospun gelatin nanofibers by DSC data using water/acetic acid 3/7 ratios in solution. The third thermal peak is located for the GLESA sample at 263.74 °C (Figure 5.5; inset image). At this eutectic point, an exothermic reaction may be related to a change in the phase of Au_3Sn to gas which the confirms interaction of Au-Sn nanostructures (Naderi et al, 2012; Tabatabaei et al, 2012). Morsy (2022) determined position change in the endothermic peaks of GL nanofibers to higher temperatures when the diameter of the fibers was higher. This observation is explained by easy solvent evaporation due to the shorter diffusion paths. This statement is in accordance with our results since fiber diameters proportionally increased with increasing T_m.

The addition of BE extract, SnO_2 and Au nanopowder, lowered the value of ΔH_m (Figure 5.5) compared to the control samples, confirming that the formation of triple helix could be impeded by different networks, ionic bond groups, etc., during the electrospinning process (Liu et al, 2016).

Change in DSC curves of nanofibers after absorption of volatiles can be seen in Figure 5.6. The melting, decomposition, or oxidation peaks can disappear, widen, or shift as a result of interaction between components (Celebioglu and Uyar, 2021). Compared

to initial forms, extra endothermic meltings were observed for GLE, GLES, and GLESA samples. Tabatabaei et al. (2012) indicated that metal nanoparticle compositions may exhibit multiple melting temperatures. Third melting was observed at 99.16 °C for the GLESA sample. Although T_m values were decreased on the 30th hour for GLE (133.64 °C), GLES (135.18 °C), and GLESA (137.63 °C), they were still in line with initial results (GLE<GLES<GLESA). Amjadi et al. (2019) examined the gelatin film with ZnO nanoparticles and attributed multiple endothermic peaks to the different crystal structures in the sample. So, higher thermal stability for GLESA may be related to the overall crystallinity of the sample. The incorporation of SnO_2 and Au nanopowders in gelatin nanofiber may be enhanced thermal stability by acting as a thermal dielectric barrier of volatile compounds (Sahraee et al, 2017). ΔH_m value was lowest for GLESA (88.82 J/g) which was also in accordance with the initial GLESA curve.

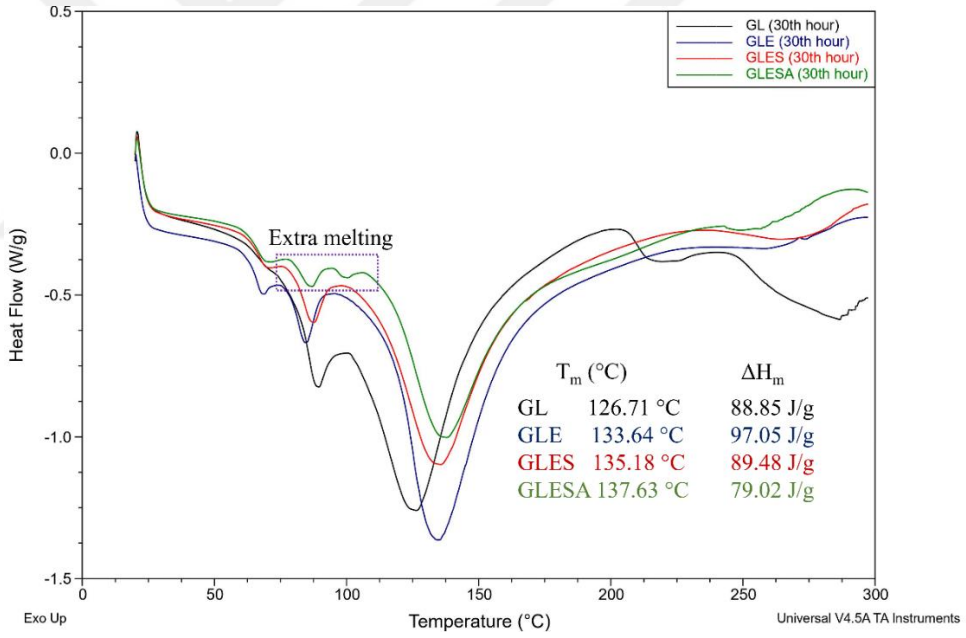

Figure 5.6 : DSC curves of GL, GLE, GLES, and GLESA nanofiber samples on the 30th hour.

5.4.3.2 Thermogravimetric analysis

Thermogravimetric analysis curves (Figure 5.7) show a typical decomposition profile with three distinct weight loss steps regarding (1) water evaporation, (2) organic template decomposition and (3) oxidation of residual organic compounds (Xu et al, 2014). The initial weight loss occured in the range of 40–150 °C, which was attributed to the elimination of absorbed water from the nanofibers during the process of heating.

In the first step of weight change, GLE, GLES, and GLESA decreased weight more slowly than GL, which may be attributed to the entrapment of the moisture by BE extract's hydrophilic anthocyanins (Kim et al, 2022).

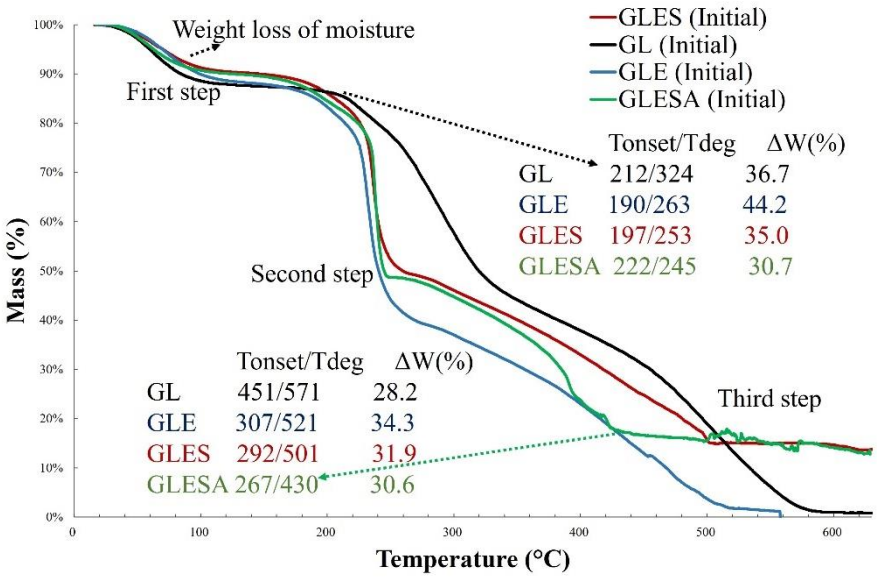

Figure 5.7 : TGA curves of GL, GLE, GLES, and GLESA nanofiber samples on the initial hour.

In the second step of weight change, the significant loss of weight for GL took place in the range of ~210–330 °C, related to the degradation of gelatin. The addition of BE extracts into the gelatin results in a slightly lower thermal resistance than the neat gelatin nanofiber, evidenced by a shift of temperature which starts degradation (T_{onset}) from 212 °C to ~190 °C and a maximum peak of degradation T_{deg} from 324°C to 263 °C. Similar results were expressed by Cabrera-Barjas et al. (2021) for chitin/elderberry extract films. A drastic weight loss between ~200-250 °C for GLES and GLESA may correspond to the oxidation of metal oxides and reduction, which turns carbon to carbon/combined oxygen (Zhang et al, 2016).

In the second step, more weight loss of GLE was observed in comparison with that of GLES, indicating that the existence of SnO_2 NPs improved the thermal stability. Chen et al. (2015) observed similar results by incorporating Au NPs into zein nanofibers. Since Au and Sn metals have different melting points, the combined effect of Au and Sn morphology and element immiscibility could affect T_{deg}, shifting from 253 °C (GLES) to 245 °C (GLESA) on thermograms (Naderi et al, 2012; Vykoukal et al, 2020). GLES and GLESA samples had a lower decomposition rate in the second and third steps than the GLE sample. The formation of bonds between metallic NPs and

gelatin molecules, as confirmed in FTIR results, may yield a stronger network and cause the nanofibers to be stiffer and more compact with improved thermal stability (Baniasad & Ghorbani, 2016).

Unlike GL and GLE samples, there were still residues at 600 °C for GLES and GLESA (14%), probably due to the non-ignitable minerals, and mass ratios were constant over this temperature (Kim et al, 2022). Kwak et al. (2019) stated that as the amount of silver NPs in the gelatin nanofiber increased, the residue at the end also increased. Dai et al. (2011) examined SnO_2 NPs added waterborne polyurethane and indicated that the char residue at 700 °C increased from 1.87% (neat polymer) to 18.31% with SnO_2 addition. In another study by Mousdis et al. (2008), it was found that there was not any loss of mass for Au nanoparticle/SnO_2-based films over 500 °C.

TGA data of samples on the 30th hour was shown in Figure 5.8. Results indicated that weight loss ratios were changed after the absorption of volatiles. Interestingly, the GL sample had more moisture evaporation (14.51%) compared to initial data (11.22%) between 40-150 °C. On the other hand, weight loss was reduced especially for GLES during heating compared to initial data. The weight loss difference could be attributed to changes in nanofibers' structure and drying with the absorption of volatiles on the SnO_2 integrated surface.

The curve slope appears approximately at 313 °C (T_{deg}) for GL is related to gelatin decomposition (Sahraee et al, 2017). This process was slower for GLES and GLESA. Weight loss is reduced and slowed because of the high flexibility acquired after SnO_2 NPs and Au nanopowders embedding where the amorphous regions content increases. Morsi and Abdelghany (2017) stated that up to 366 °C elimination of CO_2, NO_2, NH_3, and hydrocarbons can show weight loss. This range may be related to the thermal decomposition of absorbed volatiles in present data.

After absorption of volatiles, GLES and GLESA samples were more thermally stable compared to the GL and GLE, indicating that more stable structures or groups were generated by the interaction between volatiles, SnO_2 NPs and Au nanopowders. Shifting toward higher temperatures can be assigned to the catalysis ability of SnO_2 and Au nanopowders and their synergistic capability in raising the crosslinking density. The slowed diffusion of degradation products from the bulk polymer to the gas phase results in an improved heating barrier to protect the GLES and GLESA with

enhancement in thermal resistance (Gaabour, 2017; Morsi et al, 2019). The atoms of NPs are generally unstable because of their large surface area and defective structure (Moon et al, 2005). Therefore, with the presence of Au nanopowders, third weight loss could occur at a lower T_{onset} for GLESA (443 °C) sample compared to GLES (452 °C).

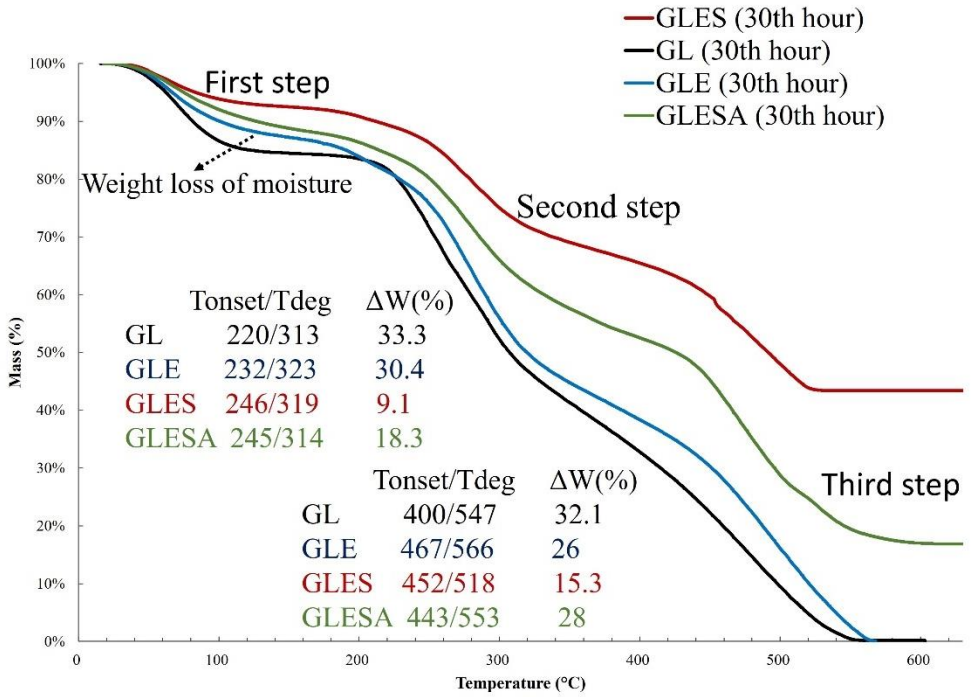

Figure 5.8 : TGA curves of GL, GLE, GLES, and GLESA nanofiber samples on the 30th hour.

Abla et al. (2021) synthesized Au/SnO_2 core-shell nanostructures and found that the organic removal started at 540 °C. Although there was not any residiue left for GL and GLE at 570 °C, similar to mentioned study, there were still residues for GLES (43.41%) and GLESA (17.75%) samples. Drastic residue amount difference may be attributed to the more absorption capability of GLESA nanomaterial surface, which resulted in higher weight loss.

5.4.4 Colorimetric measurements

5.4.4.1 Response to NH_3 and TMA

The color parameters of nanofibers during their exposition to TMA or NH_3 were studied, in order to evaluate the "smart" function of nanofiber layers.

L values of all samples decreased with exposing to TMA at 0.05M (Table 5.5). GLES sample had lowest *L* value (49.3% decrease) after 24 min. The changes in a values had

different trends for GL, GLE and GLES samples. The a values of GL samples had no consistent trend, whereas they decreased for GLE and GLES. The a value changes were higher for GLES sample than other samples, they decreased to 1.29 from 5.15. The b values of GL and GLE samples increased with time whereas they had no consistent trend for GLES.

Table 5.5 : *L*, *a*, and *b* response of the nanofiber samples after exposed to 0.05 M TMA.

	Time (min)	GL	GLE	GLES
L	0	93.96±0.04^{a}	79.55±0.02^{a}	79.47±0.02^{a}
	4	91.98±0.11^{b}	67.54±0.20^{b}	74.12±0.06^{b}
	8	87.58±0.24^{c}	60.70±0.13^{c}	74.35±0.04^{c}
	12	83.70±0.16^{d}	58.17±0.22^{d}	54.84±0.10^{d}
	16	80.93±0.01^{e}	54.82±0.04^{e}	53.13±0.06^{e}
	20	76.32±0.17^{f}	53.67±0.40^{f}	43.37±0.02^{f}
	24	74.90±0.17^{g}	52.39±0.04^{g}	40.33±0.02^{g}
a	0	0.79±0.01^{c}	5.36±0.01^{e}	5.15±0.00^{a}
	4	0.93±0.02^{b}	3.28±0.02^{d}	2.67±0.02^{b}
	8	0.60±0.01^{f}	2.91±0.15^{ac}	2.29±0.09^{c}
	12	0.74±0.02^{d}	2.85±0.12^{ac}	2.26±0.09^{c}
	16	0.65±0.02^{e}	2.97±0.12^{c}	1.50±0.06^{d}
	20	1.07±0.02^{a}	2.41±0.15^{ab}	1.54±0.09^{d}
	24	0.81±0.00^{c}	2.65±0.06^{ab}	1.29±0.09^{e}
b	0	-0.53±0.01^{f}	-1.16±0.01^{f}	-1.32±0.00^{a}
	4	-0.04±0.02^{e}	-1.64±0.01^{e}	-0.94±0.01^{b}
	8	1.42±0.03^{d}	-0.42±0.06^{c}	-1.02±0.00^{bc}
	12	2.59±0.05^{c}	-0.92±0.18^{d}	-1.13±0.02^{c}
	16	2.70±0.10^{c}	-0.52±0.04^{c}	0.99±0.07^{d}
	20	2.84±0.04^{b}	0.82±0.09^{b}	-1.59±0.06^{e}
	24	3.58±0.03^{a}	1.42±0.02^{a}	-1.44±0.09^{a}

$^{a-c}$ Different superscript lowercase letters show differences between the storage hours within same sample and same parameter in columns (p<0.05).

L values of all samples decreased with exposing to TMA at 78x10^{-5} M (Table 5.6). Comparing to the first concentration of TMA, the results were very similar, except for GLES samples. The decrease for GLES samples was less at this concentration of TMA, whereas the decreases for GL and GLE were similar. The a value changes had no distinct trend. On the other hand, the *b* values increased for GL and GLE. The *b* values fo GLES increased up to 16th min, then they decreased.

As a result, the *a* and *b* values were more sensitive to the TMA concentration in terms of trends and values. However, the *L* values appeared to be similar at both concentration, except for the decrase in *L* values of GLES.

Table 5.6 : *L*, *a*, and *b* response of the nanofiber samples after exposed to $78x10^{-5}$ M TMA.

	Time (min)	GL	GLE	GLES
L	0	95.89 ± 0.01^{a}	78.25 ± 0.01^{a}	78.72 ± 0.18^{a}
	4	89.77 ± 0.00^{bc}	75.91 ± 0.06^{b}	78.42 ± 0.04^{b}
	8	93.60 ± 0.19^{ac}	74.67 ± 0.06^{c}	77.7 ± 0.02^{c}
	12	89.68 ± 0.50^{c}	73.32 ± 0.11^{d}	78.32 ± 0.01^{b}
	16	75.78 ± 0.28^{d}	68.13 ± 0.01^{e}	77.99 ± 0.03^{d}
	20	72.82 ± 0.08^{d}	69.25 ± 0.08^{f}	77.64 ± 0.04^{c}
	24	75.77 ± 3.87^{d}	45.67 ± 0.21^{g} (30th min)	76.97 ± 0.01^{e}
a	0	0.32 ± 0.01^{a}	5.11 ± 0.00^{e}	4.91 ± 0.01^{d}
	4	0.43 ± 0.00^{a}	6.17 ± 0.01^{d}	4.52 ± 0.01^{f}
	8	0.30 ± 0.09^{a}	6.01 ± 0.03^{c}	4.65 ± 0.02^{e}
	12	0.08 ± 0.10^{a}	6.27 ± 0.10^{c}	5.39 ± 0.03^{c}
	16	0.35 ± 0.03^{a}	6.26 ± 0.05^{c}	5.75 ± 0.02^{b}
	20	0.57 ± 0.03^{a}	6.86 ± 0.01^{b}	5.69 ± 0.03^{a}
	24	0.77 ± 0.44^{a}	8.70 ± 0.08^{a} (30th min)	4.60 ± 0.03^{e}
b	0	0.17 ± 0.01^{e}	-0.9 ± 0.01^{f}	-1.92 ± 0.02^{g}
	4	1.22 ± 0.00^{d}	-0.55 ± 0.00^{e}	-1.33 ± 0.02^{f}
	8	1.00 ± 0.06^{d}	-0.55 ± 0.01^{e}	-1.04 ± 0.01^{e}
	12	1.89 ± 0.31^{c}	-0.09 ± 0.03^{d}	0.35 ± 0.01^{c}
	16	6.88 ± 0.38^{b}	1.70 ± 0.02^{b}	0.51 ± 0.01^{a}
	20	8.35 ± 0.09^{a}	1.18 ± 0.01^{c}	0.39 ± 0.00^{b}
	24	6.66 ± 0.25^{b}	2.87 ± 0.06^{a} (30th min)	-0.61 ± 0.01^{d}

$^{a-c}$ Different superscript lowercase letters show differences between the storage hours within same sample and same parameter in columns ($p<0.05$).

The color parameters of nanofibers during their exposition to NH_3 were given in Table 5.7 and Table 5.8.

L values of all samples decreased with exposing to NH_3 at 0.05M (Table 5.7). GLE sample had lowest *L* value after 24 min. The changes in a values had different trends for GL, GLE and GLES samples. The *a* values of GL and GLE samples had no consistent trend, whereas they decreased for GLES. The *b* values of GL and GLE samples increased with time whereas they had no consistent trend for GLES.

Table 5.7 : *L*, *a*, and *b* response of the nanofiber samples after exposed to 0.05 M NH_3.

	Time (min)	GL	GLE	GLES
L	0	94.80±0.00^{a}	79.28±0.03^{a}	78.72±0.18^{a}
	4	94.52±0.01^{ac}	73.95±0.06^{b}	76.43±0.02^{b}
	8	93.75±0.00^{b}	68.90±0.06^{c}	74.26±0.01^{c}
	12	94.02±0.14^{b}	66.55±0.04^{d}	67.22±0.12^{d}
	16	94.27±0.39^{c}	62.51±0.18^{e}	68.91±0.22^{e}
	20	83.77±0.01^{d}	61.82±0.03^{f}	64.21±0.63^{f}
	24	82.12±0.04^{e}	60.19±0.03^{g}	64.20±0.23^{f}
a	0	0.43±0.01^{a}	5.28±0.00^{a}	4.91±0.01^{a}
	4	0.39±0.01^{b}	2.19±0.08^{b}	1.87±0.04^{b}
	8	0.35±0.01^{c}	2.24±0.08^{b}	0.81±0.06^{c}
	12	0.29±0.01^{d}	1.94±0.08^{b}	0.54±0.01^{d}
	16	-0.08±0.02^{e}	2.60±0.27^{c}	0.86±0.03^{c}
	20	0.33±0.01^{c}	1.97±0.09^{b}	-0.07±0.04^{e}
	24	0.38±0.02^{b}	2.16±0.04^{b}	-0.87±0.04^{f}
b	0	0.22±0.01^{e}	-0.78±0.01 ^{b}	-1.92±0.02^{e}
	4	0.28±0.02^{e}	-0.62±0.06 ^{c}	-2.71±0.02^{g}
	8	0.6±0.02^{d}	-0.66±0.04 ^{bc}	-2.31±0.01^{f}
	12	0.63±0.02^{d}	-0.39±0.05 ^{ad}	-0.95±0.13^{d}
	16	0.90±0.06^{c}	-0.49±0.14 ^{abcd}	2.59±0.03^{b}
	20	4.46±0.03^{b}	-0.84±0.11 ^{b}	3.30±0.21^{a}
	24	4.64±0.06^{a}	-0.29±0.05^{a}	2.14±0.05^{c}

$^{a–c}$ Different superscript lowercase letters show differences between the storage hours within same sample and same parameter in columns (p<0.05).

L values of all samples decreased with exposing to NH_3 at $3.9x10^{-5}$ M (Table 5.8). Comparing to the first concentration of NH_3, the decrease of *L* values for all samples was less at this concentration of NH_3. The *a* and *b* values generally increased with time.As a result, the trends of *L* values were more consistent compared to the *a* and *b* values at both NH_3 concentration.

As shown in Table 5.9 the color of the GLE and GLES changed from light purple to dark purple when exposed to 0.05 M TMA at the end of 24 min. ΔE of GLE increased faster than GLES in first 8 minutes. However, after 24 minutes of GLES was higher than GLE which could be attributed to stronger sensitivity against TMA. On the other hand ΔE of GL was lower than other samples. These findings indicated that GLES sensing layer possessed high sensitivity to TMA.

Table 5.8 : *L*, *a*, and *b* response of the nanofiber samples after exposed to $3.9x10^{-5}$ M NH_3.

	Time (min)	GL	GLE	GLES
L	0	95.95±0.01[a]	80.96±0.04[a]	80.98±1.42[a]
	4	94.40±0.01[b]	80.40±0.01[a]	80.48±0.01[a]
	8	94.81±0.01[c]	76.35±0.03[b]	77.41±0.06[b]
	12	93.87±0.03[d]	73.37±0.06[c]	77.17±0.02[b]
	16	88.73±0.07[e]	70.83±0.28[d]	77.26±0.02[b]
	20	85.90±0.11[f]	72.45±0.02[e]	77.03±0.40[b]
	24	87.52±0.03[g]	68.57±0.50[f]	76.45±0.02[b]
a	0	-0.65±0.01[f]	4.95±0.01[f]	4.59±0.16[d]
	4	-0.61±0.01[e]	5.32±0.02[e]	5.38±0.02[c]
	8	-0.48±0.01[d]	6.05±0.01[d]	5.56±0.02[bc]
	12	-0.46±0.01[d]	7.69±0.04[c]	5.90±0.02[ab]
	16	-0.30±0.01[c]	7.61±0.04[c]	5.93±0.03[ab]
	20	-0.08±0.00[a]	7.10±0.02[b]	6.11±0.35[ab]
	24	-0.55±0.00[b]	7.48±0.07[a]	4.25±0.03[d]
b	0	0.87±0.01[g]	-0.60±0.01[a]	-2.00±0.01[d]
	4	1.67±0.01[f]	-1.24±0.02[b]	0.04±0.01[c]
	8	1.74±0.02[e]	-1.27±0.01[b]	0.45±0.01[b]
	12	1.60±0.02[d]	-4.13±0.02[c]	0.48±0.01[b]
	16	3.02±0.02[c]	-3.76±0.01[d]	0.68±0.01[a]
	20	1.97±0.01[b]	-3.58±0.01[e]	0.72±0.06[a]
	24	4.59±0.01[a]	-3.34±0.06[f]	-1.05±0.02[e]

[a–c] Different superscript lowercase letters show differences between the storage hours within same sample and same parameter in columns (p<0.05).

Table 5.9 : ΔE response of the nanofiber samples after exposed to 0.05 M TMA.

Time (min)	GL	Photograph	GLE	Photograph	GLES	Photograph
0	5.70±0.03[g]		20.16±0.12[g]		20.27±0.02[g]	
4	7.28±0.10[f]		31.64±0.19[f]		25.00±0.05[f]	
8	11.23±0.24[e]		38.27±0.13[e]		24.75±0.03[e]	
12	15.07±0.16[d]		40.79±0.22[d]		44.12±0.10[d]	
16	17.84±0.01[c]		44.13±0.03[c]		45.68±0.06[c]	
20	22.45±0.17[b]		45.18±0.41[b]		55.55±0.02[b]	
24	23.89±0.17[a]		46.46±0.04[a]		58.57±0.02[a]	

[a–c] Different superscript lowercase letters show differences between the storage hours within same sample and same parameter in columns (p<0.05).

As shown in Table 5.10 the color of the GLE changed from light purple to dark purple when exposed to $78x10^{-5}$ M TMA at the end of 24 min., whereas GLES had almost no change. This can be attributed to that GLES had a sensivitity to TMA concentration. On the other hand ΔE of GL was lower than other samples.

Table 5.10 : ΔE response of the nanofiber samples after exposed to $78x10^{-5}$ M TMA.

Time (min)	GL	GLE	GLES
0	3.69 ± 0.01^{c}	21.35 ± 0.01^{g}	20.90 ± 0.17^{e}
4	9.08 ± 0.00^{c}	23.81 ± 0.05^{f}	21.54 ± 0.04^{d}
8	5.38 ± 0.16^{bc}	24.95 ± 0.07^{e}	22.17 ± 0.03^{b}
12	9.11 ± 0.47^{b}	26.28 ± 0.13^{d}	21.60 ± 0.03^{cd}
16	23.40 ± 0.20^{a}	31.23 ± 0.02^{c}	21.77 ± 0.04^{c}
20	26.59 ± 0.08^{a}	30.27 ± 0.07^{b}	22.32 ± 0.04^{b}
24	23.38 ± 3.75^{a}	43.64 ± 0.05^{a} (30th min)	23.56 ± 0.03^{a}

[a–c] Different superscript lowercase letters show differences between the storage hours within same sample and same parameter in columns ($p<0.05$).

Similar results observed when nanofibers exposed to NH_3 (Table 5.11). The highest total color change was occured later for GLES (between 8^{th}-12^{th} min) compared to GLE (4^{th}-8^{th} min).

Table 5.11 : ΔE response of the nanofiber samples after exposed to 0.05 M NH_3.

Time (min)	GL	Photo graph	GLE	Photo graph	GLES	Photo graph
0	4.58 ± 0.01^{c}		20.39 ± 0.03^{f}		20.93 ± 0.17^{f}	
4	4.79 ± 0.01^{c}		25.08 ± 0.06^{e}		22.67 ± 0.02^{e}	
8	5.36 ± 0.007^{d}		30.09 ± 0.06^{d}		24.83 ± 0.01^{d}	
12	5.09 ± 0.79^{cd}		32.39 ± 0.04^{d}		31.74 ± 0.12^{c}	
16	4.78 ± 0.36^{c}		36.45 ± 0.17^{c}		30.14 ± 0.20^{b}	
20	15.12 ± 0.01^{b}		37.13 ± 0.03^{b}		34.78 ± 0.63^{a}	
24	15.78 ± 0.03^{a}		38.72 ± 0.03^{a}		34.76 ± 0.22^{a}	

[a–c] Different superscript lowercase letters show differences between the storage hours within same sample and same parameter in columns ($p<0.05$).

As shown in Table 5.12 the color of all samples changed when they were exposed to $3.9x10^{-5}$ M NH_3. It appears that the change in GLE had more prominent than the

changes of other two samples. In addition, the changes affacted by the NH_3 concentration.

Table 5.12 : ΔE response of the nanofiber samples after exposed to $3.9x10^{-5}$ M NH_3.

Time (min)	GL	GLE	GLES
0	3.37 ± 0.01^{g}	18.68 ± 0.04^{e}	18.66 ± 1.34^{c}
4	4.52 ± 0.01^{e}	19.42 ± 0.01^{e}	19.47 ± 0.01^{c}
8	4.09 ± 0.01^{f}	23.46 ± 0.03^{d}	22.57 ± 0.05^{b}
12	5.02 ± 0.03^{d}	27.28 ± 0.06^{c}	23.94 ± 0.01^{a}
16	10.06 ± 0.07^{c}	29.56 ± 0.27^{ac}	23.73 ± 0.00^{a}
20	12.88 ± 0.11^{a}	27.86 ± 0.02^{bc}	23.73 ± 0.37^{a}
24	11.46 ± 0.03^{b}	31.59 ± 0.49^{a}	24.32 ± 0.04^{a}

$^{a-c}$ Different superscript lowercase letters show differences between the storage hours within same sample and same parameter in columns ($p<0.05$).

5.4.4.2 Real sample analysis

Color is an important property for smart the packaging functions of nanofibers. As can be seen from Figure 5.9 visually, on the initial hour the GL film was colorless, the GLE and GLES nanofiber was slightly violet, and the GLESA nanofibers were dark violet/light purple color.

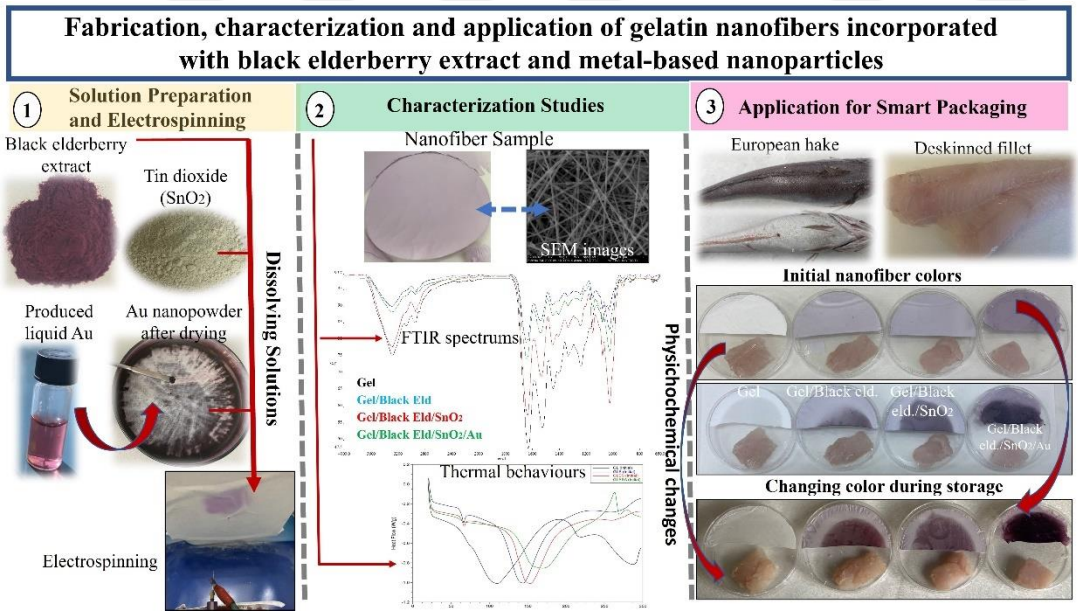

Figure 5.9 : Fabrication, characterization, and application of gelatin nanofibers incorporated with BE extract and metal-based nanoparticles.

GL nanofiber showed the highest *L* value (94.98), and the least *a* (0.02) value (Table 5.13). After the addition of BE extract, the lightness values of GLE and GLES

considerably decreased (L=77.44 and 76.44) with a significant increase in the redness (a=5.80 and 5.71) and decrease in b (-2.44 and -3.73) values (p<0.05).

Table 5.13 : Color measurements of nanofiber samples during storage period.

	Time (h)	GL	GLE	GLES	GLESA
L	Initial	94.98 ± 0.34^{Aa}	77.44 ± 0.14^{Ab}	76.44 ± 0.61^{Ac}	64.23 ± 0.22^{Ad}
	3rd	80.00 ± 3.47^{Ba}	49.87 ± 1.63^{Bb}	49.01 ± 1.32^{Bb}	31.49 ± 0.60^{Bc}
	6th	79.33 ± 2.66^{Ba}	39.39 ± 1.88^{Cb}	45.67 ± 2.70^{Bc}	30.64 ± 0.12^{Bd}
	24th	78.99 ± 1.50^{Ba}	34.68 ± 6.75^{Cb}	42.86 ± 3.90^{Bb}	24.14 ± 0.33^{Cc}
	30th	76.45 ± 2.23^{Ba}	31.64 ± 4.56^{Cbd}	42.07 ± 5.19^{Bc}	24.51 ± 0.13^{Cbd}
a	Initial	0.02 ± 0.01^{Aa}	5.80 ± 0.26^{Cb}	5.71 ± 0.37^{Cb}	10.37 ± 0.05^{Ac}
	3rd	-0.09 ± 0.03^{Aa}	11.24 ± 0.96^{Bb}	13.85 ± 0.64^{ABc}	5.79 ± 1.15^{Bd}
	6th	-0.01 ± 0.05^{Aa}	7.80 ± 1.52^{Cb}	12.91 ± 0.83^{Bc}	4.92 ± 0.30^{Bd}
	24th	-0.01 ± 0.05^{Aa}	14.55 ± 0.70^{Ab}	15.18 ± 1.09^{Ab}	5.76 ± 0.48^{Bc}
	30th	-0.06 ± 0.16^{Aa}	14.87 ± 1.24^{Ab}	15.13 ± 0.83^{Ab}	6.14 ± 0.64^{Bc}
b	Initial	0.44 ± 0.27^{Aa}	-2.44 ± 0.30^{Cb}	-3.73 ± 0.34^{Bc}	-5.01 ± 0.10^{Cd}
	3rd	-0.24 ± 0.33^{Aa}	0.65 ± 0.98^{ABa}	-1.84 ± 0.39^{Ab}	-2.02 ± 0.21^{Bb}
	6th	-0.23 ± 0.09^{Aa}	-0.18 ± 0.07^{Ba}	-2.05 ± 0.46^{Ab}	-2.05 ± 0.04^{Bb}
	24th	-0.24 ± 0.42^{Aa}	1.70 ± 0.32^{Ab}	-1.87 ± 0.21^{Ac}	-3.11 ± 0.14^{Ad}
	30th	0.32 ± 0.16^{Aab}	1.38 ± 1.05^{ABa}	-1.64 ± 0.87^{Abc}	-3.04 ± 0.23^{Ac}

$^{A–C}$ Different superscript uppercase letters show differences between the storage hours within same sample and same parameter in columns (p<0.05). $^{a-d}$ Different superscript lowercase letters show differences between the nanofiber samples within same hour and same parameter in rows (p<0.05).

Similarly, in a study by Alizadeh-Sani et al. (2021) methylcellulose/chitosan-based films containing anthocyanins extracted from barberry showed lower L values (54.33) with higher a (22.5) compared to colorless film (L=90.00; a=-0.33). The higher a values were associated with red color, due to the presence of pigments. Eze et al. (2022) stated that there can be an interaction between flavonoids/phenolic acids and metal ions, which modify the color produced by the anthocyanins (co-pigmentation effect). This could be attributed to the lowest L values (64.23) with the highest a (10.37) for the GLESA nanofiber that contains gold nanopowders (p<0.05).

L, a, b change ratios for GLE, GLES, and GLESA samples were higher relative to the GL sample during the storage period. For instance, there was no significant difference between a and b during the 30th hour for GL (p>0.05). The higher color changes for other samples are mainly attributed to changes in anthocyanin's chemical structure. Alizadeh-Sani et al. (2021) indicated that barberry anthocyanins are converted to quinoid anhydrous bases with violet color, since the pH rises. As confirmed by FTIR results in previous sections, the removal of H atoms from OH groups create structural transformations, leading to the formation of N-O bands because of the free oxygen

anions. Volatile ions may stimulate the creation of an alkaline condition on the surface or inside the nanofiber with the production of end products (NO_2). The reason for the variation in *L, a, b* could be also related to combination of volatile compounds with H_2O embedded in the nanofiber, which leads to the production of ions of NH_4^+ and OH^-. The OH ions produced an alkaline environment, which consequently changes the color of the nanofiber (Jamróz *et al.*, 2019).

In the first 24 hours, *L* values decreased regularly for all samples. However, the color of the GLESA sample became more intense and turned to dark purple with lowest *b* value (-3.11) and the lowest *L* value (24.14) on the 24th hour ($p<0.05$). Alizadeh Sani et al. (2022b) indicated that the addition of TiO_2 NPs may be led to less light penetration through films and be reflected by the white back plate, which can reduce the lightness more. Furthermore, it has been stated that amines with electron-rich N atoms are easily bound to the surface of metallic NPs through the interactions between N and the electron-deficient surface of metallic NPs (Vilela, González & Escarpa, 2012). Thus, absorbed gases could induce the Au NPs aggregation through the cross-linking effect producing a stronger *L* and *b* change for the GLESA sample.

The degree of fish spoilage is increase with the growth of bacteria and lipid oxidation, which causes the release of more volatiles such as amines, aldehydes, and gases. As confirmed by FTIR results, functional groups such as Au-OCO, Au-Sn-C, or N–H in nanofibers can absorb volatile gases and an H bond can be formed between the carboxyl group and amines leading to the formation of N-O or other bonds (Naghdi *et al.*, 2022). All these findings could be attributed interaction of volatiles and newly formed Au-Sn metallic nanostructures in the GLESA sample with color change.

5.4.5 Physicochemical analysis

As known fish spoils faster than meat under chilled conditions (Kanatt, 2020). Moreover, hake fish's short shelf life and poor quality remain challenging. Biochemical reactions are key reasons for fish freshness loss during storage. The accumulation of metabolites such as amines, aldehydes, ketones, and esters, causes off-flavors conducting sensory product rejection. The other spoilage volatile compounds found hake fish were alcohols, ketones, organic acid, amines, esters, sulphur-containing compounds, and esters (Opara et al, 2022). In this context, it is important to trace physiochemical changes in hake fillets (González et al, 2022). In

this section, the ability of the developed nanofibers to detect spoilage was evaluated by analyzing the physicochemical characteristics of fillets (pH, TMA, TVBN) together with ΔE changes occurring in the nanofibers. Mendes et al. (2021) stated that, hake products with TVBN between 10 mg and ≤20 mg/100 g refer to good quality, 20 mg to ≤35 mg/100 g inferior quality and >35 mg/100 g should be rejected. The initial TVBN value of the hake fillet was found as 21.93±1.97 mg/100 g. It has been indicated that higher initial TVBN values could be observed by using hake fillets instead of whole fish (Simeonidou et al, 1997; Ruiz-Capillas and Moral, 2001). Furthermore, upon checking the literature there are many similar studies indicating >20 mg/100 g content in the first analysis period for *Merluccius Merluccius* fillets (Pérez-Villarreal and Howgate, 1987; Sotelo et al, 1995; Å Nia Baixas-nogueras et al, 2002; Rodríguez et al., 2004). This trend was also observed in other hake species. For instance, in a study by Mendes et al. (2021) 20 different deep-frozen hake fillets (consisting of *M. hubbsi, M. capensis, M. paradoxus,* and *M. productus* species) had a high initial TVBN range, and samples that contains TVBN ≥18.8 mg N/100 g accounted for 10% of the total, with the highest value of 23.5±2.8 mg/100 g. In another study reported by Simeonidou et al. (1997), initial TVBN levels (25.46±0.26 mg N/100 g) of *M. Mediterraneus* increased to 42.26±0.47 mg N/100 g in fillets, after 12 months of frozen storage at −18 °C. According to the above-mentioned studies, the initial TVBN level of the fresh *M. Merluccius* fillets in the current study can be considered as satisfactory. As expected, on the 3rd hour TVBN values increased to 28.28±0.1 mg/100 g. Volatile amines such as NH_3, and DMA collectively recognized as TVBN are produced due to the proteolysis of fish meat during storage which is an important parameter for indicating spoilage (Kanatt, 2020). TVBN accumulation showed that the breakdown of proteins and nitrogen-containing compounds was begun. In the 6th hour it was increased to 30.52±0.36 mg/100 g. As mentioned before, the TVBN value is an essential freshness indicator that may also be responsible for the odor and taste present in fish (Mendes *et al.*, 2021). Opara et al. (2022) indicated that TVBN levels below the limit of 35 mg N/100 g, allowed for hake species. TVBN already exceed the limit on the 24th hour (38.36±1.63 mg N/100 g) and increased to 39.57±1.16 on the 30th hour. Similar increase with storage has also been observed by previously mentioned authors.

Other variations such as pH changes may also occur with biochemical and/or microbiological changes in fish muscle. The changes in pH and TVBN of hake fillets and ΔE of GLESA sample during 30 hours storage period are shown in Figure 5.10. As can be seen from the graph, results showed similar trends with each other. According to Howgate (2009), the post-mortem pH could be found up to 6.8. Previously, the mean pH values of 6.8 (Ciarlo et al, 1985) and 6.85 (Sánchez-Valencia et al, 2014) were reported for *M. hubbsi* and *M. merluccius* species respectively. So, the initial pH of (6.8±0.06) hake samples in this study was within the previous reports, which was dropped to 6.44±0.01 in the 3rd hour. Neira et al. (2019) stated the approximate limit value for the safe consumption of hake of products as 7.3. In their study, the pH value of unpacked *Merluccius hubbsi* is increased up to 7.32 after 28 days of −4±1 °C. Based on previous studies pH 7.3 can be recommended as the threshold for the *Merlucciidae* family, which was found to be 7.36±0.01 on the 6th hour in the current study. At room temperature, pH values were increased to 7.82±0.01 and 7.92±0.02, in the 24th and 30th hours, respectively. In a study by Opara et al. (2022) fresh cape hake (*Merluccius capensis*) fillets stored at 8 °C for 3 days had 7.4 and 8.2 pH on active and passive modified atmosphere conditions, respectively. In another study by Ordóñez et al. (2000) pH of *M. merluccius* hake steaks stored in air at 2±1°C was increased from 6.7 to 7.7 in 14 days. In this context, storage temperature and time are considered important factors that affect pH because when storage temperature increases, the pH increase accelerated for the 24th hour and 30th. Increases in the pH value of fish muscle during storage above 0 °C have been reported to indicate the release of NH_3, TMA, derived with microbial action and or/lipid autoxidation with enzymatic reactions (Sullivan et al, 2020; Mendes et al, 2021), resulting in the change in color of the nanofibers with absorption. So, especially before the 24th hour, the pH value of the samples exceeded the limit value.

The TMA value of fish meat samples was determined as 1.94 mg/100g at the end of 3rd hour. Especially, a more rapid increase was observed during the 6th hour of the analysis (6.32 mg/100g, $p<0.05$). Initial values of urea in hake muscle degraded and converted to NH_3 by the microbiota which increases TMA content Ordóñez et al. (2000). Despite of increase in TMA, on the 24th hour in other words 1 day later, the TMA value of fish meat samples observed at room temperature in sterile plates was found to be 7.45 mg/100g. Following this analysis period, the TMA value reached the

limit value determined as unfit for human consumption 8 mg/100g. TMA concentration of fish samples is evaluated as an important indicator to reflect the freshness (Orban et al, 2011; Ceylan et al, 2017a). In this sense, as stated by Malle and Poumeyrol (1989) and Souza et al. (2010), values between 5 mg/100 g and 10 mg/100 g were recommended as limit value for human consumption. In the present study, an 8 mg/100g TMA value was accepted as the limit value. As can be seen from the results fish meat samples kept in plates were spoilt over time and the color changes in nanofibers hold in the plate confirmed with TVBN, pH, and TMA increased at the same conditions. Based on the data, it can be concluded that the hake maintained freshness up to the 3rd hour, began to decay after the 6th hour, and already spoiled on the 24th hour. This study showed that in conjunction with TMA, TVBN, and pH, esters and sulphur-related compounds that were confirmed by FTIR could be used as spoilage markers for *M. Merluccius* fillets. The visible color change of gelatin nanofibers with BE extract is evaluated as an important indicator of hake products to alert the consumer of its spoilage. Previously, similar methods for anthocyanin-added materials were used to reflect the freshness of seafood products. For instance, gelatin films that are integrated with anthocyanin are used for a color change when fish or shrimp are spoiled (Kanatt, 2020; Kim et al, 2022).

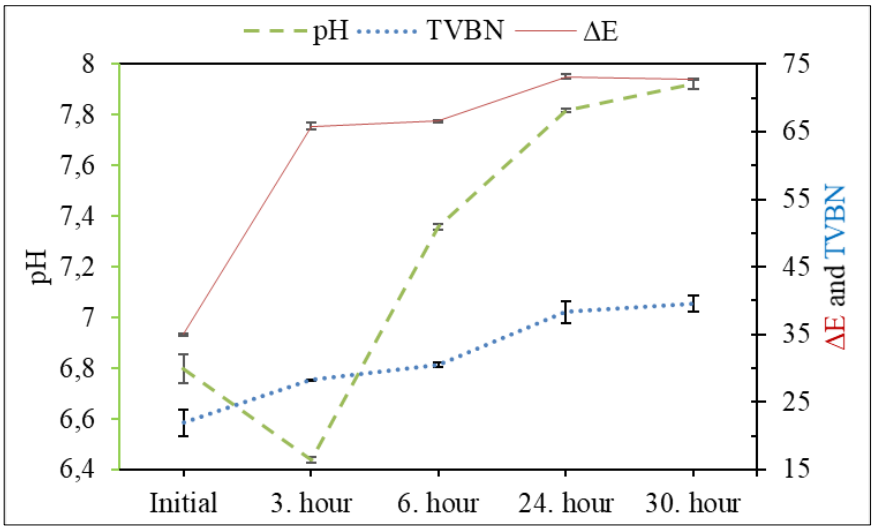

Figure 5.10 : TVBN, pH of fish fillets and *ΔE* changes (GLESA sample) during the storage period.

Correlations of color parameters of nanofibers versus TVBN, pH, and TMA values of the hake fillets during storage at room temperature were also presented in Table 5.14. The TVBN values of hake fillets appear to be correlated with L and ΔE of GLE nanofiber (R^2 = -0.920 and R^2 =0.927, respectively). The correlations of TVBN and

the color parameters of other nanofibers were relatively weak compared to the GLE nanofiber. The correlation of pH values of hake fillets and color parameters seemed very low, the best correlation belonged to the GLE nanofiber (R^2=0.720). On the other hand, the correlations between TMA values and color parameters such as L and ΔE of GLE nanofiber were the highest ones (R^2=-0.987 and R^2=0.979, respectively). In addition, the correlation between the TMA and L value of GLES nanofiber was also high (R^2=-0.965). These results suggest that the color parameters, mostly L value, of GLE and GLES nanofibers correlated with TVBN or TMA, meaning that GLE and GLES nanofiber layers were more responsive to volatiles than to pH values of hake fillets.

Table 5.14 : Correlation measurements of color values against chemical results.

Sample	Color parameter	TVBN	pH	TMA
GL	*L*	-0.831	-0.524	-0.711
	a	-0.316	0.171	0.678
	B	-0.234	0.051	0.494
	ΔE	0.870	0.581	0.678
GLE	*L*	-0.920	-0.717	-0.987
	a	0.872	0.553	0.295
	B	0.906	0.571	0.401
	ΔE	0.927	0.720	0.979
GLES	*L*	-0.855	-0.572	-0.965
	a	0.863	0.524	-0.683
	B	0.861	0.552	0.636
	ΔE	0.857	0.571	0.580
GLESA	*L*	-0.865	-0.561	-0.805
	a	-0.653	-0.364	0.072
	B	0.399	0.043	-0.764
	ΔE	0.872	0.570	0.800

5.5 Conclusion

Structure and integrity of the nanofibers were affected after SnO_2 and Au nanopowder integration. SEM images indicated that SnO_2 and Au nanopowders were deposited on the surface. Increasing the solid material concentration showed thickening and swelling in the nanofibers with a higher average diameter that confirms successful integration.

FTIR spectrums proved the presence of functional groups of anthocyanins. For instance, the intensity of the absorption peak at 1735.93 cm^{-1} was reduced and moved to the lower wavenumber, which is probably associated with the H bonding and dipole dipole interactions between the anthocyanin's aromatic rings-polymer matrix. These changed peak intensities proved that there is an H bonding interaction between gelatin, BE, SnO_2, and Au molecules. The transmittance distance ratios confirmed a close relationship between the degree of spoilage of metabolic activities. Compared to other spectrums, band intensities are wider but weaker at 3700-3100 cm^{-1}, 1700-1600 cm^{-1}, 1050-950 cm^{-1}, and 870-840 cm^{-1} for GLESA. Changes after 30 hours might reflect an increase in the concentrations of peptides and free amino acids because of autolytic activities and microbiological proteolysis in meat. Specific spectral changes may also associate with the degradation of hydroperoxides and the formation of saturated aldehydes, alcohols, ketones, acids, and esters which may be indicative of the absorption of volatile gases by nanofibers. Chemical interactions with volatiles affected the *L*, *a*, and *b* values of the nanofibers with BE extract and metallic nanoparticles which shows favorable practical application. Producing volatile compounds such as amines and NH_3, was confirmed with the increase in TVBN, pH, and TMA due to the activity of endogenous and microbial proteolytic enzymes, that degrade proteins. Changing the color of nanofibers is attributed to the absorption of volatile compounds such as NH_2, H_2S, etc. The incorporation of metal NPs improved nanofiber sample's thermal stability in terms of DSC and TGA results. Segmental motions of polymer molecular changes were restrained by incorporated NPs, causing the increase of T_m that suggested thermally stable hydrogen bonding. The introduction of SnO_2 and Au nanopowders in gelatin fibers leads to a change in the second-stage degradation process in TGA thermograms probably because of the various binding interactions. The lower weight loss observed for GLESA in comparison with that of GL, and GLE, indicates that the existence of nanoparticles improved the thermal degradation stability of gelatin nanofibers. The TGA curve of GLES and GLESA showed that thermal stability enhanced because of the interaction between the nanofiber and volatiles after 30 hours. Lower weight losses in GLES and GLESA samples were observed probably due to higher NP contents. When all results are evaluated together, it can be concluded that changing *L, a,* and *b* values of nanofibers during spoilage of hake fish is related to chemical reactions that are confirmed by spectral changes, which also affected the nanofiber thermal behavior and even

morphology. The high thermal stability of the GLESA sample greatly showed it possible applications as a smart food packaging layer. However, regarding the correlation between color parameters and TVBN, pH and TMA values, GLE and GLES nanofiber layers were more responsive to volatiles than to pH values of hake fillets.

The results of the present work suggest the possible application of the gelatin nanofibers incorporated with BE extract and metal-based nanoparticles permits the visual monitoring of the quality of European hake fish and can be applied as a color-changing indicator for flesh foods.

6. CONCLUSIONS

In this dissertation, biopolymer-based nanofiber systems fabricated with antimicrobial or volatile gas sensing functions and characterized. Chapter 2 indicated the recommended consumption time (24h) for smoked fish products after opening the package. Revealing quickly the seafood products' quality changes is important. In this sense, Chapter 2 also revealed that dielectric loss factor increases and surface tension, the electrical conductivity of fish meat changes during the storage and these measurements can be used as fast quality index methods that guide future scientific studies. Chapter 3 results revealed that the dielectric changes could be limited by using Au-zein-based nanofibers. Furthermore, the TMAB load of fillets treated with Au-zein nanofibers was more slowly increased as compared to the control groups (up to 21.64% difference) during the storage period, showing successful limitation of microbiological spoilage. In Chapter 4, molecular characterization proved that gold ion-zein molecule binding promotes the successful integration of the gold nanospheres. In addition, translational diffusion coefficient, major axis values, aggregated nanofibers hydrodynamic radius, and PDI analyses were developed with long rod equation calculations which were also innovative parts of this chapter. In Chapter 5, gelatin nanofibers without (GL) and with 10wt% BE extract (GLE), with 5wt% SnO_2 (GLES), and with 2wt% Au nanopowders were fabricated. The outcomes of this chapter have demonstrated the color properties of nanofibers that contains BE extract and NPs to trace fish spoilage. Fish spoilage is mainly due to the degradation of protein by microorganisms which leads to the generation of volatile compounds such as NH_3 and amines, which also increase the pH and TMA.

An increase in pH was due to the activity of endogenous and microbial proteolytic enzymes, that degrade proteins, producing compounds such as NH_3 and amines. The use of color indicator nanofibers to monitor changes in the quality of fish during 30-hour storage is applied in real fresh fish samples that are placed in Petri dishes. So, alterations in the quality of hake fish are monitored by measuring changes in nanofiber samples. The nanofiber color changed over time to dark purple, and the TMA content

of the hake proved that it deteriorated at the time of the color change. In this context, deep characterization of nanofibers by DSC, TGA, and FTIR gave an insight into the autolytic and/or microbiological proteolysis of fish meat because the spoilage of fish meat is often accompanied by the formation of nitrogenous gases and changes in pH and TMA, caused by the degradation of proteins and lipids. Changes in color parameters attributed to the production of nitrogenous compounds.

The transmittance changes between 1500-1000 cm^{-1} revealed non-protein nitrogenous constituents and ethyl esters, intensity changes of the N-O revealed the presence of NO_2 and changing shoulder positions revealed Sulphur compounds vibrations. Moreover, thermal behaviors and color measurements indicated that metal-based nanoparticles inside and the on the surface of gelatin nanofibers allow more interaction with gaseous amines.

Overall, this dissertation indicated that spoilage can be predicted rapidly with novel parameters that have been explained in previous sections. Moreover, the successful fabrication and application of nanofibers with nanoparticles presented in this dissertation showed that these systems will provide valuable data about the potential usage of electrospinning for extending storage time and for the detection of volatile amines in fresh seafood products. In this sense, considering their ellipse shape, the characterization of nanofibers with long rod equation calculations will shed light on further characterization studies along with aggregation behavior and stability properties. Specific spectral changes can be used to predict spoilage rates and should be further examined since to the best of our knowledge, the band distances were compared to reveal the relationship between spoilage and absorption of volatiles on nanofibers for the first time. Furthermore, transmittance band area ratios are associated with the thermal stability of nanofiber samples. Changes in DSC and TGA curves of nanofibers after absorption of produced metabolites should be further examined to define the interaction between volatiles, and NPs which will also lead to comparing thermal resistance between samples. Whereas the active coating layer function of Au-integrated zein nanofiber mats was effective, GLE and GLES nanofiber layers exhibited a smart packaging layer function for fresh fish fillets.

Since it is a simple, and low-cost technique, electrospinning has been increasing utilization to fabricate nanofibers in the seafood industry. In this dissertation, an overview of the practical application of biodegradable zein and gelatin-based

electrospun fibers as smart and active packaging layers has been given. It has been concluded that they can be fabricated in combination with extracts and metallic nanomaterials to increase their color, thermal, and absorption properties. Therefore, NPs and plant extracts have the potential to be used as an active and smart food packaging ingredients for further practical applications on seafood and meat products. However, the incorporation of plant extracts and metallic NPs to active/smart coating or packaging layer of nanofibers, their mechanical properties, and water vapor permeabilities must be investigated. In the future, it will be important to determine the cost-effectiveness, of these nanomaterials in real-time applications in a rapid way. Moreover, biodegradability, economic and high-scale production should be considered to create sufficiently large quantities of non-toxic functional materials for application within the seafood industry.

REFERENCES

Å Nia Baixas-nogueras, S., Bover-cid, S., Veciana-nogue Ä, T.S. and Carmen Vidal-carou, M. (2002) Chemical and Sensory Changes in Mediterranean Hake (*Merluccius merluccius*) under Refrigeration (6−8 °C) and Stored in Ice. *Journal of Agricultural and Food Chemistry*, *50*(22), 6504-6510.

Abbas, K.A., Mohamed, A., Jamilah, B. and Ebrahimian, M. (2008) A review on correlations between fish freshness and pH during cold storage. *American Journal of Biochemistry and Biotechnology*, *4*(4), 416-421.

Abla, F., Kanan, S.M., Park, Y., Han, C., Omastova, M., Chehimi, M.M. and Mohamed, A.A. (2021) Exceptionally redox-active precursors in the synthesis of gold core-tin oxide shell nanostructures. *Colloids and Surfaces A: Physicochemical and Engineering Aspects*, *616*, 126266.

Afonso, B.S., Azevedo, A.G., Gonçalves, C., Amado, I.R., Ferreira, E.C., Pastrana, L.M. and Cerqueira, M.A. (2020) Bio-Based Nanoparticles as a Carrier of β-Carotene: Production, Characterisation and In Vitro Gastrointestinal Digestion. *Molecules*. *25*, 4497.

Agbodaze, D., Nmai, P., Robertson, F., Yeboah-Manu, D., Owusu-Darko, K. and Addo, K. (2006) Microbiological quality of "Khebab" consumed in the Accra metropolis. *Ghana Medical Journal*, *39*, 46–49.

Aghaei, Z., Emadzadeh, B., Ghorani, B. and Kadkhodaee, R. (2018) Cellulose Acetate Nanofibres Containing Alizarin as a Halochromic Sensor for the Qualitative Assessment of Rainbow Trout Fish Spoilage. *Food Bioprocess Technology*, *11*, 1087–1095. https://doi.org/10.1007/s11947-017-2046-5

Ahmed, F., Soliman, F.M., Adly, M.A., Soliman, H.A.M., El-Matbouli, M. and Saleh, M. (2019) Recent progress in biomedical applications of chitosan and its nanocomposites in aquaculture: A review. *Research in Veterinary Science*, *126*, 68–82.

Alizadeh Sani, M., Maleki, M., Eghbaljoo-Gharehgheshlaghi, H., Khezerlou, A., Mohammadian, E., Liu, Q. and Jafari, S.M. (2022a) Titanium dioxide nanoparticles as multifunctional surface-active materials for smart/active nanocomposite packaging films. *Advence in Colloid and Interface Science*, *300*, 102593.

Alizadeh Sani, M., Tavassoli, M., Salim, S.A., Azizi-lalabadi, M. and McClements, D.J. (2022b) Development of green halochromic smart and active packaging materials: TiO2 nanoparticle- and anthocyanin-loaded gelatin/κ-carrageenan films. *Food Hydrocolloids*, *124*, 107324. https://doi.org/10.1016/j.foodhyd.2021.107324

Alizadeh-Sani, M., Tavassoli, M., Mohammadian, E., Ehsani, A., Khaniki, G.J., Priyadarshi, R. and Rhim, J.W. (2021) pH-responsive color indicator films based on methylcellulose/chitosan nanofiber and barberry anthocyanins for real-time monitoring of meat freshness. *International Journal of Biological Macromolecules, 166*, 741–750. https://doi.org/10.1016/j.ijbiomac.2020.10.231

Altay, F. and Okutan, N. (2015) Nanofibre Encapsulation of Active Ingredients and their Controlled Release. In *Advances in Food Biotechnology* ed. Ravishankar, R. v. pp.607–616. John Wiley & Sons, Ltd.

Amalric-Popescu, D. and Bozon-Verduraz, F. (2001) Infrared studies on SnO2 and Pd/SnO2. *Catalysis Today, 70*, 139–154.

Aman Mohammadi, M., Ramezani, S., Hosseini, H., Mortazavian, A.M., Hosseini, S.M. and Ghorbani, M. (2021) Electrospun Antibacterial and Antioxidant Zein/Polylactic Acid/Hydroxypropyl Methylcellulose Nanofibers as an Active Food Packaging System. *Food and Bioprocess Technology, 14*, 1529–1541.

Amjadi, S., Almasi, H., Ghorbani, M. and Ramazani, S. (2020) Preparation and characterization of TiO2NPs and betanin loaded zein/sodium alginate nanofibers. *Food Packaging Shelf Life*, *24*, 100504.

Amjadi, S., Emaminia, S., Heyat Davudian, S., Pourmohammad, S., Hamishehkar, H. and Roufegarinejad, L. (2019) Preparation and characterization of gelatin-based nanocomposite containing chitosan nanofiber and ZnO nanoparticles. *Carbohydrate Polymers*, *216*, 376–384. https://doi.org/10.1016/j.carbpol.2019.03.062

Ansarifar, E. and Moradinezhad, F. (2021) Preservation of strawberry fruit quality via the use of active packaging with encapsulated thyme essential oil in zein nanofiber film. *International Journal of Food Science and Technology*, *56*(9), 4239-4247.

Arenas-Guerrero, P., Delgado, Á. v., Donovan, K.J., Scott, K., Bellini, T., Mantegazza, F. and Jiménez, M.L. (2018) Determination of the size distribution of non-spherical nanoparticles by electric birefringence-based methods. *Scientific Reports, 8*, 9502. https://doi.org/10.1038/s41598-018-27840-0.

Arkoun, M., Daigle, F., Heuzey, M.-C. and Ajji, A. (2017) Antibacterial electrospun chitosan-based nanofibers: A bacterial membrane perforator. *Food Science Nutrition*, *5*, 865–874.

Arvanitoyannis, I.S. and Tsarouhas, P. (2010) Food Packaging Materials for Irradiation. In *Irradiation of Food Commodities*. pp.43–64. Elsevier.

Ashfaq, A., Khursheed, N., Fatima, S., Anjum, Z. and Younis, K. (2022) Application of nanotechnology in food packaging: Pros and Cons. *Journal of Agriculture and Food Research, 7*, 100270.

Aslaner, G., Sumnu, G. and Sahin, S. (2021) Encapsulation of Grape Seed Extract in Rye Flour and Whey Protein–Based Electrospun Nanofibers. *Food and Bioprocess Technology, 14*, 1118–1131.

Aydar, A.Y. and Bağdatlıoğlu, N. (2014) Yemeklik Yağların Yüzey Gerilimi ve Temas Açılarının Belirlenmesinde Uygulanan Yöntemler. *Akademik Gıda*, *12*, 108–114.

Ayofemi Olalekan Adeyeye, S. and Joshua Ashaolu, T. (2021) Applications of nano-materials in food packaging: A review. *Journal of Food Processing Engineering*, *44*, e13708.

Aytac, Z., Huang, R., Vaze, N., Xu, T., Eitzer, B.D., Krol, W., MacQueen, L.A., Chang, H., Bousfield, D.W., Chan-Park, M.B., Ng, K.W., Parker, K.K., White, J.C. and Demokritou, P. (2020) Development of Biodegradable and Antimicrobial Electrospun Zein Fibers for Food Packaging. *ACS Sustainable Chemistry & Engineering*, *8*, 15354–15365.

Babapour, H., Jalali, H., Nafchi, A.M. and Jokar, M. (2022) Effects of Active Packaging Based on Potato Starch/Nano Zinc Oxide/Fennel (*Foeniculum vulgare Miller*) Essential Oil on Fresh Pistachio during Cold Storage. *Journal of Nuts*, *13*, 105–123.

Bagchi, S., Achla, R. and Mondal, S.K. (2017) Optical Fiber Sensor With ZnO Hierarchical Nano-Structures Grown on Electrospun ZnO Mat Base on the Sensor for Trace Level Detection of Volatile Amines. *IEEE Sensors Letters*, *2*, 1–4.

Baniasad, A. and Ghorbani, M. (2016) Thermal stability enhancement of modified carboxymethyl cellulose films using SnO2 nanoparticles. *International Journal of Biological Macromolecules*, *86*, 901–906. https://doi.org/10.1016/j.ijbiomac.2016.02.029

Bankar, A., Joshi, B., Kumar, A.R. and Zinjarde, S. (2010) Banana peel extract mediated novel route for the synthesis of silver nanoparticles. *Colloids and Surfaces A: Physicochemical and Engineering Aspects*, *368*(1-3), 58-63.

Basaran, P., Basaran-Akgul, N. and Rasco, B.A. (2010) Dielectric properties of chicken and fish muscle treated with microbial transglutaminase. *Food Chemistry*, *120*, 361–370. https://doi.org/10.1016/j.foodchem.2009.09.050

Bendini, A., Cerretani, L., Carrasco-Pancorbo, A., Gómez-Caravaca, A.M., Segura-Carretero, A., Fernández-Gutiérrez, A. and Lercker, G. (2007) Phenolic molecules in virgin olive oils: A survey of their sensory properties, health effects, antioxidant activity and analytical methods. An overview of the last decade. *Molecules*, *12*(8), 1679-1719.

Berger, F., Beche, E., Berjoan, R., Klein, D. and Chambaudet, A. (1996) An XPS and FTIR study of SO2 adsorption on SnO2 surfaces. *Applied Surface Science*, *93*(1), 9–16.

Berik, N. and Kahraman, D. (2010) Kefal Balığı Sucuklarında Duyusal ve Besin Kompozisyonun Belirlenmesi. *Kafkas Universitesi Veterinerlik Fakultesi Dergisi*, *16*, S59–S63.

Bhushani, J.A., Kurrey, N.K. and Anandharamakrishnan, C. (2017) Nanoencapsulation of green tea catechins by electrospraying technique and its effect on controlled release and in-vitro permeability. *Journal of Food Engineering*, *199*, 82–92. https://doi.org/10.1016/j.jfoodeng.2016.12.010

Bi, F., Qin, Y., Chen, D., Kan, J. and Liu, J. (2021) Development of active packaging films based on chitosan and nano-encapsulated luteolin. *International Journal of Biolological Macromolecules*, *182*, 545–553.

Bircan, C. and Barringer, S.A. (2002) Determination of Protein Denaturation of Muscle Foods Using the Dielectric Properties. *Journal of Food Science*, *67*, 202–205.

Boatemaa, M.A., Ragunathan, R. and Naskar, J. (2019) Nanogold for in vitro inhibition of Salmonella strains. *Journal of Nanomaterials*.

Bogale Teseme, W. and Weldemichael Weldeselassie, H. (2020) Review on the Study of Dielectric Properties of Food Materials. *American Journal of Engineering and Technology Management*, *5*, 76–83.

Borzenkov, M., Pallavicini, P., Taglietti, A., D'Alfonso, L., Collini, M. and Chirico, G. (2020) Photothermally active nanoparticles as a promising tool for eliminating bacteria and biofilms. *Beilstein Journal of Nanotechnology*, *11*, 1134–1146.

Bouletis, A.D., Arvanitoyannis, I.S. and Hadjichristodoulou, C. (2017) Application of modified atmosphere packaging on aquacultured fish and fish products: A review. *Critical reviews in food science and nutrition*, *57*(11), 2263-2285.

Cabrera-Barjas, G., Radovanović, N., Arrepol, G.B., de la Torre, A.F., Valdés, O. and Nešić, A. (2021) Valorization of food waste to produce intelligent nanofibrous β-chitin films. *International Journal of Biological Macromolecules*, *186*, 92–99. https://doi.org/10.1016/j.ijbiomac.2021.07.045

Cai, Z. and Park, S. (2020) Synthesis of Pd nanoparticle-decorated SnO2 nanowires and determination of the optimum quantity of Pd nanoparticles for highly sensitive and selective hydrogen gas sensor. *Sensors and Actuators: B Chemical*, *322*, 128651.

Cai, Z., Goo, E. and Park, S. (2021) Synthesis of tin dioxide (SnO2) hollow nanospheres and its ethanol-sensing performance augmented by gold nanoparticle decoration. *Journal of Alloys and Compounds*, *883*, 160868.

Cakmak-Arslan, G. (2022) Monitoring of Hazelnut oil quality during thermal processing in comparison with extra virgin olive oil by using ATR-FTIR spectroscopy combined with chemometrics. *Spectrochimica Acta Part A: Molecular and Biomolecular Spectroscopy*, *266*, 120461.

Cano-Sarmiento, C., Téllez-Medina, D.I., Viveros-Contreras, R., Cornejo-Mazón, M., Figueroa-Hernández, C.Y., García-Armenta, E., Alamilla-Beltrán, L., García, H.S. and Gutiérrez-López, G.F. (2018) Zeta Potential of Food Matrices. *Food Engineering Reviews*, *10*, 113-138.

Cao, H., Fan, D., Jiao, X., Huang, J., Zhao, J., Yan, B., Zhou, W., Zhang, W., Ye, W. and Zhang, H. (2019) Importance of thickness in electromagnetic properties and gel characteristics of surimi during microwave heating. *Journal of Food Engineering*, *248*, 80–88. https://doi.org/10.1016/j.jfoodeng.2019.01.003

Carbone, M., Donia, D.T., Sabbatella, G. and Antiochia, R. (2016) Silver nanoparticles in polymeric matrices for fresh food packaging. *Journal of King Saud University-Science*, *28*, 273–279.

Celebioglu, A. and Uyar, T. (2021) Electrohydrodynamic encapsulation of eugenol-cyclodextrin complexes in pullulan nanofibers. *Food Hydrocolloids*, *111*, 106264. https://doi.org/10.1016/j.foodhyd.2020.106264

Cetinkaya, T., Altay, F. and Ceylan, Z. (2021a) A new application with characterized oil-in-water-in-oil double emulsions: Gelatin-xanthan gum complexes for the edible oil industry. *LWT*, *138*, 110773. https://doi.org/10.1016/j.lwt.2020.110773

Cetinkaya, T., Mendes, A.C., Jacobsen, C., Ceylan, Z., Chronakis, I.S., Bean, S.R. and García-Moreno, P.J. (2021b) Development of kafirin-based nanocapsules by electrospraying for encapsulation of fish oil. *LWT*, *136, 110297*. https://doi.org/10.1016/j.lwt.2020.110297

Cetinkaya, T., Wijaya, W., Altay, F. and Ceylan, Z. (2022) Fabrication and characterization of zein nanofibers integrated with gold nanospheres. *LWT, 155*, 112976. https://doi.org/10.1016/j.lwt.2021.112976

Ceylan, Z. (2017) *Elektrodöndürme yöntemiyle üretilen biyopolimer tabanlı nanoliflerle balık filetolarının kaplanması ve depolama stabilitesinin artırılması* (Doctoral dissertation). Retrieved from https://tez.yok.gov.tr/

Ceylan, Z. (2019) A new cost-effective process for limitation of microbial growth in fish fleshes: Wrapping by aluminum foil coated with electrospun nanofibers. *Journal of Food Safety*, *39*, 1–8.

Ceylan, Z. and Meral, R. (2018) Determination of Textural and Color Parameters of Fish Fillets Stored at Refrigerated Conditions. *International Journal of Scientific and Technological Research, 4*, 320–326.

Ceylan, Z. and Özoğul, Y. (2019) Irradiation Technology. In *Innovative Technologies in Seafood Processing* ed. Ozogul, Y. pp.115–129. Edited by Yesim Ozogul, 600 Broken Sound Parkway, NW, Suite 300, Boca Raton, FL: CRC Press.

Ceylan, Z. and Unal, K. (2019) The Effect of Different Thawing Methods on Quality Parameters of Frozen Mussels and Shrimp Meats. *Turkish Journal of Agriculture - Food Science and Technology*, *7*, 927–933.

Ceylan, Z. and Ünal Şengör, G.F. (2015) Dumanlanmış Su Ürünüleri ve Polisiklik Aromatik Hidrokarbonlar (PAH's). *Journal of Food and Feed Science-Technology*, *15*, 27–33.

Ceylan, Z., Meral, R., Alav, A., Karakas, C.Y. and Yilmaz, M.T. (2020a) Determination of Textural Deterioration in Fish Meat Processed with Electrospun Nanofibers. *Journal of Texture Studies*, *51*(6), 917-924.

Ceylan, Z., Meral, R., Cavidoglu, I., Yagmur Karakas, C. and Tahsin Yilmaz, M. (2018a) A new application on fatty acid stability of fish fillets: Coating with probiotic bacteria-loaded polymer-based characterized nanofibers. *Journal of food safety*, *38*, e12547.

Ceylan, Z., Meral, R., Karakaş, C.Y., Dertli, E. and Yilmaz, M.T. (2018b) A novel strategy for probiotic bacteria: Ensuring microbial stability of fish fillets using characterized probiotic bacteria-loaded nanofibers. *Innovative Food Science & Emerging Technologies*, *48*, 212–218. https://doi.org/10.1016/j.ifset.2018.07.002

Ceylan, Z., Meral, R., Özogul, F. and Yilmaz, M.T. (2020b) Importance of electrospun chitosan-based nanoscale materials for seafood products safety. *Handbook of Chitin and Chitosan: Volume 1: Preparation and Properties*, 195–223.

Ceylan, Z., Sengor, G.F.U. and Yilmaz, M.T. (2017a) A Novel Approach to Limit Chemical Deterioration of Gilthead Sea Bream (Sparus aurata) Fillets: Coating with Electrospun Nanofibers as Characterized by Molecular, Thermal, and Microstructural Properties. *Journal of Food Science*, *82*, 1163–1170.

Ceylan, Z., Unal Sengor, G.F. and Yilmaz, M.T. (2017c) Amino acid composition of gilthead sea bream fillets (*Sparus aurata*) coated with thymol-loaded chitosan nanofibers during cold storage. *Journal of Biotechnology*, *256*, S28. https://doi.org/10.1016/j.jbiotec.2017.06.645

Ceylan, Z., Unal Sengor, G.F. and Yilmaz, M.T. (2018d) Nanoencapsulation of liquid smoke/thymol combination in chitosan nanofibers to delay microbiological spoilage of sea bass (*Dicentrarchus labrax*) fillets. *Journal of Food Engineering*, *229*, 43–49. https://doi.org/10.1016/j.jfoodeng.2017.11.038

Ceylan, Z., Unal Sengor, G.F., Basahel, A. and Yilmaz, M.T. (2018c) Determination of quality parameters of gilthead sea bream (*Sparus aurata*) fillets coated with electrospun nanofibers. *Journal of Food Safety*, *38*, 1–7.

Ceylan, Z., Unal Sengor, G.F., Sağdıç, O. and Yilmaz, M.T. (2017b) A novel approach to extend microbiological stability of sea bass *(Dicentrarchus labrax*) fillets coated with electrospun chitosan nanofibers. *LWT-Food Science and Technology*, *79*, 367–375. https://doi.org/10.1016/j.lwt.2017.01.062

Ceylan, Z., Uslu, E., İspirli, H., Meral, R., Gavgalı, M., 'Yilmaz, M.T. and Dertli, E. (2019) A novel perspective for *Lactobacillus reuteri*: Nanoencapsulation to obtain functional fish fillets. *LWT- Food Science and Technology*, *115*, 108427. https://doi.org/10.1016/j.lwt.2019.108427

Ceylan, Z., Yilmaz, M.T. and Sengor, G.F. (2016) Microbiological stability of sea bass (*Dicentrarchus labrax*) fillets coated with chitosan based liquid smoke loaded electrospun nanofibers. *Journal of Biotechnology*, S, S16. https://doi.org/j.biotec.2016.05.080

Chandran, S.P., Chaudhary, M., Pasricha, R., Ahmad, A. and Sastry, M. (2006) Synthesis of Gold Nanotriangles and Silver Nanoparticles Using Aloe vera Plant Extract. *Biotechnol Progress*, *22*, 577–583.

Chellaram, C., Murugaboopathi, G., John, A.A., Sivakumar, R., Ganesan, S., Krithika, S. and Priya, G. (2014) Significance of Nanotechnology in Food Industry. *APCBEE Procedia*, *8*, 109–113.

Chen, T., Cheng, G., Ahmed, S., Wang, Y., Wang, X., Hao, H. and Yuan, Z. (2017) New methodologies in screening of antibiotic residues in animal-derived foods: Biosensors. *Talanta*, *175*, 435–442.

Chen, X., Li, D., Li, G., Luo, L., Ullah, N., Wei, Q. and Huang, F. (2015) Facile fabrication of gold nanoparticle on zein ultrafine fibers and their application for catechol biosensor. *Applied Surface Science*, *328*, 444–452.

Chen, Y., Qiu, F., Tang, C., Xing, Z. and Zhao, X. (2021) Controllable self-patterning behaviours of flexible self-assembling peptide nanofibers. *Nanoscale Advances*, *3*, 1603–1611.

Chotimarkorn, C. (2014) Quality changes of anchovy (Stolephorus heterolobus) under refrigerated storage of different practical industrial methods in Thailand. *Journal of Food Science and Technology*, *51*, 285–293. https://doi.org/10.1007/s13197-011-0505-y

Chung, F.C., Wu, R.J. and Cheng, F.C. (2014) Fabrication of a Au@SnO2 core–shell structure for gaseous formaldehyde sensing at room temperature. *Sensors and Actuators: B Chemical*, *190*, 1–7.

Ciarlo, A.S., Boeri, R.L. and Giannini, D.H. (1985) Storage Life of Frozen Blocks of Patagonian Hake (Merluccius hubbsi) Filleted and Minced. *Journal of Food Science*, *50*, 723–726.

Clark, D.S. and Thatcher, F.S. (1978) *Microorganisms in foods : their significance and methods of enumeration*. 2nd ed. Toronto: University of Toronto Press.

Cobley, C.M., Chen, J., Cho, E.C., Wang, L. v. and Xia, Y. (2011) Gold nanostructures: a class of multifunctional materials for biomedical applications. *Chemical Society Reviews*, *40*, 44–56.

Çetinkaya, T. and Ceylan, Z. (2020) Balıketi Kalitesinin Tanımlanmasında Kullanılabilecek Alternatif Yaklaşımlar. In *Ziraat, Orman ve Su Ürünleri Alanında Akademik Çalışmalar – II*. pp.75–85. Ankara: Gece Kitaplığı Yayınevi.

Çetinkaya, T., Altay, F. and Ceylan Zafer (2021a) Determination of Fish Meat Quality Changes by Fast and Novel Methods During Storage Period. *Journal of the Institute of Science and Technology*. *11*.

Çetinkaya, T., Ceylan, Z., Meral, R., Kılıçer, A. and Altay, F. (2021b) A novel strategy for Au in food science: Nanoformulation in dielectric, sensory properties, and microbiological quality of fish meat. *Food Bioscience, 41*, 101024. https://doi.org/10.1016/j.fbio.2021.101024

da Silva, G.R., Lima, T.H., Oréfice, R.L., Fernandes-Cunha, G.M., Silva-Cunha, A., Zhao, M. and Behar-Cohen, F. (2015) In vitro and in vivo ocular biocompatibility of electrospun poly(ε-caprolactone) nanofibers. *European Journal of Pharmaceutical Sciences, 73*, 9–19.

Dai, Z., Li, Z., Li, L. and Xu, G. (2011) Synthesis and thermal properties of antimony doped tin oxide/waterborne polyurethane nanocomposite films as heat insulating materials. *Polymers for Advances Technologies, 22*, 1905–1911.

Dar, A.H., Rashid, N., Majid, I., Hussain, S. and Dar, M.A. (2019) Nanotechnology interventions in aquaculture and seafood preservation. *Critical Reviews in Food Science and Nutrition*, *60*(11), 1912-1921.

Dashdorj, U., Reyes, M.K., Unnithan, A.R., Tiwari, A.P., Tumurbaatar, B., Park, C.H. and Kim, C.S. (2015) Fabrication and characterization of electrospun zein/Ag nanocomposite mats for wound dressing applications. *International Journal of Biological Macromolecules, 80*, 1–7. https://doi.org/10.1016/j.ijbiomac.2015.06.026

Dede, S. and Lokumcu Altay, F. (2021) Investigation of Electrophoretic Mobility of Various Nanofibers in Ethanol or Water. *Turkish Journal of Science & Technology Research Paper, 16*, 269–274.

Dias Antunes, M., da Silva Dannenberg, G., Fiorentini, Â.M., Pinto, V.Z., Lim, L.-T., da Rosa Zavareze, E. and Dias, A.R.G. (2017) Antimicrobial electrospun ultrafine fibers from zein containing eucalyptus essential oil/cyclodextrin inclusion complex. *International Journal of Biological Macromolecules, 104*, 874–882. https://doi.org/10.1016/j.ijbiomac.2017.06.095

Díaz, P., Garrido, M.D. and Bañón, S. (2011) Spoilage of sous vide cooked salmon (*Salmo salar*) stored under refrigeration. *Food Science and Technology International, 17*, 31–37.

Duan, N., Li, Q., Meng, X., Wang, Z. and Wu, S. (2021) Preparation and characterization of k-carrageenan/konjac glucomannan/TiO2 nanocomposite film with efficient anti-fungal activity and its application in strawberry preservation. *Food Chemistry, 364*, 130441. https://doi.org/10.1016/j.foodchem.2021.130441

Dunnewind, B., Janssen, A.M., van Vliet, T. and Weenen, H. (2004) Relative importance of cohesion and adhesion for sensory stickiness of semisolid foods. *Journal of Texture Studies, 35*, 603–620.

Durlu-Özkaya, F. and Cömert, M. (2008) Gıda Zehirlenmelerinde Etken Faktörler. *Türk Hijyen ve Deneysel Biyoloji Dergisi*. *65*, 149–158.

Durmus, M., Ozogul, Y., Küley Boga, E., Uçar, Y., Kosker, A.R., Balikci, E. and Gökdogan, S. (2019) The effects of edible oil nanoemulsions on the chemical, sensory, and microbiological changes of vacuum packed and refrigerated sea bass fillets during storage period at 2 ± 2°C. *Journal of Food Processing and Preservation, 43,* e14282.

Dutta, M., Rani Majumdar, P., Rakeb-Ul Islam, M. and Saha, D. (2018) Bacterial and Fungal Population Assessment in Smoked Fish during Storage Period. *Journal of Food: Microbiology, Safety & Hygiene, 3*.

Duymuş, H.G., Göger, F. and Başer, K.H.C. (2014) In vitro antioxidant properties and anthocyanin compositions of elderberry extracts. *Food Chemistry, 155*, 112–119. https://doi.org/10.1016/j.foodchem.2014.01.028

EEC (1995) Commission Decision of 8 March 1995 fixing the total volatile basic nitrogen (TVB-N) limit values for certain categories of fishery products and specifying the analysis methods to be used. *Official Journal of the European Communities*, 84–87.

El-Lahamy, A.A., Khalil, K.I., A El-Sherif, S. and Mahmud, A.A. (2018) Effect of Smoking Methods (Hot and Cold) and Refrigeration Storage on the Chemical Composition of Catfish Fillets (*Clarias Gariepinus*). *Journal of Food Processing Technology, 9, 1-4*.

Ertaş, H.A. (1998) Chemical Composition of Smoke. *Gıda, 23,* 177–185.

Espinosa-Acosta, G., Ramos-Jacques, A.L., Molina, G.A., Maya-Cornejo, J., Esparza, R., Hernandez-Martinez, A.R., Sánchez-González, I. and Estevez, M. (2018) Stability Analysis of Anthocyanins Using Alcoholic Extracts from Black Carrot (*Daucus Carota ssp. Sativus Var. Atrorubens Alef*.). *Molecules, 23*, 2744.

Eze, F.N., Jayeoye, T.J. and Singh, S. (2022) Fabrication of intelligent pH-sensing films with antioxidant potential for monitoring shrimp freshness via the fortification of chitosan matrix with broken Riceberry phenolic extract. *Food Chemistry, 366*, 130574. https://doi.org/10.1016/j.foodchem.2021.130574

Facchi, D.P., Souza, P.R., Almeida, V.C., Bonafé, E.G. and Martins, A.F. (2021) Optimizing the Ecovio® and Ecovio®/zein solution parameters to achieve electrospinnability and provide thin fibers. *Journal of Molecular Liquids, 321*, 114476.

Fan, W., Sun, J., Chen, Y., Qiu, J., Zhang, Y. and Chi, Y. (2009) Effects of chitosan coating on quality and shelf life of silver carp during frozen storage. *Food Chemistry,* 115. https://doi.org/10.1016/j.foodchem.2008.11.060

Fang, Q., Ma, N., Ding, K., Zhan, S., Lou, Q. and Huang, T. (2021) Interaction between Negatively Charged Fish Gelatin and Cyclodextrin in Aqueous Solution: Characteristics and Formation Mechanism. *Gels, 7,* 260.

Feng, K., Wen, P., Yang, H., Li, N., Lou, W.Y., Zong, M.H. and Wu, H. (2017) Enhancement of the antimicrobial activity of cinnamon essential oil-loaded electrospun nanofilm by the incorporation of lysozyme. *RSC Adv*ances, *7*, 1572–1580.

Fengou, L.C., Lianou, A., Tsakanikas, P., Gkana, E.N., Panagou, E.Z. and Nychas, G.J.E. (2019) Evaluation of Fourier transform infrared spectroscopy and multispectral imaging as means of estimating the microbiological spoilage of farmed sea bream. *Food Microbiology*, *79*, 27–34.

Fernandes, P. (2016) Enzymes in fish and seafood processing. *Frontiers in Bioengineering and Biotechnology*, *4*, 59.

Fernández-Saiz, P., Sánchez, G., Soler, C., Lagaron, J.M. and Ocio, M.J. (2013) Chitosan films for the microbiological preservation of refrigerated sole and hake fillets. *Food Control*, *34*, 61–68. https://doi.org/10.1016/j.foodcont.2013.03.047

Forghani, S., Almasi, H. and Moradi, M. (2021) Electrospun nanofibers as food freshness and time-temperature indicators: A new approach in food intelligent packaging. *Innovative Food Science & Emerging Technologies*, *73*, 102804. https://doi.org/10.1016/j.ifset.2021.102804

Franceschelli, L., Berardinelli, A., Dabbou, S., Ragni, L. and Tartagni, M. (2021) Sensing technology for fish freshness and safety: A review. *Sensors (Switzerland)*, *21*(4), 1373.

Gaabour, L.H. (2017) Spectroscopic and thermal analysis of polyacrylamide/chitosan (PAM/CS) blend loaded by gold nanoparticles. *Results in Physics*, *7*, 2153–2158.

Gallocchio, F., Cibin, V., Biancotto, G., Roccato, A., Muzzolon, O., Losasso, C., Simone, B., Manodori, L., Fabrizi, A., Patuzzi, I. and Ricci, A. (2016) Testing nano-silver food packaging to evaluate silver migration and food spoilage bacteria on chicken meat. *Food Additives & Contaminants: Part A*, *33*(6), 1063-1071.

García-Moreno, P.J., Mendes, A.C., Jacobsen, C. and Chronakis, I.S. (2018) Biopolymers for the Nano-microencapsulation of Bioactive Ingredients by Electrohydrodynamic Processing. In *Polymers for Food Applications*. pp.447–479. Cham: Springer International Publishing.

Gaudin, V. (2017) Advances in biosensor development for the screening of antibiotic residues in food products of animal origin – A comprehensive review. *Biosensors and Bioelectronics*, *90*, 363-377.

Gerdes, D.L. and Santos Valdez, C. (1991) Modified atmosphere packaging of commercial Pacific red snapper (*Sebastes entomelas, Sebastes flavidus or Sebastes goodei*). *LWT- Food Science and Technology*, *24*, 256–258.

Getu, A. and Misganaw, K. (2015) Post-harvesting and Major Related Problems of Fish Production. *Fisheries and Aquaculture Journal*, 06.

Ghaly, A.E., Dave, D., Budge, S. and Brooks, M.S. (2010) Fish Spoilage Mechanisms and Preservation Techniques: Review. *American Journal of Applied Sciemces*, *7*, 859–877.

Gharibshahi, L., Saion, E., Gharibshahi, E., Shaari, A. and Matori, K. (2017) Structural and Optical Properties of Ag Nanoparticles Synthesized by Thermal Treatment Method. *Materials*, *10*, 402.

Giteru, S.G., Azam Ali, M. and Oey, I. (2021) Elucidating the pH influence on pulsed electric fields-induced self-assembly of chitosan-zein-poly(vinyl alcohol)-polyethylene glycol nanostructured composites. *Journal of Colloid and Interface Science, 588*, 531–546.

Gokoglu, N. (2019) Novel natural food preservatives and applications in seafood preservation: a review. *Journal of the Science of Food and Agriculture, 99*(5), 2068-2077. https://doi.org/10.1002/jsfa.9416

González, C.M.O., Schelegueda, L.I., Ruiz-Henestrosa, V.M.P., Campos, C.A., Basanta, M.F. and Gerschenson, L.N. (2022) Cassava Starch Films with Anthocyanins and Betalains from Agroindustrial by-Products: Their Use for Intelligent Label Development. *Foods, 11,3361*.

Govari, M., Tryfinopoulou, P., Parlapani, F.F., Boziaris, I.S., Panagou, E.Z. and Nychas, G.J.E. (2021) Quest of Intelligent Research Tools for Rapid Evaluation of Fish Quality: FTIR Spectroscopy and Multispectral Imaging Versus Microbiological Analysis. *Foods, 10, 264*.

Göksen, G., Fabra, M.J., Ekiz, H.I. and López-Rubio, A. (2020) Phytochemical-loaded electrospun nanofibers as novel active edible films: Characterization and antibacterial efficiency in cheese slices. *Food Control*, *112*, 107133. https://doi.org/10.1016/j.foodcont.2020.107133

Göksen, G., Fabra, M.J., Pérez-Cataluña, A., Ekiz, H.I., Sanchez, G. and López-Rubio, A. (2021) Biodegradable active food packaging structures based on hybrid cross-linked electrospun polyvinyl alcohol fibers containing essential oils and their application in the preservation of chicken breast fillets. *Food Packaging Shelf Life, 27*, 100613.

Göktan, D. (1990) *Gıdaların Mikrobiyal Ekolojisi*. İzmir: Ege Üniversitesi Basımevi.

Günlü, A. and Koyun, E. (2013) Effects of Vacuum Packaging and Wrapping with Chitosan-Based Edible Film on the Extension of the Shelf Life of Sea Bass (*Dicentrarchus labrax*) Fillets in Cold Storage (4 °C). *Food Bioprocess Technology, 6*, 1713–1719. https://doi.org/10.1007/s11947-012-0833-6

Güzel, N. and Bahçeci, K.S. (2020) Çorum Yöresi Ballarının Bazı Kimyasal Kalite Parametrelerinin Değerlendirilmesi. *Gıda, 45*(2), 230–241.

Halkman, A. (2005) *Gıda Mikrobiyolojisi Uygulamaları*. Ankara: Başak Matbaacılık.

Heising, J.K., Dekker, M., Bartels, P. v. and van Boekel, M.A.J.S. (2012) A non-destructive ammonium detection method as indicator for freshness for packed fish: Application on cod. *Journal of Food Engineering, 110*, 254–261. https://doi.org/10.1016/j.jfoodeng.2011.05.008

Howgate, P. (2009) Traditional Methods. In *Fishery Products*. pp.19–41. Oxford, UK: Wiley-Blackwell.

Huss, H.H. (1994) Assurance of seafood quality. *FAO Fisheries Technical Paper*.

Icier, F. and Baysal, T. (2004) Dielectrical properties of food materials - 1: Factors affecting and industrial uses. *Critical reviews in food science and nutrition, 44*(6), 465-471.

ICMSF (1986) Sampling for microbiological analysis: Principles and specific applications Second edition ICMSF . In *Micro Organisms In Foods*. Blackwell Scientific Publications.

ICMSF (1992) Sampling for microbiological analysis. In *Microorganisms in food*. Toronto, Canada: University of Toronto Press.

Isik, B.S., Altay, F. and Capanoglu, E. (2018) The uniaxial and coaxial encapsulations of sour cherry (*Prunus cerasus L*.) concentrate by electrospinning and their in vitro bioaccessibility. *Food chemistry*, *265*, 260-273. https://doi.org/10.1016/j.foodchem.2018.05.064

Iturriaga, L., Olabarrieta, I. and de Marañón, I.M. (2012) Antimicrobial assays of natural extracts and their inhibitory effect against Listeria innocua and fish spoilage bacteria, after incorporation into biopolymer edible films. *International journal of food microbiology*, *158*(1), 58-64.

Ivanovskaya, M., Ovodok, E., Gaevskaya, T., Kotsikau, D., Kormosh, V., Bilanych, V. and Micusik, M. (2021) Effect of Au nanoparticles on the gas sensitivity of nanosized SnO_2. *Materials Chemistry and Physics*, *258*, 123858.

Iwamoto, S., Lee, S.-H. and Endo, T. (2014) Relationship between aspect ratio and suspension viscosity of wood cellulose nanofibers. *Polymer journal*, *46*(1), 73-76.

İnal, M. and Mülazımoğlu, G. (2019) Production and characterization of bactericidal wound dressing material based on gelatin nanofiber. *International Journal of Biological Macromolecules*, *137*, 392-404. https://doi.org/10.1016/j.ijbiomac.2019.06.119

İnal, T. (1992) *Besin Hijyen; Hayvansal Gıdaların Sağlık Kontrolu, .* İstanbul: Final Ofset.

İnanç Horuz, T. and Belibağlı, K.B. (2018) Nanoencapsulation by electrospinning to improve stability and water solubility of carotenoids extracted from tomato peels. *Food Chemistry*, *268*, 86–93. https://doi.org/10.1016/j.foodchem.2018.06.017

Jamróz, E., Kulawik, P., Guzik, P. and Duda, I. (2019) The verification of intelligent properties of furcellaran films with plant extracts on the stored fresh Atlantic mackerel during storage at 2 °C. *Food Hydrocolloids*, *97*, 105211. https://doi.org/10.1016/j.foodhyd.2019.105211

Jang, J.H., Kang, H.J., Adedeji, O.E., Kim, G.Y., Lee, J.K., Kim, D.H. and Jung, Y.H. (2023) Development of a pH indicator for monitoring the freshness of minced pork using a cellulose nanofiber. *Food Chemistry*, *403*, 134366. https://doi.org/10.1016/j.foodchem.2022.134366

Jay, J.M. (2000) Food Preservation with Modified Atmospheres. *Modern Food Microbiology*. 283–300.

Jayakumar, R., Divya Rani, V. v., Shalumon, K.T., Kumar, P.T.S., Nair, S. v., Furuike, T. and Tamura, H. (2009) Bioactive and osteoblast cell attachment studies of novel α- and β-chitin membranes for tissue-engineering applications. *International Journal of Biolological Macromolecules*, *45*, 260–264.

Jha, S.N., Narsaiah, K., Basediya, A.L., Sharma, R., Jaiswal, P., Kumar, R. and Bhardwaj, R. (2011) Measurement techniques and application of electrical properties for nondestructive quality evaluation of foods-a review. *Journal of food science and technology*, *48*, 387-411. https://doi.org/10.1007/s13197-011-0263-x

Jørgensen, L., Qvortrup, K. and Chronakis, I.S. (2015) Phospholipid electrospun nanofibers: Effect of solvents and co-axial processing on morphology and fiber diameter. *RSC Advances*, *5*, 53644–53652.

K. Adeyemo, O. and Foyle, L. (2022) Fundamentals of aquatic veterinary medicine. In *Fundamentals of Aquatic Veterinary Medicine* ed. Urdes, L., Walster, C. and Tepper, J. pp.181–209. Wiley.

Kaba, N., Özer, Ö. and Çorapçı, B. (2012) The determination of some quality parameters of smoked gar fish meat balls. *Journal of FisheriesSciences.com*, *6*, 357–367.

Kanatt, S.R. (2020) Development of active/intelligent food packaging film containing Amaranthus leaf extract for shelf life extension of chicken/fish during chilled storage. *Food Packaging Shelf Life*, *24*, 100506.

Kasaai, M.R. (2018) Zein and zein -based nano-materials for food and nutrition applications: A review. *Trends in Food Science & Technology*, *79*, 184–197. https://doi.org/10.1016/j.tifs.2018.07.015

Kaya, O. and İçier, F. (2019) İndüksiyon ve Ohmik Isıtma İşlemlerinin Gıdalara Uygulanabilirliğinin Karşılaştırılması. *Akademik Gıda*, *17*, 111–120.

Kayim, M. and Can, E. (2010) The pH and total fat values of fish meat in different iced storage period. *Asian Journal of Animal and Veterinary Advances*, 2010, 5.5: 346-348.

Kiessling, A., Ruohonen, K. and Bjørnevik, M. (2006) Muscle fibre growth and quality in fish. *Arch Tierz, Dummerstorf*, *49*, 137–146.

Kim, H.-J., Roy, S. and Rhim, J.-W. (2022) Gelatin/agar-based color-indicator film integrated with Clitoria ternatea flower anthocyanin and zinc oxide nanoparticles for monitoring freshness of shrimp. *Food Hydrocolloids*, *124*, 107294. https://doi.org/10.1016/j.foodhyd.2021.107294

Kolsarıcı, N. and Güven, T. (1998) The Effects of Using Liquid Smoke on Storage Stability of Frankfurters. *Turkish Journal of Veterinary & Animal Sciences*, *22*(4), 379-388.

Komarov, V., Wang, S. and Tang, J. (2005) Permittivity and Measurements. In *Encyclopedia of RF and Microwave Engineering*. pp.3693–3711. Hoboken, NJ, USA: John Wiley & Sons, Inc.

Korotcenkov, G., Gulina, L.B., Cho, B.K., Han, S.H. and Tolstoy, V.P. (2011) SnO2–Au nanocomposite synthesized by successive ionic layer deposition method: Characterization and application in gas sensors. *Materials Chemistry and Physics*, *128*(3), 433-441.

Křenek, T., Murafa, N., Bezdička, P., Šubrt, J., Masoudi, H.M. and Pola, J. (2012) IR laser-induced breakdown in tetramethyltin adjacent to Ag or Au: deposition of β-Sn nanograin-containing amorphous Au–Sn/C and Ag–Sn/C films. *Applied Organometallic Chemistry*, *26*(3), 135-139.

Krishnaswamy, K. and Orsat, V. (2015) Insight into the nanodielectric properties of gold nanoparticles synthesized from maple leaf and pine needle extracts. *Industrial Crops and Products*, *66*, 131-136.

Kurek, M., Garofulić, I.E., Bakić, M.T., Ščetar, M., Uzelac, V.D. and Galić, K. (2018) Development and evaluation of a novel antioxidant and pH indicator film based on chitosan and food waste sources of antioxidants. *Food Hydrocolloids*, *84*, 238–246. https://doi.org/10.1016/j.foodhyd.2018.05.050

Küçüköner, E. and Küçüköner, Z. (1990) Balık Mikroflorası ve Balıklarda Meydana Gelen Mikrobiyal Değişmeler. *The Journal of Food*, *15*, 339–341.

Külcü, D.B. (2017) Farklı sıcaklıklarda muhafaza edilen palamut (sarda sarda) balığının bazı kimyasal kalite niteliklerinin belirlenmesi. *Sakarya Üniversitesi Fen Bilimleri Enstitüsü Dergisi*, *21*, 403–410.

Kwak, H.W., Kim, J.E. and Lee, K.H. (2019) Green fabrication of antibacterial gelatin fiber for biomedical application. *Reactive and Functional Polymers*, *136*, 86-94.

Kyrana, V.R. and Lougovois, V.P. (2002) Sensory, chemical and microbiological assessment of farm-raised European sea bass (*Dicentrarchus labrax*) stored in melting ice. *International Journal of Food Science and Technology*, *37*, 319–328.

Lafferty, K.D., Harvell, C.D., Conrad, J.M., Friedman, C.S., Kent, M.L., Kuris, A.M., Powell, E.N., Rondeau, D. and Saksida, S.M. (2015) Infectious Diseases Affect Marine Fisheries and Aquaculture Economics. *Annual review of marine science*, *7*, 471-496.

le Corre-Bordes, D., Hofman, K. and Hall, B. (2018) Guide to electrospinning denatured whole chain collagen from hoki fish using benign solvents. *International Journal of Biological Macromolecules*, *112*, 1289–1299. https://doi.org/10.1016/j.ijbiomac.2018.02.088

Li, M., Yu, H., Xie, Y., Guo, Y., Cheng, Y., Qian, H. and Yao, W. (2021) Fabrication of eugenol loaded gelatin nanofibers by electrospinning technique as active packaging material. *LWT-Food Science and Technology*, *139*, 110800. https://doi.org/10.1016/j.lwt.2020.110800

Li, S., Li, F., Tang, J., Koral, T. and Jiao, Y. (2019) Influence of composition, temperature, and frequency on dielectric properties of selected saltwater and freshwater fish. *International Journal of Food Properties*, *22*(1), 1920-1934.

Liao, X., Su, Y., Liu, D., Chen, S., Hu, Y., Ye, X., Wang, J. and Ding, T. (2018) Application of atmospheric cold plasma-activated water (PAW) ice for preservation of shrimps (*Metapenaeus ensis*). *Food Control*, *94*, 307–314. https://doi.org/10.1016/j.foodcont.2018.07.026

Lin, J., Wang, Y., Pan, D., Sun, Y., Ou, C. and Cao, J. (2018) Physico-mechanical properties of gelatin films modified with Lysine, Arginine and Histidine. *International Journal of Biological Macromolecules*. *108*, 947–952.

Lin, M.-H., Sun, L., Kong, F. and Lin, M. (2021) Rapid detection of paraquat residues in green tea using surface-enhanced Raman spectroscopy (SERS) coupled with gold nanostars. *Food Control*, *130*, 108280. https://doi.org/10.1016/j.foodcont.2021.108280

Linh, N.T.B., Min, Y.K., Song, H.Y. and Lee, B.T. (2010) Fabrication of polyvinyl alcohol/gelatin nanofiber composites and evaluation of their material properties. *Journal of Biomedical Materials Research Part B: Applied Biomaterials*, *95*(1), 184-191.

Linklater, D.P., Baulin, V.A., Guével, X. le, Fleury, J.-B., Hanssen, E., Nguyen, T.H.P., Juodkazis, S., Bryant, G., Crawford, R.J., Stoodley, P. and Ivanova, E.P. (2020) Antibacterial Action of Nanoparticles by Lethal Stretching of Bacterial Cell Membranes. *Advanced Materials*, *32*, 2005679.

Liu, F., Majeed, H., Antoniou, J., Li, Y., Ma, Y., Yokoyama, W., Ma, J. and Zhong, F. (2016) Tailoring physical properties of transglutaminase-modified gelatin films by varying drying temperature. *Food Hydrocolloids*, *58*, 20–28. https://doi.org/10.1016/j.foodhyd.2016.01.026

Liu, J., Yong, H., Liu, Y., Qin, Y., Kan, J. and Liu, J. (2019) Preparation and characterization of active and intelligent films based on fish gelatin and haskap berries (*Lonicera caerulea L.*) extract. *Food Packaging Shelf Life*, *22*, 100417.

Liu, L., Zhang, J., Zou, X., Arslan, M., Shi, J., Zhai, X., Xiao, J., Wang, X., Huang, X., Li, Z. and Li, Y. (2022) A high-stable and sensitive colorimetric nanofiber sensor based on PCL incorporating anthocyanins for shrimp freshness. *Food Chemistry*, *377*, 131909. https://doi.org/10.1016/j.foodchem.2021.131909

Liu, Y., Zhu, J., Weng, G., Li, J. and Zhao, J. (2020) Gold nanotubes: synthesis, properties and biomedical applications. *Microchimica Acta*, *187*, 612.

Lougovois, V.P., Kyranas, E.R. and Kyrana, V.R. (2003) Comparison of selected methods of assessing freshness quality and remaining storage life of iced gilthead sea bream (*Sparus aurata*). *Food Research International*, *36*, 551–560.

Mahendia, S., Tomar, A.K. and Kumar, S. (2010) Electrical conductivity and dielectric spectroscopic studies of PVA-Ag nanocomposite films. *Journal of Alloys and Compounds*, *508*(2), 406-411.

Malle, P. and Poumeyrol, M. (1989) A New Chemical Criterion for the Quality Control of Fish: Trimethylamine/Total Volatile Basic Nitrogen (%). *Journal of food protection*, *52*(6), 419-423.

Marega, C., Maculan, J., Andrea Rizzi, G., Saini, R., Cavaliere, E., Gavioli, L., Cattelan, M., Giallongo, G., Marigo, A. and Granozzi, G. (2015) Polyvinyl alcohol electrospun nanofibers containing Ag nanoparticles used as sensors for the detection of biogenic amines. *Nanotechnology*, *6*, 075501.

Masette, M. and Magnússon, M.H. (1999) A Comparative Study of Storage Time of Warm and Cold Water Fish In View of the Current Market Demand. *Methods*, *3*, 4.

Masniyom, P. (2011) Deterioration and shelf-life extension of fish and fishery products by modified atmosphere packaging. *Songklanakarin Journal of Science and Technology, 33*, 181–192.

Maturin, L. and Peeler, J.T. (2001) Aerobic Plate Count. In *Bacteriological Analytical Manual*.

Maturin, L.J. and Peeler, J.T. (1988) Aerobic plate count. In *Food and Drug Administration Bacteriological Analytical Manual*.

Medina, I., Gallardo, J.M. and Aubourg, S.P. (2009) Quality preservation in chilled and frozen fish products by employment of slurry ice and natural antioxidants. *International journal of food science & technology*, *44*(8), 1467-1479.

Mehrasa, M., Asadollahi, M.A., Ghaedi, K., Salehi, H. and Arpanaei, A. (2015) Electrospun aligned PLGA and PLGA/gelatin nanofibers embedded with silica nanoparticles for tissue engineering. *International Journal of Biological Macromolecules, 79*, 687–695. https://doi.org/10.1016/j.ijbiomac.2015.05.050

Mendes, A.C. and Chronakis, I.S. (2019) Functional Phospholipid Nano-Microfibers and Nano-Microparticles by Electrohydrodynamic Processing: A Review. *Journal of Self-Assembly and Molecular Electronics (SAME), 7*, 23–44.

Mendes, A.C. and Chronakis, I.S. (2021) Electrohydrodynamic encapsulation of probiotics: A review. *Food Hydrocolloids, 117*, 106688. https://doi.org/10.1016/j.foodhyd.2021.106688

Mendes, R., Silva, H., Oliveira, P., Oliveira, L. and Teixeira, B. (2021) Quality of Frozen Hake Fillets in the Portuguese Retail Market: A Case Study of Inadequate Practices in the European Frozen White Fish Market. *Foods*, *10*, 848.

Meral, R., Alav, A., Karakas, C.Y., Dertli, E., Yilmaz, M.T. and Ceylan, Z. (2019a) Effect of electrospun nisin and curcumin loaded nanomats on the microbial quality, hardness and sensory characteristics of rainbow trout fillet. *LWT-Food Science and Technology, 113*, 108292. https://doi.org/10.1016/j.lwt.2019.108292

Meral, R., Ceylan, Z. and Kose, S. (2019b) Limitation of microbial spoilage of rainbow trout fillets using characterized thyme oil antibacterial nanoemulsions. *Journal of Food Safety, 39,* e12644.

Meral, R., Ceylan, Z., Kutlu, N., Kılıçer, A., Çağlar, A. and Tomar, O. (2022) Antimicrobial nanocoating for food industry. *Handbook of Microbial Nanotechnology*, 255–283.

Mercante, L.A., Scagion, V.P., Migliorini, F.L., Mattoso, L.H.C. and Correa, D.S. (2017) Electrospinning-based (bio)sensors for food and agricultural applications: A review. *TrAC Trends in Analytical Chemistry, 91,* 91–103.

Michalski, M.C., Desobry, S. and Hardy, J. (1997) Food materials adhesion: A review. *Critical reviews in food science and nutrition*, *37*(7), 591-619.

Miguel, G.A., Jacobsen, C., Prieto, C., Kempen, P.J., Lagaron, J.M., Chronakis, I.S. and García-Moreno, P.J. (2019) Oxidative stability and physical properties of mayonnaise fortified with zein electrosprayed capsules loaded with fish oil. *Journal of Food Engineering, 263,* 348–358. https://doi.org/10.1016/j.jfoodeng.2019.07.019

Mikulic-Petkovsek, M., Schmitzer, V., Slatnar, A., Todorovic, B., Veberic, R., Stampar, F. and Ivancic, A. (2014) Investigation of Anthocyanin Profile of Four Elderberry Species and Interspecific Hybrids. *Journal of agricultural and food chemistry*, *62*(24), 5573-5580.

Ministry of Agriculture and Forest Food Control Laboratory Directorate (2022) Turkish Food Codex Regulation on Microbiological Criteria-Legislation Draft. https://www.tarimorman. gov.tr / GKGM / Duyuru / 493 / Mevzuat – Taslagi – Turk – Gida -Kodeksi-Mikrobiyolojik-Kriterler-Yonetmelik-Taslagi.

Ministry of Agriculture and Forestry (2011) *Prime Ministry Legislation Development and Publication General Directorate*. Forestry Sensory Properties Of Fishery Products And Total Volatile Basic Nitrogen Limits Communique.

Mohamady Hussein, M.A., Guler, E., Rayaman, E., Cam, M.E., Sahin, A., Grinholc, M., Sezgin Mansuroglu, D., Sahin, Y.M., Gunduz, O., Muhammed, M., El-Sherbiny, I.M. and Megahed, M. (2021) Dual-drug delivery of Ag-chitosan nanoparticles and phenytoin via core-shell PVA/PCL electrospun nanofibers. *Carbohydrate Polymers, 270,* 118373. https://doi.org/10.1016/j.carbpol.2021.118373

Moharam, M.A. and Abbas, L.M. (2010) A study on the effect of microwave heating on the properties of edible oils using FTIR spectroscopy. *African Journal of Microbiological Research, 4,* 1921-1927.

Mohseni-Shahri, F., Mehrzad, A., Khoshbin, Z., Sarabi-Jamab, M., Khanmohamadi, F. and Verdian, A. (2023) Polyphenol-loaded bacterial cellulose nanofiber as a green indicator for fish spoilage. *International Journal of Biological Macromolecules, 224,* 1174-1182. https://doi.org/10.1016/j.ijbiomac.2022.10.203

Monaghan, B.R. and White, H.L. (1936) Effect of proteins on electrophoretic mobilitiy and sedimentation velocitiy of red cells. *Journal of General Physiology*, *19*, 715–726.

Moon, K.S., Dong, H., Maric, R., Pothukuchi, S., Hunt, A., Li, Y.I. and Wong, C.P. (2005) Thermal behavior of silver nanoparticles for low-temperature interconnect applications. *Journal of Electronic Materials 34*, 168–175.

Moosavi-Nasab, M., Khoshnoudi-Nia, S., Azimifar, Z. and Kamyab, S. (2021) Evaluation of the total volatile basic nitrogen (TVB-N) content in fish fillets using hyperspectral imaging coupled with deep learning neural network and meta-analysis. *Scientific Reports*, *11*, 1–11.

Moradkhannejhad, L., Abdouss, M., Nikfarjam, N., Mazinani, S. and Heydari, V. (2018) Electrospinning of zein/propolis nanofibers; antimicrobial properties and morphology investigation. *Journal of Materials Science: Materials in Medicine*, *29*, 1-10.

Morsi, M.A. and Abdelghany, A.M. (2017) UV-irradiation assisted control of the structural, optical and thermal properties of PEO/PVP blended gold nanoparticles. *Materials Chemistry and Physics*, *201*, 100-112.

Morsi, M.A., Rajeh, A. and Menazea, A.A. (2019) Nanosecond laser-irradiation assisted the improvement of structural, optical and thermal properties of polyvinyl pyrrolidone/carboxymethyl cellulose blend filled with gold nanoparticles. *Journal of Materials Science: Materials in Electronics*, *30*, 2693–2705.

Morsy, R. (123AD) Influence of substrate temperature parameter on electrospinning process: example of application to the formation of gelatin fibers. *Polymer Bulletin*, 1-12.

Mousdis, G.A., Kompitsas, M., Fasaki, I., Suchea, M. and KiriakIDis, G. (n.d.) The Effect Of Au Nanoclusters In Tin OxIDe Film Gas Sensors. In *Nanostructured Materials for Advanced Technological Applications*, pp.219–222. Dordrecht: Springer Netherlands.

Naderi, S., Ghaderi, A., Solaymani, S. and Golzan, M.M. (2012) Structural, optical and thermal properties of silver colloidal nanoparticles. *The European Physical Journal - Applied Physics*, *58*, 20401.

Naghdi, S., Rezaei, M., Bahramifar, N. and Kuswandi, B. (2022) Preparation and characterization of intelligent color-changing nanosensor based on bromophenol blue and GONH2 nanosheet for freshness evaluation of minced Caspian sprat (*Clupeonella cultriventris caspia*) stored at 4 °C. *Chemical Papers*, *1*, 1–14.

Nair, K. (2002) Handling of Fish Onboard Fishing Vessels. *Central Institute of Fisheries Technology*, Cochin-682 029.

Najafi, Z., Cetinkaya, T., Bildik, F., Altay, F. and Yeşilçubuk, N.Ş. (2022) Nanoencapsulation of saffron (*Crocus sativus L.*) extract in zein nanofibers and their application for the preservation of sea bass fillets. *LWT-Food Science and Technology*, *163*, 113588. https://doi.org/10.1016/j.lwt.2022.113588

Neira, L.M., Agustinelli, S.P., Ruseckaite, R.A. and Martucci, J.F. (2019) Shelf life extension of refrigerated breaded hake medallions packed into active edible fish gelatin films. *Packaging Technology and Science*, *32*, 471–480.

Neves, D., Andrade, P.B., Videira, R.A., de Freitas, V. and Cruz, L. (2022) Berry anthocyanin-based films in smart food packaging: A mini-review. *Food Hydrocolloids*, *133*, 107885. https://doi.org/10.1016/j.foodhyd.2022.107885

Nguyen, L.T., Ahmad, I. and Jayanath, N.Y. (2020) Dielectric Properties of Selected Seafood and their Products. In *Encyclopedia of Marine Biotechnology*, pp.2867–2880. Wiley.

Nikolic, M.V., Vasiljevic, Z.Z., Auger, S. and Vidic, J. (2021) Metal oxide nanoparticles for safe active and intelligent food packaging. *Trends in Food Science & Technology*, 116, 655–668. https://doi.org/10.1016/j.tifs.2021.08.019

Oğuzhan, P. and Angiş, S. (2012) Effect of Salting and Packaging Treatments on Fresh Rainbow Trout (Oncorhynchus mykiss) Fillets During Storage at Refrigerator Temperatures. *Kafkas Universitesi Veterinerlik Fakultesi Dergisi*, *18*, 443–448.

Okkeh, M., Bloise, N., Restivo, E., Vita, L. de, Pallavicini, P. and Visai, L. (2021) Gold Nanoparticles: Can They Be the Next Magic Bullet for Multidrug-Resistant Bacteria? *Nanomaterials*, *11*, 312.

Okutan, N., Terzi, P. and Altay, F. (2014) Affecting parameters on electrospinning process and characterization of electrospun gelatin nanofibers. *Food Hydrocolloids*, *39*, 19–26. https://doi.org/10.1016/j.foodhyd.2013.12.022

Olatunde, O.O. and Benjakul, S. (2018) Natural Preservatives for Extending the Shelf-Life of Seafood: A Revisit. *Comprehensive Reviews in Food Science and Food Safety*, *17*(6), 1595-1612.

Omerović, N., Djisalov, M., Živojević, K., Mladenović, M., Vunduk, J., Milenković, I., Knežević, N.Ž., Gadjanski, I. and Vidić, J. (2021) Antimicrobial nanoparticles and biodegradable polymer composites for active food packaging applications. *Comprehensive Reviews in Food Science and Food Safety*, *20*(3), 2428-2454.

Opara, U.L., Fadiji, T., Caleb, O.J. and Oluwole, A.O. (2022) Changes in Volatile Composition of Cape Hake Fillets under Modified Atmosphere Packaging Systems during Cold Storage. *Foods*, *11*, 1292.

Orban, E., Nevigato, T., di Lena, G., Masci, M., Casini, I., Caproni, R. and Rampacci, M. (2011) Total volatile basic nitrogen and trimethylamine nitrogen levels during ice storage of European hake (*Merluccius merluccius*): A seasonal and size differentiation. *Food Chemistry*, *128*, 679–682. https://doi.org/10.1016/j.foodchem.2011.03.086

Ordóñez, J.A., López-Gálvez, D.E., Fernández, M., Hierro, E. and de La Hoz, L. (2000) Microbial and physicochemical modifications of hake (*Merluccius merluccius*) steaks stored under carbon dioxide enriched atmospheres. *Journal of the Science of Food and Agriculture*, *80*(13), 1831-1840.

Otero, L., Pérez-Mateos, M. and López-Caballero, M.E. (2017) Hyperbaric cold storage versus conventional refrigeration for extending the shelf-life of hake loins. *Innovative Food Science & Emerging Technologies*, *41*, 19–25. https://doi.org/10.1016/j.ifset.2017.01.003

Ozogul, Y., Durmus, M., Uçar, Y., Köşker, A.R. and Ozogul, F. (2017a) The combined impact of nanoemulsion based on commercial oils and vacuum packing on the fatty acid profiles of sea bass fillets. *Journal of Food Processing Preservation*, *41*, e13222.

Ozogul, Y., Kuley Boğa, E., Akyol, I., Durmus, M., Ucar, Y., Regenstein, J.M. and Köşker, A.R. (2020) Antimicrobial activity of thyme essential oil nanoemulsions on spoilage bacteria of fish and food-borne pathogens. *Food Bioscience*, *36*, 100635.

Ozogul, Y., Yuvka, İ., Ucar, Y., Durmus, M., Kösker, A.R., Öz, M. and Ozogul, F. (2017b) Evaluation of effects of nanoemulsion based on herb essential oils (rosemary, laurel, thyme and sage) on sensory, chemical and microbiological quality of rainbow trout (*Oncorhynchus mykiss*) fillets during ice storage. *LWT-Food Science and Technology*, *75*, 677–684. https://doi.org/10.1016/j.lwt.2016.10.009

Özogul, Y., Durmus, M., Ucar, Y., Özogul, F. and Regenstein, J.M. (2016) Comparative study of nanoemulsions based on commercial oils (sunflower, canola, corn, olive, soybean, and hazelnut oils): Effect on microbial, sensory, and chemical qualities of refrigerated farmed sea bass. *Innovative Food Science and Emerging Technologies*, *33*, 422–430. https://doi.org/10.1016/j.ifset.2015.12.018

Pandey, S., Sharma, K. and Gundabala, V. (2022) Antimicrobial bio-inspired active packaging materials for shelf life and safety development: A review. *Food Bioscience*, *48*, 101730.

Panicker, S., Ahmady, I.M., Han, C., Chehimi, M. and Mohamed, A.A. (2020) On demand release of ionic silver from gold-silver alloy nanoparticles: fundamental antibacterial mechanisms study. *Materials Today Chemistry*, *16*, 100237.

Park, J.S. (2011) Electrospinning and its applications. *Advances in Natural Sciences: Nanoscience and Nanotechnology*, 1, 043002.

Parlapani, F.F., Mallouchos, A., Haroutounian, S.A. and Boziaris, I.S. (2014) Microbiological spoilage and investigation of volatile profile during storage of sea bream fillets under various conditions. *International journal of food microbiology*, *189*, 153-163.

Parlapani, F.F., Mallouchos, A., Haroutounian, S.A. and Boziaris, I.S. (2017) Volatile organic compounds of microbial and non-microbial origin produced on model fish substrate un-inoculated and inoculated with gilt-head sea bream spoilage bacteria. *LWT-Food Science and Technology*, *78*, 54–62. https://doi.org/10.1016/j.lwt.2016.12.020

Pecora, R. (1985) Dynamic light scattering : applications of photon correlation spectroscopy. 420.

Penders, J., Stolzoff, M., Hickey, D.J., Andersson, M. and Webster, T.J. (2017) Shape-dependent antibacterial effects of non-cytotoxic gold nanoparticles. *International journal of nanomedicine*, *12*, 2457.

Peng, J., Tang, Y., Lin, J., Li, J., Shi, K., Ng, A.M.C. and He, Y. (2018) Surface-plasmon-enhanced SnO2 nanofiber gas sensor. In *Nanophotonics and Micro/Nano Optics IV* ed. Zhou, Z. and Wada, K. p.48. SPIE.

Pérez-Guzmán, C.J. and Castro-Muñoz, R. (2020) A review of zein as a potential biopolymer for tissue engineering and nanotechnological applications. *Processes*, *8*(11), 1376.

Pérez-Villarreal, B. and Howgate, P. (1987) Spoilage of European hake (*Merluccius merluccius*) in ice. *Journal of the Science of Food and Agriculture*, *41*(4), 335-350.

Perry, J.H. (1950) Chemical engineers' handbook. *Journal of Chemical Education*, 27, 533.

Pliquett, U., Altmann, M., Pliquett, F. and Schöberlein, L. (2003) Py - A parameter for meat quality. *Meat Science*, *65*, 1429–1437.

Prietto, L., Pinto, V.Z., el Halal, S.L.M., de Morais, M.G., Costa, J.A.V., Lim, L.T., Dias, A.R.G. and Zavareze, E. da R. (2018) Ultrafine fibers of zein and anthocyanins as natural pH indicator. *Journal of the Science of Food and Agriculture*, *98*(7), 2735-2741.

Puthiyaveetil Yoosaf, M.A., Jayaprakash, A., Ghosh, S., Jaswal, V.S., Singh, K., Mandal, S., Shahid, M., Yadav, M., Das, S. and Kumar, P. (2019) Zein film functionalized with gold nanoparticles and the factors affecting its mechanical properties. *RSC Advances*, *9*, 25184–25188.

R Sharma, M.R. and S Ahmad, M.A. (2013) Nanotechnology: A Novel Tool for Aquaculture and Fisheries Development. A Prospective Mini-Review. *Fisheries and Aquaculture Journal*, *16*(1-5), 3.

Raba, D.N., Poiana, M.A., Borozan, A.B., Stef, M., Radu, F. and Popa, M.V. (2015) Investigation on Crude and High-Temperature Heated Coffee Oil by ATR-FTIR Spectroscopy along with Antioxidant and Antimicrobial Properties. *PLoS One*, *10*, e0138080.

Rajar, K., Alveroglu, E., Caglar, M. and Caglar, Y. (2021) Highly selective colorimetric onsite sensor for Co2+ ion detection by povidone capped silver nanoparticles. *Materials Chemistry and Physics*, *273*, 125082.

Ranjbar-Mohammadi, M., Zamani, M., Prabhakaran, M.P., Bahrami, S.H. and Ramakrishna, S. (2016) Electrospinning of PLGA/gum tragacanth nanofibers containing tetracycline hydrochloride for periodontal regeneration. *Materials Science and Engineering: C*, *58*, 521–531.

Rath, G., Hussain, T., Chauhan, G., Garg, T. and Goyal, A.K. (2016) Development and characterization of cefazolin loaded zinc oxide nanoparticles composite gelatin nanofiber mats for postoperative surgical wounds. *Materials Science and Engineering: C, 58*, 242–253.

Rawdkuen, S., Faseha, A., Benjakul, S. and Kaewprachu, P. (2020) Application of anthocyanin as a color indicator in gelatin films. *Food Bioscience, 36*, 100603.

Reddy Panyala, N., María Peña-Méndez, E. and Havel, J. (2009) Gold and nano-gold in medicine: overview, toxicology and perspectives. *Journal of applied biomedicine, 7*(2).

Rey, M.S., García-Soto, B., Fuertes-Gamundi, J.R., Aubourg, S. and Barros-Velázquez, J. (2012) Effect of a natural organic acid-icing system on the microbiological quality of commercially relevant chilled fish species. *LWT-Food Science and Technology*, *46*, 217–223. https://doi.org/10.1016/j.lwt.2011.10.003

Rezaei, A., Fathi, M. and Jafari, S.M. (2019) Nanoencapsulation of hydrophobic and low-soluble food bioactive compounds within different nanocarriers. *Food Hydrocolloids*, *88*, 146–162. https://doi.org/10.1016/j.foodhyd.2018.10.003

Ringø, E. and Strøm, E. (1994) Microflora of Arctic charr, Salvelinus alpinus (L.): gastrointestinal microflora of free-living fish and effect of diet and salinity on intestinal microflora. *Aquaculture Research, 25*, 623–629.

Rodrigues Arruda, T., Campos Bernardes, P., Robledo Fialho e Moraes, A. and de Fátima Ferreira Soares, N. (2022) Natural bioactives in perspective: The future of active packaging based on essential oils and plant extracts themselves and those complexed by cyclodextrins. *Food Research International, 156*, 111160.

Rodríguez, Ó., Losada, V., Aubourg, S.P. and Barros-Velázquez, J. (2004) Enhanced shelf-life of chilled European hake (*Merluccius merluccius*) stored in slurry ice as determined by sensory analysis and assessment of microbiological activity. *Food Research International*, *37*, 749–757.

Rozemarie Manea, L. and Bertea, A.-P. (2019) Sensors from Electrospun Nanostructures. In *Nanostructures in Energy Generation, Transmission and Storage*, IntechOpen.

Ruiz-Capillas, C. and Moral, A. (2001) Correlation between biochemical and sensory quality indices in hake stored in ice. *Food Research International, 34*, 441–447.

Sahraee, S., Milani, J.M., Ghanbarzadeh, B. and Hamishehkar, H. (2017) Physicochemical and antifungal properties of bio-nanocomposite film based on gelatin-chitin nanoparticles. *International Journal of Biological Macromolecules, 97*, 373–381. https://doi.org/10.1016/j.ijbiomac.2016.12.066

Saleh, M., Kumar, G., Abdel-Baki, A.A., Al-Quraishy, S. and El-Matbouli, M. (2016) In vitro antimicrosporidial activity of gold nanoparticles against Heterosporis saurida. *BMC veterinary research*, *12*(1), 1-6.

Sameen, D.E., Ahmed, S., Lu, R., Li, R., Dai, J., Qin, W., Zhang, Q., Li, S. and Liu, Y. (2021) Electrospun nanofibers food packaging: trends and applications in food systems. *Critical Reviews in Food Science and Nutrition*, *62*(22), 6238-6251.

Samuel, D. and Trabelsi, S. (2012) Influence of color on dielectric properties of marinated poultry breast meat. *Poultry Science*, *91*, 2011–2016. https://doi.org/10.3382/ps.2011-01837

Sánchez-Valencia, J., Sánchez-Alonso, I., Martinez, I. and Careche, M. (2014) Estimation of frozen storage time or temperature by kinetic modeling of the Kramer shear resistance and water holding capacity (WHC) of hake (*Merluccius merluccius, L*.) muscle. *Journal of Food Engineering*, *120*, 37–43. https://doi.org/10.1016/j.jfoodeng.2013.07.012

Sant'Ana, L.S., Soares, S. and Vaz-Pires, P. (2011) Development of a quality index method (QIM) sensory scheme and study of shelf-life of ice-stored blackspot seabream (*Pagellus bogaraveo*). *LWT-Food Science and Technology*, *44*, 2253–2259. https://doi.org/10.1016/j.lwt.2011.07.004

Saraiva, C., Vasconcelos, H. and de Almeida, J.M.M.M. (2017) A chemometrics approach applied to Fourier transform infrared spectroscopy (FTIR) for monitoring the spoilage of fresh salmon (*Salmo salar*) stored under modified atmospheres. *International Journal of Food Microbiology*, *241*, 331–339.

Saunders, Z., Noack, C.W., Dzombak, D.A. and Lowry, G. v. (2015) Characterization of engineered alumina nanofibers and their colloidal properties in water. *Journal of Nanoparticle Research*, *17*, 140.

Schiffman, J.D. and Schauer, C.L. (2007) Cross-linking chitosan nanofibers. *Biomacromolecules*, *8*, 594–601.

Scientific Opinion on the re-evaluation of gold (E 175) as a food additive (2016) *EFSA Journal*, *14*.

Seethu, B.G., Pushpadass, H.A., Emerald, F.M.E., Nath, B.S., Naik, N.L. and Subramanian, K.S. (2020) Electrohydrodynamic Encapsulation of Resveratrol Using Food-Grade Nanofibres: Process Optimization, Characterization and Fortification. *Food Bioprocess Technology*, *13*, 341–354. https://doi.org/10.1007/s11947-019-02399-4

Serdaroğlu, M. and Deniz, E.E. (2001) Balıklarda ve Bazı Su Ürünlerinde Trimetilamin (TMA) ve Dimetilamin (DMA) Oluşumunu Etkileyen Koşullar. *Ege Journal of Fisheries and Aquatic Sciences*, *18*, 575–581.

Shavisi, N. and Shahbazi, Y. (2022) Chitosan-gum Arabic nanofiber mats encapsulated with pH-sensitive Rosa damascena anthocyanins for freshness monitoring of chicken fillets. *Food Packaging Shelf Life*, *32*, 100827.

Shen, C., Cao, Y., Rao, J., Zou, Y., Zhang, H., Wu, D. and Chen, K. (2021) Application of solution blow spinning to rapidly fabricate natamycin-loaded gelatin/zein/polyurethane antimicrobial nanofibers for food packaging. *Food Packaging Shelf Life*, *29*, 100721.

Silva, P.M., Torres-Giner, S., Vicente, A.A. and Cerqueira, M.A. (2021) Electrohydrodynamic processing for the production of zein-based microstructures and nanostructures. *Current Opinion in Colloid & Interface Science*, *56*, 101504.

Silva, V.M. da, Silva, L.A., Andrade, J.B. de, Veloso, M.C. da C. and Santos, G.V. (2008) Determination of moisture content and water activity in algae and fish by thermoanalytical techniques. *Quimica Nova*, *31*, 901-905.

Simeonidou, S., Govaris, A. and Vareltzis, K. (1997) Effect of frozen storage on the quality of whole fish and fillets of horse mackerel (*Trachurus trachurus*) and mediterranean hake (*Merluccius mediterraneus*). *Zeitschrift für Lebensmitteluntersuchung und -Forschung A, 204*, 405–410.

Singh, P., König, T.A.F. and Jaiswal, A. (2018) NIR-Active Plasmonic Gold Nanocapsules Synthesized Using Thermally Induced Seed Twinning for Surface-Enhanced Raman Scattering Applications. *ACS Applied Materials Interfaces, 10*, 39380–39390.

Socrates, G. (2001) Infrared and Raman Characteristic Group Frequencies: Tables and Charts. John Wiley & Sons.

Sone, I., Olsen, R.L., Dahl, R. and Heia, K. (2011) Visible/Near-Infrared Spectroscopy Detects Autolytic Changes during Storage of Atlantic Salmon (*Salmo salar L.*). *Journal of Food Science, 76*, S203–S209.

Song, J.H., Kim, H.E. and Kim, H.W. (2008) Production of electrospun gelatin nanofiber by water-based co-solvent approach. *Journal of Materials Science: Materials in Medicine*, *19*, 95-102.

Sosa-Morales, M.E., Valerio-Junco, L., López-Malo, A. and García, H.S. (2010) Dielectric properties of foods: Reported data in the 21st century and their potential applications. *LWT-Food Science and Technology*, *43*(8), 1169-1179. https://doi.org/10.1016/j.lwt.2010.03.017

Sotelo, C.G., Gallardo, J.M., Piñeiro, C. and Pérez-Martin, R. (1995) Trimethylamine oxide and derived compounds' changes during frozen storage of hake (*Merluccius merluccius*). *Food Chemistry*, *53*, 61–65.

Souza, B.W.S., Cerqueira, M.A., Ruiz, H.A., Martins, J.T., Casariego, A., Teixeira, J.A. and Vicente, A.A. (2010) Effect of Chitosan-based coatings on the shelf life of Salmon (*Salmo salar*). *Journal of Agricultural and Food Chemistry*, *58*(21), 11456-11462. https://doi.org/10.1021/jf102366k

Speranza, B., Racioppo, A., Bevilacqua, A., Buzzo, V., Marigliano, P., Mocerino, E., Scognamiglio, R., Corbo, M.R., Scognamiglio, G. and Sinigaglia, M. (2021) Innovative Preservation Methods Improving the Quality and Safety of Fish Products: Beneficial Effects and Limits. *Foods, 10, 2854*. 10, 2854.

Sriket, C. (2014) Proteases in fish and shellfish: Role on muscle softening and prevention. *International Food Research Journal*, *21*(2).

Stagnitta, P. v., Micalizzi, B. and Stefanini De Guzmán, A.M. (2006) Prevalence of some bacteria yeasts and molds in meat foods in San Luis, Argentina. *Central European journal of public health*, *14*(3), 141-144.

Stołyhwo, A. and Sikorski, Z.E. (2005) Polycyclic aromatic hydrocarbons in smoked fish – a critical review. *Food Chemistry*, *91*, 303–311. https://doi.org/10.1016/j.foodchem.2004.06.012

Suganya, P., Vaseeharan, B., Vijayakumar, S., Balan, B., Govindarajan, M., Alharbi, N.S., Kadaikunnan, S., Khaled, J.M. and Benelli, G. (2017) Biopolymer zein-coated gold nanoparticles: Synthesis, antibacterial potential, toxicity and histopathological effects against the Zika virus vector Aedes aegypti. *Journal of Photochemistry and Photobiology B: Biology*, *173*, 404-411.

Sullivan, D.J., Cruz-Romero, M.C., Hernandez, A.B., Cummins, E., Kerry, J.P. and Morris, M.A. (2020) A novel method to deliver natural antimicrobial coating materials to extend the shelf-life of European hake (*Merluccius merluccius*) fillets. *Food Packaging Shelf Life*, *25*, 100522.

Sun, B., Long, Y.Z., Zhang, H.D., Li, M.M., Duvail, J.L., Jiang, X.Y. and Yin, H.L. (2014) Advances in three-dimensional nanofibrous macrostructures via electrospinning. *Progress in Polymer Science*, *39*, 862–890.

Tabatabaei, S., Kumar, A., Ardebili, H., Loos, P.J. and Ajayan, P.M. (2012) Synthesis of Au–Sn alloy nanoparticles for lead-free electronics with unique combination of low and high melting temperatures. *Microelectronics Reliability*, *52*, 2685–2689.

Tanaka, Y., Yamamoto, T., Satomi, Y., Kubota, H. and Makita, T. (1977) Specific volume and viscosity of ethanol-water mixtures under high pressure. *The Review of Physical Chemistry of Japan*, *47*, 12–24.

Taşkaya, L., Hasanhocaoğlu Yapıcı, H., Metin Cansu and Alparslan, Y. (2017) The effect of lavender (Lavandula stoechas) on the shelf life of a traditional food: hamsi kaygana. *Food Science and Technology*, *38*, 711–718.

Teixeira, B. and Mendes, R. (2022) Analysis of added phosphates in hake fillets by ion-exchange chromatography: A case study of false positives induced by nucleotides coelution. *Food Chemistry*, *368*, 130841. https://doi.org/10.1016/j.foodchem.2021.130841

Thirumurugan, A., Ramachandran, S. and Shiamala Gowri, A. (2013) Combined effect of bacteriocin with gold nanoparticles against food spoiling bacteria-an approach for food packaging material preparation. *International Food Research Journal*, *20*, 1909–1912.

Tıraş, B., Dede, S. and Altay, F. (2019) Dielectric Properties of Foods. *Turkish Journal of Agriculture - Food Science and Technology*, *7*, 1805–1816.

Tito, N.B., Rodemann, T. and Powell, S.M. (2012) Use of near infrared spectroscopy to predict microbial numbers on Atlantic salmon. *Food Microbiology*, *32*, 431–436.

Toranzo, A.E., Magariños, B. and Romalde, J.L. (2005) A review of the main bacterial fish diseases in mariculture systems. *Aquaculture*, *246*, 37–61.

Torres-Giner, S., Gimenez, E. and Lagaron, J.M. (2008) Characterization of the morphology and thermal properties of Zein Prolamine nanostructures obtained by electrospinning. *Food Hydrocolloids*, *22*, 601–614.

TUİK (2021) *SU ÜRÜNLERİ İSTATİSTİKLERİ*. Ankara.

Turasan, H. and Kokini, J.L. (2017) Advances in Understanding the Molecular Structures and Functionalities of Biodegradable Zein-Based Materials Using Spectroscopic Techniques: A Review. *Biomacromolecules*, *18*, 331–354.

Turasan, H., Cakmak, M. and Kokini, J. (2019) Fabrication of zein-based electrospun nanofiber decorated with gold nanoparticles as a SERS platform. *Journal of Materials Science*, *54*, 8872–8891.

Tyson, W.R. and Miller, W.A. (1977) Surface free energies of solid metals: Estimation from liquid surface tension measurements. *Surface Science*, *62*(1), 267-276.

Ucar, Y., Ceylan, Z., Durmus, M., Tomar, O. and Cetinkaya, T. (2021) Application of cold plasma technology in the food industry and its combination with other emerging technologies. *Trends in Food Science & Technology*, *114*, 355–371. https://doi.org/10.1016/j.tifs.2021.06.004

Uçar, Y. (2020) Antioxidant Effect of Nanoemulsions Based on Citrus Peel Essential Oils: Prevention of Lipid Oxidation in Trout. *European Journal of Lipid Science and Technology*, *122*, 1900405.

Uygun, E., Yildiz, E., Sumnu, G. and Sahin, S. (2020) Microwave Pretreatment for the Improvement of Physicochemical Properties of Carob Flour and Rice Starch–Based Electrospun Nanofilms. *Food Bioprocess Technology*, *13*, 838–850. https://doi.org/10.1007/s11947-020-02440-x

Ünal Şengör, G.F., Balaban, M.O., Ceylan, Z. and Doğruyol, H. (2018) Determination of shelf life of gilthead seabream (Sparus aurata) with time temperature indicators. *Journal of Food Processing and Preservation*, *42*(2), e13426.

Vilela, D., González, M.C. and Escarpa, A. (2012) Sensing colorimetric approaches based on gold and silver nanoparticles aggregation: Chemical creativity behind the assay. A review. *Analytica chimica acta*, *751*, 24-43.

Vykoukal, V., Zelenka, F., Bursik, J., Kana, T., Kroupa, A. and Pinkas, J. (2020) Thermal properties of Ag@Ni core-shell nanoparticles. *Calphad*, *69*, 101741.

Wahyuningsih, S., Wulandari, L., Wartono, M.W., Munawaroh, H. and Ramelan, A.H. (2017) The Effect of pH and Color Stability of Anthocyanin on Food Colorant. *IOP conference series: Materials science and engineering*, *193*, 012047. https://doi.org/10.1088/1757-899X/193/1/012047

Wang, K., Qi, Z., Pan, S., Zheng, S., Wang, H., Chang, Y.X., Li, H., Xue, P., Yang, X. and Fu, C. (2020) Preparation, characterization and evaluation of a new film based on chitosan, arginine and gold nanoparticle derivatives for wound-healing efficacy. *RSC Advances*, *10*, 20886–20899.

Wang, Y. de, Wu, X.H., Su, Q., Li, Y.F. and Zhou, Z.L. (2001) Ammonia-sensing characteristics of Pt and SiO2 doped SnO2 materials. *Solid State Electron*, *45*, 347–350.

Wang, Y., Tang, J., Rasco, B., Kong, F. and Wang, S. (2008) Dielectric properties of salmon fillets as a function of temperature and composition. *Journal of Food engineering*, *87*(2), 236-246. https://doi.org/10.1016/j.jfoodeng.2007.11.034

Wang, Y.H., Zhao, M., Barker, S.A., Belton, P.S. and Craig, D.Q.M. (2019) A spectroscopic and thermal investigation into the relationship between composition, secondary structure and physical characteristics of electrospun zein nanofibers. *Materials Science and Engineering C*, *98*, 409–418. https://doi.org/10.1016/j.msec.2018.12.134

Wei, D., Sun, W., Qian, W., Ye, Y. and Ma, X. (2009) The synthesis of chitosan-based silver nanoparticles and their antibacterial activity. *Carbohydrarte Research*, *344*, 2375–2382.

Wei, X. qing, Li, X. peng, Wu, C. ling, Yi, S. min, Zhong, K. li, Sun, T. and Li, J. rong (2018a) The Modification of In Situ SiOx Chitosan Coatings by ZnO/TiO2 NPs and Its Preservation Properties to Silver Carp Fish Balls. *Journal of food science*, *83*(12), 2992-3001

Wei, Y., Li, C., Zhang, L., Dai, L., Yang, S., Liu, J., Mao, L., Yuan, F. and Gao, Y. (2020) Influence of calcium ions on the stability, microstructure and in vitro digestion fate of zein-propylene glycol alginate-tea saponin ternary complex particles for the delivery of resveratrol. *Food Hydrocolloids*, *106*, 105886. https://doi.org/10.1016/j.foodhyd.2020.105886

Wei, Y., Sun, C., Dai, L., Zhan, X. and Gao, Y. (2018b) Structure, physicochemical stability and in vitro simulated gastrointestinal digestion properties of β-carotene loaded zein-propylene glycol alginate composite nanoparticles fabricated by emulsification-evaporation method. *Food Hydrocolloids*, *81*, 149–158. https://doi.org/10.1016/j.foodhyd.2018.02.042

Wen, P., Zong, M.H., Linhardt, R.J., Feng, K. and Wu, H. (2017) Electrospinning: A novel nano-encapsulation approach for bioactive compounds. *Trends in Food Science & Technology*, 70, 56–68. https://doi.org/10.1016/j.tifs.2017.10.009

Westfall, A., Sigurdson, G.T., Rodriguez-Saona, L.E. and Giusti, M.M. (2020) Ex Vivo and In Vivo Assessment of the Penetration of Topically Applied Anthocyanins Utilizing ATR-FTIR/PLS Regression Models and HPLC-PDA-MS. *Antioxidants,486*, 9.

Wu, Z., Deng, W., Luo, J. and Deng, D. (2019) Multifunctional nano-cellulose composite films with grape seed extracts and immobilized silver nanoparticles. *Carbohydrate Polymers, 205*, 447–455. https://doi.org/10.1016/j.carbpol.2018.10.060

Xu, D., Li, X. and Zhang, D. (2014) A facile one-pot method to Au–SnO2-graphene ternary hybrid. *Materials Research Bulletin*, *59*, 77-83.

Yabuki, A., Motonobu, E. and Fathona, I.W. (2017) Controlling the length of short electrospun polymer nanofibers via the addition of micro-spherical silica particles. *Journal of Materials Science*, *52*, 4016-4024. https://doi.org/10.1007/s10853-016-0663-4

Yazgan, H., Ozogul, Y. and Kuley, E. (2019) Antimicrobial influence of nanoemulsified lemon essential oil and pure lemon essential oil on food-borne pathogens and fish spoilage bacteria. *International Journal of Food Microbiology, 306*, 108266. https://doi.org/10.1016/j.ijfoodmicro.2019.108266

Yazgan, H., Ozogul, Y., Durmuş, M., Balikçi, E., Gökdoğan, S., Uçar, Y. and Aksun, E.T. (2017) Effects of Oil-in-Water Nanoemulsion Based on Sunflower Oil on the Quality of Farmed Sea Bass and Gilthead Sea Bream Stored at Chilled Temperature (2 ± 2°C). *Journal of Aquatic Food Product Technology*, *26*(8), 979-992. https://doi.org/10.1080/10498850.2017.1366610

Yilmaz, A., Bozkurt, F., Cicek, P.K., Dertli, E., Durak, M.Z. and Yilmaz, M.T. (2016) A novel antifungal surface-coating application to limit postharvest decay on coated apples: Molecular, thermal and morphological properties of electrospun zein–nanofiber mats loaded with curcumin. *Innovative Food Science and Emerging Technologies, 37*, 74–83. https://doi.org/10.1016/j.ifset.2016.08.008

Yilmaz, M.T., Akman, P.K., Bozkurt, F. and Karasu, S. (2021) An effective polydopamine coating to improve stability and bioactivity of carvacrol-loaded zein nanoparticles. *International Journal of Food Science & Technology*, *56*, 6011–6024.

Yilmaz, M.T., Yilmaz, A., Akman, P.K., Bozkurt, F., Dertli, E., Basahel, A., Al-Sasi, B., Taylan, O. and Sagdic, O. (2019) Electrospraying method for fabrication of essential oil loaded-chitosan nanoparticle delivery systems characterized by molecular, thermal, morphological and antifungal properties. *Innovative Food Science & Emerging Technologies*, *52*, 166–178. https://doi.org/10.1016/j.ifset.2018.12.005

Yurchenko, S. and Mölder, U. (2005) The determination of polycyclic aromatic hydrocarbons in smoked fish by gas chromatography mass spectrometry with positive-ion chemical ionization. *Journal of Food Composition and Analysis, 18*, 857–869. https://doi.org/10.1016/j.jfca.2004.11.004

Yurova, N.S., Danchuk, A., Mobarez, S.N., Wongkaew, N., Rusanova, T., Baeumner, A.J. and Duerkop, A. (2018) Functional electrospun nanofibers for multimodal sensitive detection of biogenic amines in food via a simple dipstick assay. *Analytical and bioanalytical chemistry, 410,* 1111-1121. https://doi.org/10.1007/s00216-017-0696-9

Zare, Y. and Shabani, I. (2016) Polymer/metal nanocomposites for biomedical applications. *Materials Science and Engineering: C, 60,* 195-203. https://doi.org/10.1016/j.msec.2015.11.023

Zarei, M., Ramezani, Z., Ein-Tavasoly, S. and Chadorbaf, M. (2015) Coating Effects of Orange and Pomegranate Peel Extracts Combined with Chitosan Nanoparticles on the Quality of Refrigerated Silver Carp Fillets. *Journal of food processing and preservation*, *39*(6), 2180-2187.

Zhang, B., Luo, Y. and Wang, Q. (2010) Development of silver-zein composites as a promising antimicrobial agent. *Biomacromolecules, 11,* 2366–2375.

Zhang, H. (2007) Electrical Properties of Foods. In *Food Engineering* ed. Barbosa-Canovas, G. pp.110–119. Oxford: Eolss Publisher Co. Ltd.

Zhang, H., Zhang, Y., Zhou, Y., Zhang, C., Wang, Q., Xu, Y. and Zhang, M. (2016) Synthesis and characterization of a multifunctional nanocatalyst based on a novel type of binary-metal-oxide-coated Fe 3 O 4 –Au nanoparticle. *RSC Advances, 6,* 18685–18694.

Zhang, X., Huang, W. and Xie, J. (2019) Effect of different packaging methods on protein oxidation and degradation of grouper (*Epinephelus coioides*) during refrigerated storage. *Foods, 8*. https://doi.org/10.3390/foods8080325

Zhang, X., Tan, L., Taxipalati, M. and Deng, L. (2021) Fabrication and characterization of fast dissolving glycerol monolaurate microemulsion encapsulated gelatin nanofibers with antimicrobial activity. *Journal of the Science of Food and Agriculture*, *101*(13), 5660-5670.

Zheng, K., Setyawati, M.I., Leong, D.T. and Xie, J. (2017) Antimicrobial Gold Nanoclusters. *ACS Nano, 11,* 6904–6910.

Zheng, K., Setyawati, M.I., Leong, D.T. and Xie, J. (2021) Overcoming bacterial physical defenses with molecule-like ultrasmall antimicrobial gold nanoclusters. *Bioactive materials*, *6*(4), 941-950.

Zheng, L., Liu, L., Yu, J. and Shao, P. (2022) Novel trends and applications of natural pH-responsive indicator film in food packaging for improved quality monitoring. *Food Control, 134,* 108769. https://doi.org/10.1016/j.foodcont.2021.108769

Zhong, Q. and Jin, M. (2009) Zein nanoparticles produced by liquid-liquid dispersion. *Food Hydrocolloids, 23*, 2380–2387. https://doi.org/10.1016/j.foodhyd.2009.06.015

Zhu, S., Shen, Y., Yu, Y. and Bai, X. (2020) Synthesis of antibacterial gold nanoparticles with different particle sizes using chlorogenic acid. *Royal Society open science*, *7*(3), 191141. https://doi.org/10.1098/rsos.191141

Zhuang, H., Nelson, S.O., Trabelsi, S. and Savage, E.M. (2007) Dielectric Properties of Uncooked Chicken Breast Muscles from Ten to One Thousand Eight Hundred Megahertz. *Poultry Science, 86*, 2433–2440. https://doi.org/10.3382/ps.2006-00434

APPENDICES

APPENDIX A: Supplemental material for Chapter 4

APPENDIX B: Supplemental material for Chapter 5

APPENDIX A

A.1-A.4 graphs were obtained by using Agilent Technologies 85070 software under the frequency range of 1 mHz-3000 MHz. First calibration was done by measuring air, short, and water. Then the probe was immersed into the zein solution (30 g/100 mL) containing the ethanol:liquid Au nanospheres (80:20 v/v). Measurements were done three times.

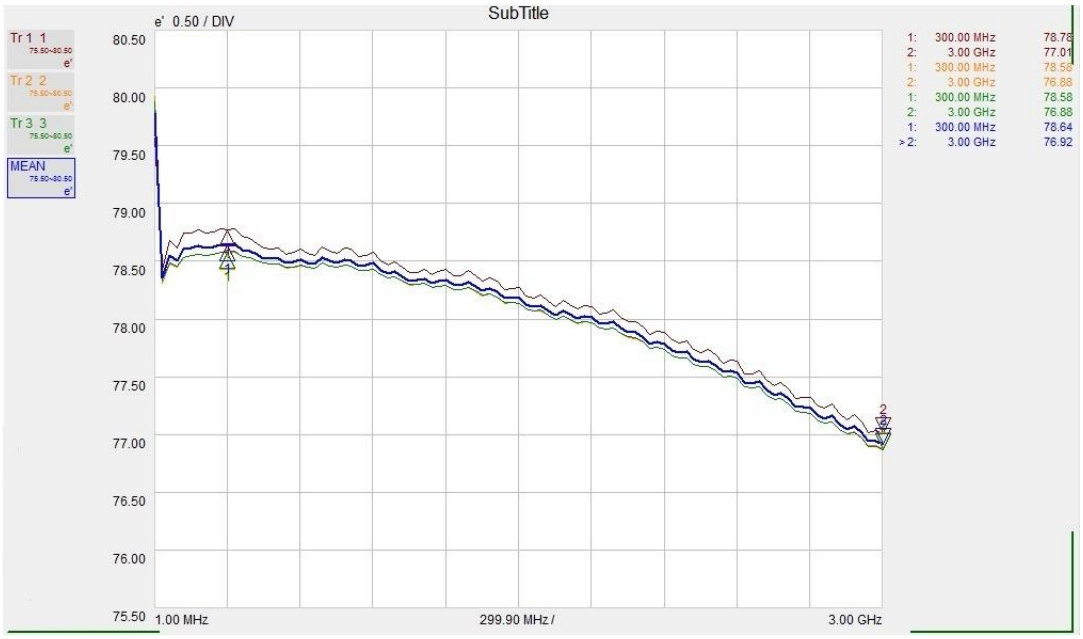

Figure A.1 : Dielectric constant values (***ε′***) of feeding solution.

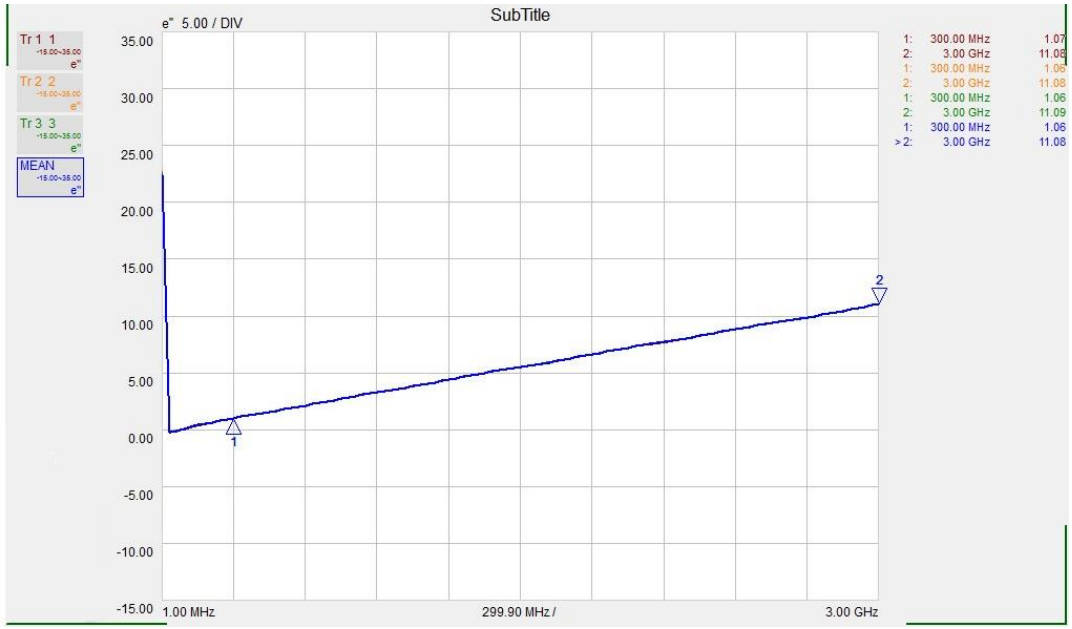

Figure A.2 : Dielectric loss factor (ε″) values of feeding solution.

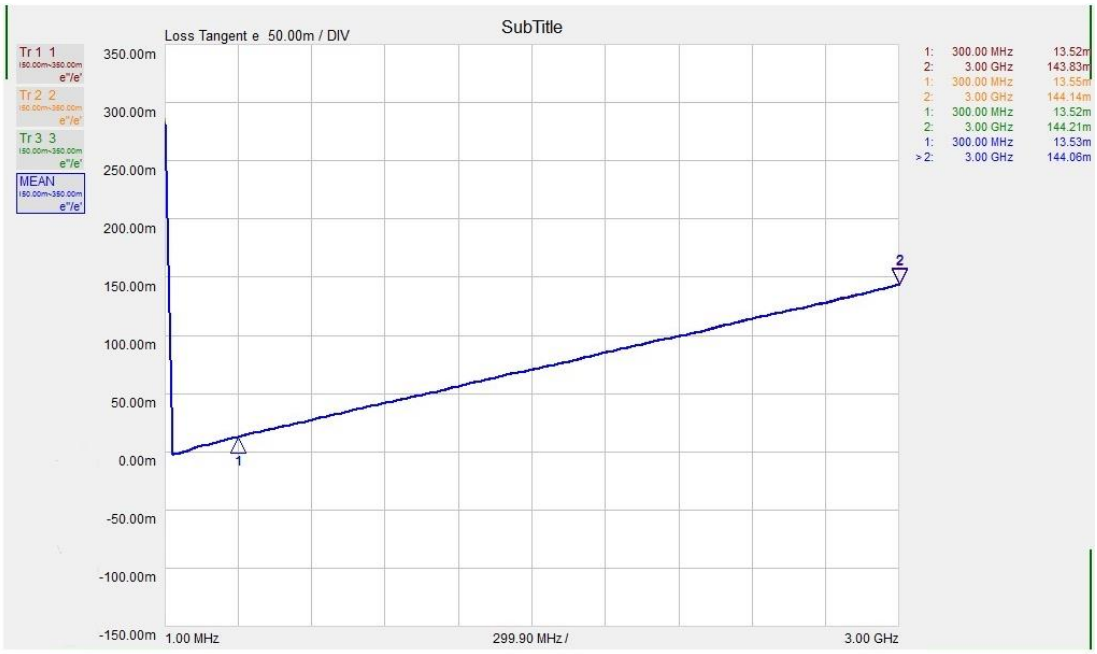

Figure A.3 : Loss tangent ($\varepsilon''/\varepsilon'$) values of feeding solution.

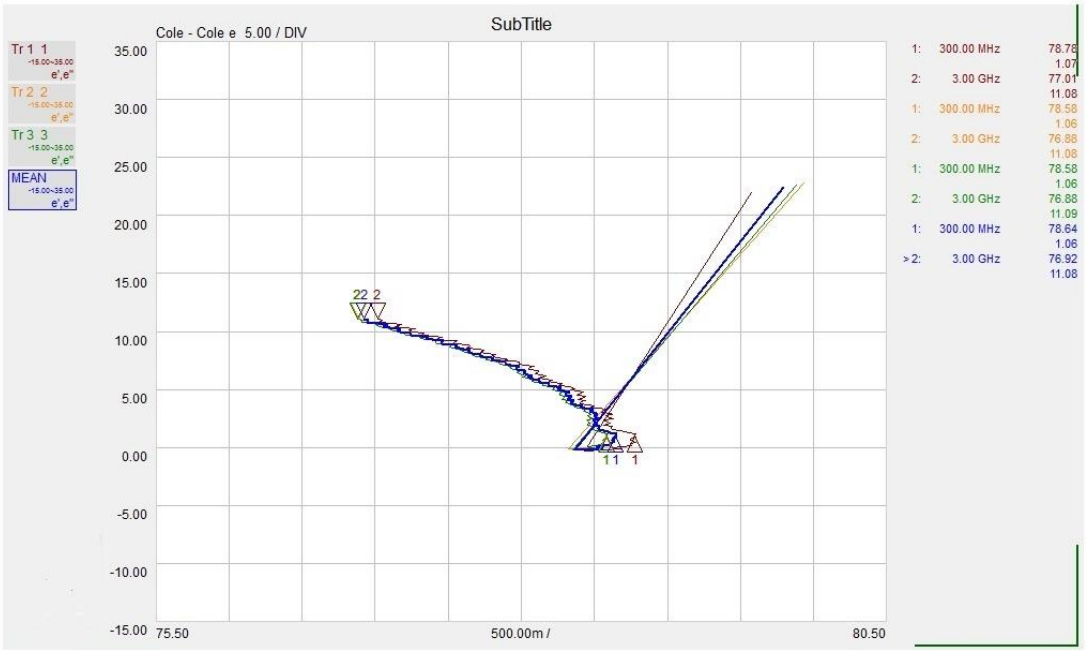

Figure A.4 : Cole-cole values of feeding solution.

APPENDIX A (Continue)

Tedpella Formvar/Carbon grid attached on the surface of aluminium foil. Aluminium foil placed on metal collector. Then nanofibers obtained on grid by electrospinning the feeding solution for 30 seconds. Nanofibers were examined with an Ultra-High Resolution Analytical Field Emission Scanning Electron Misroscope (Hitachi SU7000), at 25kV under the 10^{-5} Toor vacuum with TEM imaging module.

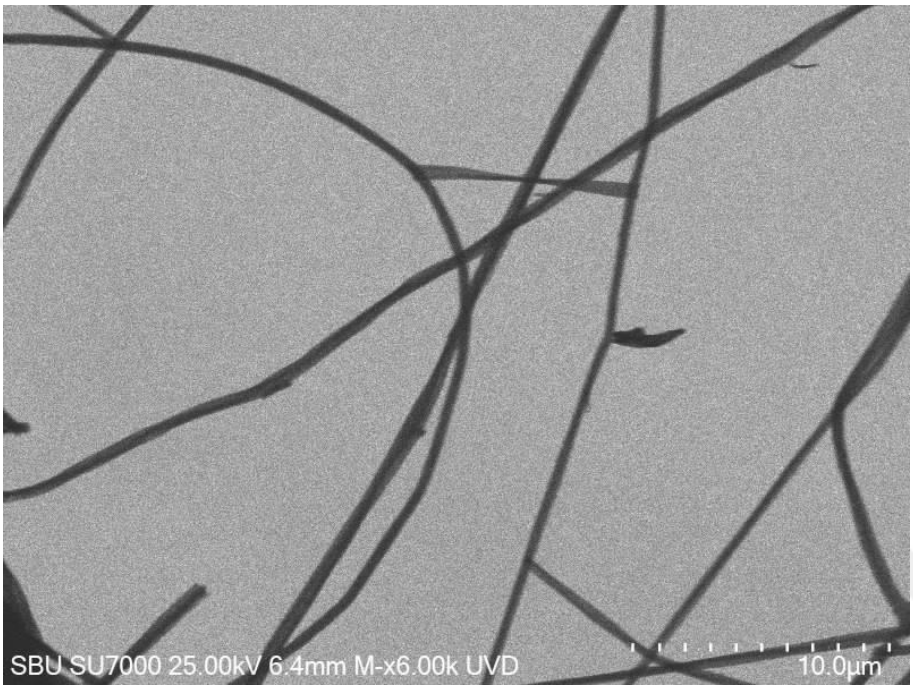

Figure A.5 : TEM image of electrospun nanofibers.

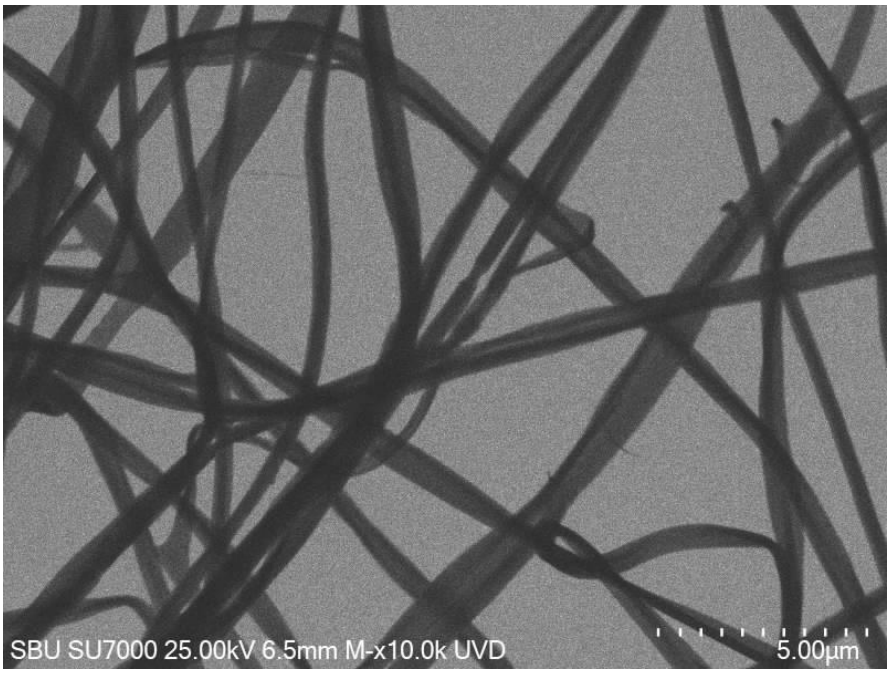

Figure A.6 : TEM image of electrospun nanofibers.

APPENDIX B

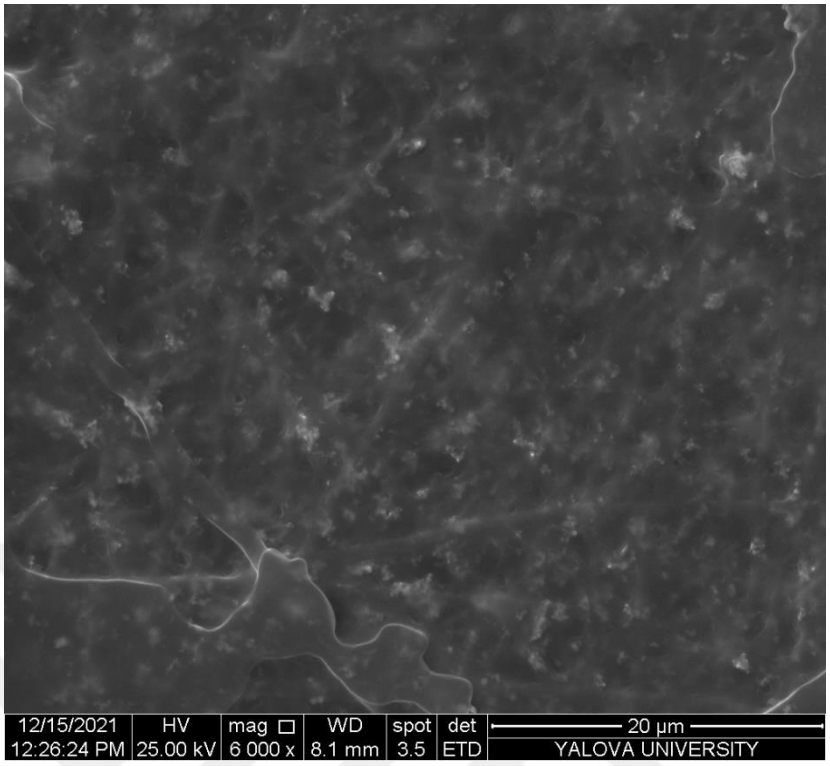

Figure B.1 : SEM image of GLES sample that absorbed volatiles (30th hour) from European hake loin (Magnification 6 000x).

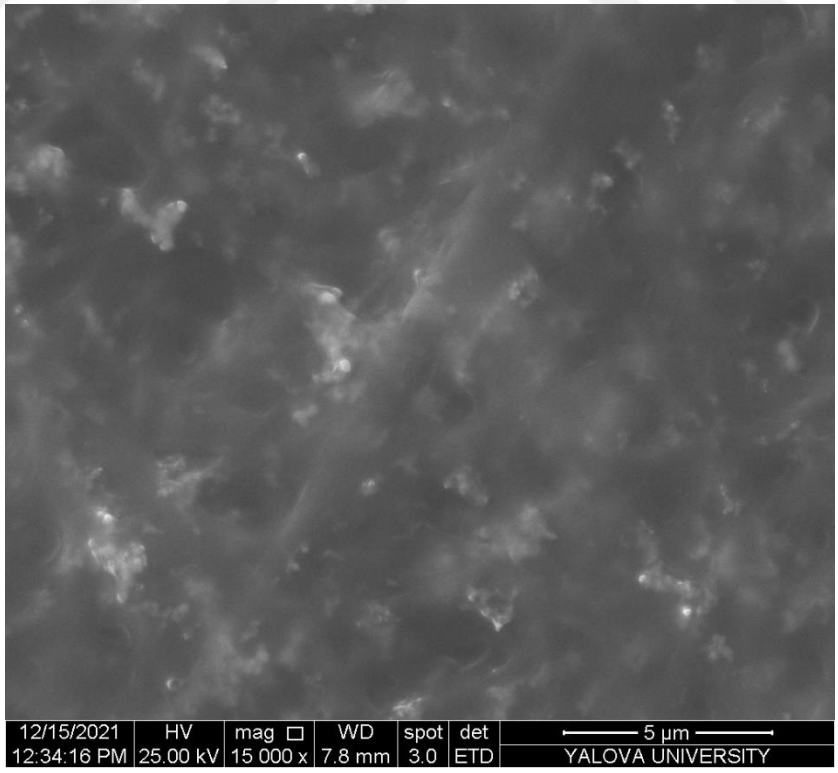

Figure B.2 : SEM image of GLES sample that absorbed volatiles (30th hour) from European hake loin (Magnification 15 000x).

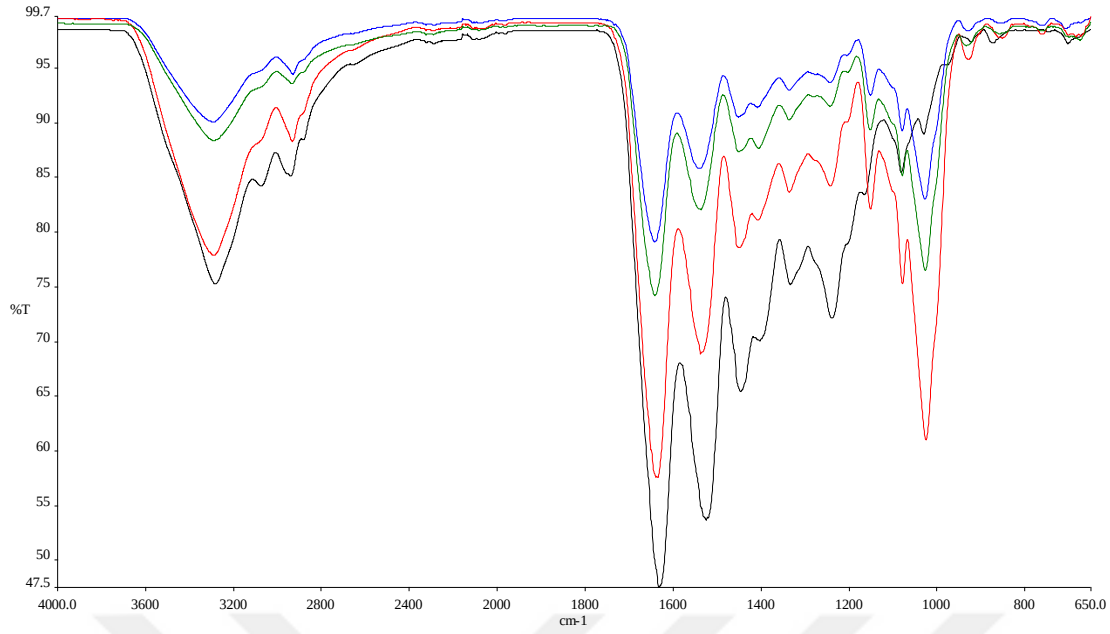

Figure B.3 : Initial FTIR spectrum of **GL**, **GLE**, **GLES**, and **GLESA** nanofibers.

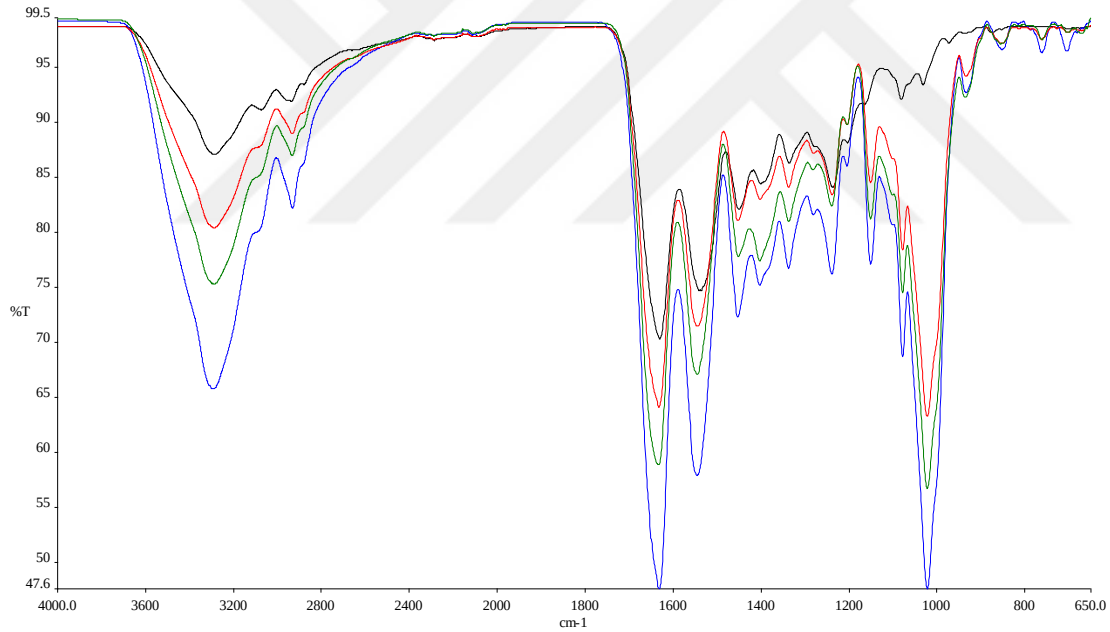

Figure B.4 : FTIR spectrum of **GL**, **GLE**, **GLES**, and **GLESA** nanofibers after absorption of volatiles (30^{th} hour).

CURRICULUM VITAE

Name Surname **:** Turgay ÇETİNKAYA

EDUCATION **:**

- **B.Sc.** **:** 2014, Sakarya University, Faculty of Engineering, Department of Food Engineering
- **M.Sc.** **:** 2016, Istanbul Technical University, Chemical and Metallurgical Faculty, Food Engineering Department
- **Ph.D.** : 2022, Istanbul Technical University, Chemical and Metallurgical Faculty, Food Engineering Department

PROFESSIONAL EXPERIENCE AND REWARDS:

- 2020-… Yalova University, Armutlu Vocational School, Department of Food Processing, Yalova, Türkiye, Lecturer
- 2016-2020 Republic of Türkiye Ministry of Agriculture and Forestry, Fatih District Agriculture and Forestry Directorate, Istanbul, Türkiye, Food Engineer
- 2019 Visiting Researcher, Denmark Technical University, National Food Institute, Lyngby, DENMARK (3 Months)
- 2018 International Symposium on Food Rheology and Texture, Istanbul, Türkiye, 2nd best poster award.
- 2015 Visiting Master Student, Ghent University, Department of Food Technology, Saferty, and Health, Ghent, BELGIUM (5 Months)
- 2012–2013 Apetito Convenience GMBH & Co, Internship, HILTER/GERMANY (6 months)

PUBLICATIONS, PRESENTATIONS AND PATENTS ON THE THESIS:

- **Çetinkaya, T.,** Ceylan, Z. 2019. An Observation of Microbial Quality Changes of Two Different Smoked Fish Products Stored at Refrigerator After Their Packages Being Opened. *European Journal of Science and Technology*, *17*, 982-988.
- **Çetinkaya, T.,** Altay, F., Ceylan, Z. 2021. Determination of Fish Meat Quality Changes by Fast and Novel Methods During Storage Period. *Journal of the Institute of Science and Technology*, *11*(3), 2030-2040.

- **Çetinkaya, T.,** Ceylan, Z., Meral, R., Kılıçer, A., Altay, F. 2021. A novel strategy for Au in food science: Nanoformulation in dielectric, sensory properties, and microbiological quality of fish meat. *Food Bioscience, 41,* 101024.
- **Cetinkaya, T.,** Wijaya, W., Altay, F., Ceylan, Z. 2022. Fabrication and characterization of zein nanofibers integrated with gold nanospheres. *LWT-Food Science and Technology*, *155*, 112976.

OTHER PUBLICATIONS, PRESENTATIONS:

International Articles:

- Ceylan, Z., Meral, R., **Cetinkaya, T.** 2020. Relevance of SARS-CoV-2 in food safety and food hygiene: potential preventive measures, suggestions and nanotechnological approaches. *VirusDisease*, 1-7. https://doi.org/10.1007/s13337-020-00611-0
- Ceylan, Z., & **Çetinkaya, T.** 2021. Definition of textural deterioration in squid samples: three different tools supported by microbial, visual and physico-chemical analysis. *Ege Journal of Fisheries and Aquatic Sciences*, *38*(3), 263-268. https://doi.org/10.12714/egejfas.38.3.01
- **Cetinkaya, T.,** Mendes, A. C., Jacobsen, C., Ceylan, Z., Chronakis, I. S., Bean, S. R., García-Moreno, P. J. 2021. Development of kafirin-based nanocapsules by electrospraying for encapsulation of fish oil. *LWT-Food Science and Technology*, *136,* 110297. https://doi.org/10.1016/j.lwt.2020.110297
- **Cetinkaya, T.,** Altay, F., Ceylan, Z. 2021. A new application with characterized oil-in-water-in-oil double emulsions: gelatin-xanthan gum complexes for the edible oil industry. *LWT-Food Science and Technology*, *138*, 110773. https://doi.org/10.1016/j.lwt.2020.110773
- Ucar, Y., Ceylan, Z., Durmus, M., Tomar, O., **Cetinkaya, T**. 2021. Application of cold plasma technology in the food industry and its combination with other emerging technologies. *Trends in Food Science & Technology*, *114*, 355-371. https://doi.org/10.1016/j.tifs.2021.06.004
- Najafi, Z., **Cetinkaya, T.**, Bildik, F., Altay, F., & Yeşilçubuk, N. Ş. 2022. Nanoencapsulation of saffron (*Crocus sativus L.*) extract in zein nanofibers and their application for the preservation of sea bass fillets. *LWT-Food Science and Technology*, 113588. https://doi.org/10.1016/j.lwt.2022.113588

Book Chapters:

- **Çetinkaya, T.,** Ceylan, Z. 2020. Balıketi Kalitesinin Tanımlanmasında Kullanılabilecek Alternatif Yaklaşımlar. In A. Bolat, (Ed.), *Ziraat, Orman ve Su Ürünleri Alanında Akademik Çalışmalar–II.* Retrieved from: https://www.gecekitapligi.com/Webkontrol/uploads/Fck/ziraatyayin.pdf
- Ceylan, Z., **Çetinkaya, T.** 2020. Taramalı Elektron Mikroskobunun Nanomateryallerle İlişkisi ve Nanoteknolojik Uygulamalar İçin Önemi. In R. İrkin, (Ed.), *Mühendislik Alanında Akademik Çalışmalar-II*. Retrieved from:

https://www.gecekitapligi.com/Webkontrol/uploads/Fck/muhendislikyayin_6.pdf

- Ceylan, Z., Ocak, E., Uçar, Y., Karakus, K., **Cetinkaya, T**. 2021. An overview of food safety and COVID-19 infection: nanotechnology and cold plasma applications, immune-boosting suggestions, hygienic precautions. In M. H. Dehghani, R. R. Karri, S. Roy, (Eds.), *Environmental and Health Management of Novel Coronavirus Disease (COVID-19)*, (Vol. 1, pp. 325-344). Retrieved from: https://www.sciencedirect.com/science/article/pii/B97803238578 0200 0044?via%3Dihub

Congress and Conference Papers:

- **Cetinkaya, T.,** Altay, F. 2016: Effects of nanofillers on plant protein based nanocomposites for food packaging applications. 6th International Seminer on Modern Polymeric Materials for Enviromental Applications, April 27-29, 2016 Krakow, Poland. (Full text paper).
- Najafi, Z., **Çetinkaya, T.,** Neşe-Şahin, Y., Altay, F. 2018: Effects of Feed Solution Viscosity on Electrospinnability of Zein With or Without Saffron. International Symposium on Food Rheology, October 19-21, 2018 Istanbul, Türkiye. (Poster Presentation).
- Ceylan, Z., Tomar, O., Çağlar, A., **Çetinkaya, T**. 2021: A Sensory Observation for Cold Stored Beef Steak and Norway Salmon. 2nd International Conference on Raw Materials to Processed Foods, June 03-04, 2021 Istanbul, Türkiye. (Full text/Oral presentation).
- Ceylan, Z., Tomar, O., Çağlar, A., **Çetinkaya, T**. 2021: A Sensory Observation at a House for Different Fish Species Stored at Room Temperature. 2nd International Conference on Raw Materials to Processed Foods, June 03-04, 2021 Istanbul, Türkiye. (Full text/Oral presentation).
- Ceylan, Z., Tomar, O., Çağlar, A., **Çetinkaya, T**. 2021: A sample Observation for Gastronomic Applications: Intercation of Lemon or Apple Vinegar Added Olive Oil with Sea Bass Fillet adn Beefsteak. III Balkan Agricultural Congress, August 30-September 1, 2021, Edirne, Türkiye (Full text/Oral presentation).

Projects:

- Evaluation of active and/or smart packaging functions of pvc films with electrospun nanofibers in terms of fresh fish fillets stability. (Istanbul Technical University, Scientific Research Projects (BAP) Unit [project number MDK-2019-42144], 25.06.2019–25.12.2022. (Researcher).